Jens Strandberg

Optimal operation of dividing wall columns

Doctoral thesis
for the degree of doctor philosophiae

Trondheim, February 2011

Norwegian University of Science and Technology

NTNU
Innovation and Creativity

NTNU

Norwegian University of Science and Technology

Doctoral thesis
for the degree of doctor philosophiae

ISBN N/A (printed version)
ISBN N/A (electronic version)
ISSN 1503-8181

Doctoral theses at NTNU, 2011:N/A

Printed by NTNU-trykk

Abstract

This thesis discusses the control and operation of dividing wall columns. In particular the attention is on the Kaibel column, a four-product dividing wall column with two side-streams.

The Kaibel column has for a given feed potentially 6 degrees of freedom available for control once inventory control loops are in place. These degrees of freedom are the vapour rate, reflux rate, two side-stream rates and the split ratios for vapour and liquid. They can be used to operate the column in such a way as to meet predefined goals and specifications. The goals of operation may be formalized by an economic cost (or objective) function. *Optimal operation* is when the best possible operation in terms of the cost function is achieved. The normal (in literature) cost function to evaluate dividing wall columns is to minimize the energy input to the column while keeping the product purities at specified values. This is a good formulation to evaluate the potential energy savings of the dividing wall compared to conventional distillation sequences, and is particularly useful in a design phase. For an existing column within a processing plant, other operational objectives may also be important, however. In this work, optimal operation of a dividing wall column is investigated from a perspective of different operational modes (objectives).

It is common to separate a control system into different layers based on the time-scale that the different control loops operate. The *supervisory control layer* should help us achieve the operational objectives - optimal operation, while the faster *regulatory control layer* should deal with stabilization and fast control. In this thesis the emphasis is on selecting the correct controlled variables for both layers. Methods for selecting self-optimizing controlled variables are applied with an aim of optimal operation, while column dynamics are more important when selecting variables to control in the regulatory control layer.

For the regulatory control layer, the importance of utilizing the liquid split for closed loop control is emphasized.

A Kaibel column pilot plant has been constructed during the work of this thesis. Initial experiments have been reported and valuable lessons were learned about the design and operation of the column. A purpose-built valve for adjusting the vapour split in the column has been included in the apparatus. The first experiment with closed loop control using the vapour split as a manipulative variable is reported.

Acknowledgements

First and foremost I would like to thank my supervisor Professor Sigurd Skogestad for giving me the opportunity to do this work and for sticking with me through all these years.

I would also like to thank Professor Heinz Preisig for his many contributions regarding the set up of the pilot plant column and especially for the close cooperation during work on the vapour split valve.

Building the pilot plant column would not have been possible without the aid and facilitation of Odd Ivar Hovin and Jan-Morten Roel from the department workshop.

I am thankful for help and encouragement from Vidar Alstad, Efstathios Skouras, Bjørn Tore Løvfall and other former colleagues in the Process Systems Engineering Group. Thanks also to former master student Martin Kverneland.

A special thank you to Olaf Trygve Berglihn whom I was lucky to share an office with for more than five years. Thanks for all your help and company during the office years and for proofreading this thesis.

Financial support for this project was provided by The Norwegian Research Council and The Chemical Engineering Department, NTNU.

Finally, I would like to thank my family for their constant support.

Last, but not least, to my girlfriend Camilla: Thank you for pushing me on to finish this. Thank you for your (im)patience!

Contents

Chapter 1

Introduction

1.1 Motivation

The concept of dividing wall distillation columns has been known for a long time. The first patents were issued in the 1930s and 40s and around 1965 Petlyuk [29] and co-workers studied the thermodynamic properties of thermally coupled columns. Although, Petlyuk worked in the then Soviet Union, and it took some time before the rest of the world was made aware of his work, it was not until 1985 that the first dividing wall column was commissioned. It was German chemical giant BASF who took the first step, and they are to this day the leader of the field when it comes to utilizing this technology.

When the work on this thesis began, the reported number of dividing wall columns in industrial use was in the region of 30 to 40. With the large potential savings in both operating- and investment costs proven by process applications and academic studies, it was striking how slow the technology was catching on in the process industry. The last 10 to 15 years have seen an increased rate of implementations, but still the total number of dividing wall columns in use is around 100. The majority of which belong to BASF plants. Compare this to the number of conventional distillation columns, and their use is by no means common practice. Dividing wall columns are of course not a viable option for all separation applications, but the potential for a more widespread use was and is still there today. In the academic world (at least), an accepted reason for the limited reach of the dividing wall column has been a fear from the process industry that the added complexity of the column arrangements will lead to more complex or difficult control and operation. Here lies the main motivation for this thesis. Are dividing wall columns inherently difficult to control or can *control structure design* procedures

and methods help us to provide guidelines to simple and workable control configurations for the columns?

At the start of this study, the dividing wall columns realized for industrial use were all (as far as reported) three-product columns (often referred to as Petlyuk columns). Dr. Gerd Kaibel of BASF had in 1987 suggested a configuration for separating four products within one column shell. The column has been dubbed the Kaibel column in tribute to its inventor, but has received little attention from academia compared to the Petlyuk arrangement. The limited studies performed and lack of operational data was a major motivation for building a pilot plant of the Kaibel column during this work. The Kaibel column configuration has therefore also been the main subject in the modelling and simulation work presented in this thesis.

1.2 Thesis overview

Chapter 2 is an introductory chapter to the concept of dividing wall distillation columns. The Petlyuk and Kaibel columns, used to separate three and four products respectively, are introduced and explained. A brief history of their evolvement from patented inventions and ideas to industrial applications is also given. The chapter then gives an overview of previously published work on control and operation of dividing wall columns, and finally a description of experimental work reported by others.

In Chapter 3 optimal operation is defined in terms of an economic objective function. First in general terms and then applied to a Kaibel distillation column. An introduction to how the plantwide control approach can be used to make structural decisions for the design of a complete control system of a plant is given. The first steps of this approach are then applied to the Kaibel column, and we show how the definition of the economic objective for the column will influence its operation. Four different operating modes are defined.

Chapter 4 looks at selecting measurements and controlled variables for the Kaibel column. The primary controlled variables should be chosen based on the economic objective of the plant (column). We give examples of how to find self-optimizing controlled variables. These are variables, either single measurements or a combination of measurements, that when kept constant will give near optimal (with acceptable loss) operation in the presence of disturbances. The examples relate to the different operating modes found in Chapter 3.

The focus of Chapter 5 is the regulatory control layer for dividing wall columns. The regulatory control layer is the base control layer for a plant

and is used mainly for stabilizing operation. Control configurations with varying number of temperature control loops are compared and the importance of using the liquid split for active feedback control is highlighted. The analysis is performed for a Kaibel column and a Petlyuk column, as well as for high-purity versions of the two.

Chapter 6 looks again at the regulatory control layer for the Kaibel column. The attention is on how to select the best locations for temperature measurements. Different selection criteria are applied and the analysis is performed for the operating modes defined in Chapter 3. Ideally, the regulatory control layer should be independent of the operating mode (and the supervisory control layer).

The last two chapters of the thesis relate to the pilot plant Kaibel column set up during the work of this thesis. In Chapter 7 the pilot plant Kaibel column is presented. The column setup is described along with its integral parts. The control and data acquisition systems are presented with details of the manipulated variables. Special attention is given to the implementation of the liquid and vapour split devices, and a new valve for modifying the vapour split is presented.

Chapter 8 is dedicated to the experimental work performed with the Kaibel pilot plant. Initial experiments include regulatory control experiments with temperature control and control of the liquid and vapour splits. After an initial period of experiments, several design flaws were identified and the column was later modified. The final sections of the chapter discuss the modifications and highlight the improvements made. An experiment with closed loop feedback control using the vapour split as a manipulated variable is reported for the first time.

1.3 Publication list

J. Strandberg and S. Skogestad, "Stabilizing control of an integrated 4-product Kaibel column", Proceedings Adchem 2006 (IFAC symp. on Advanced control of chemical processes), Gramado, Brazil, 2-5 April 2006, pp. 623-628.

J. Strandberg and S. Skogestad, "Stabilizing operation of a 4-product integrated Kaibel column", Proceedings Distillation and Apsorption, London, UK, 4-6 Sept. 2006, In: IChemE Symposium Series, 152, ISBN-13 978 0 85295 505 5, pp. 638-647 (2006).

J. Strandberg, S. Skogestad and I. J. Halvorsen, "Practical control of dividing wall columns", Proceedings Symposium Distillation and Absorption 2010, Eindhoven, The Netherlands, 12-15 September 2010, pp. 527-532, ISBN 978-90-386-2215-6.

Chapter 2

Dividing wall distillation

Distillation is the most widely used separation method in the process industry. At the same time, distillation is a highly energy intensive process. As the industry is increasingly looking for more sustainable solutions, both environmentally and financially, dividing wall distillation columns offer several benefits compared to conventional separation of multicomponent mixtures in a distillation sequence (Figure 2.1).

2.1 Dividing wall columns

Dividing wall type columns were first presented to the world as patent applications in the 1930's and 40's. Among the inventors were Monro [24], Brugma [5] and Wright[42]. However, it was not until 1985 that the dividing wall column found its first industrial application. In the former Soviet Union, Petlyuk [29] and co-workers did groundbreaking work on the thermodynamic properties of thermally coupled columns. Petlyuk showed that for a three-component mixture the fully thermally coupled column (also known as Petlyuk column, Petlyuk arrangement, prefractionator arrangement, see Figure 2.2) can considerably reduce the heat input required for separation as compared to the conventional direct and indirect sequences (Figure 2.1). In fact, the Petlyuk column will always require the lowest rate of vapour boil up for any given separation. In a Petlyuk arrangement (Figure 2.3), the feed mixture enters what is called a prefractionator and (given enough stages) the heaviest and lightest component are completely separated from each other. In other words, for the components A, B and C (in descending volatility), component A leaves the prefractionator at the top of the column while component C is drawn off the bottom. The middle boiling component (B) is allowed to go with either stream. The arrangement is

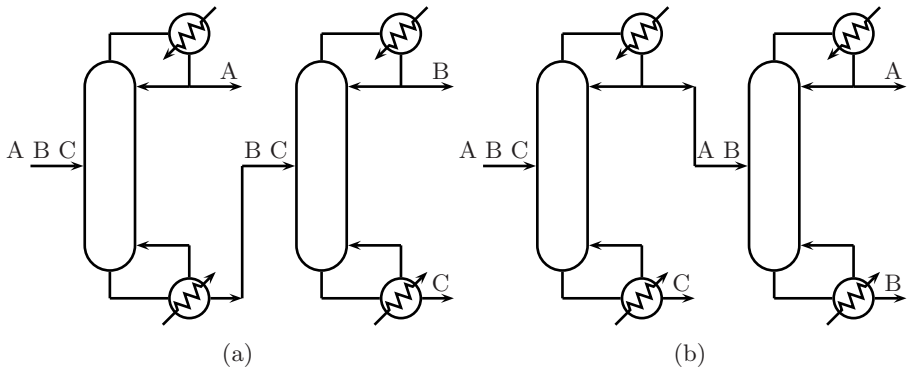

Figure 2.1: Conventional distillation sequenceses. (a) Direct split sequence. (b) Indirect split sequence.

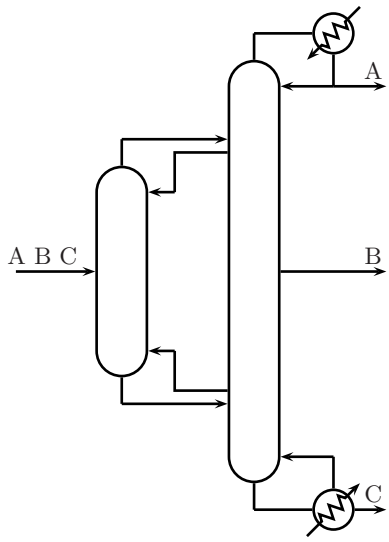

Figure 2.2: Petlyuk arrangement.

called thermally coupled because the heat to the prefractionator is supplied by a vapour stream from the "main" column. Similarly, the reflux to the prefractionator is supplied through a liquid stream from the main column. The reason for the efficiency of this arrangement is that one avoids any remixing of already separated components as will occur in a conventional column sequence.

The potential energy savings of a Petlyuk column are 20-50% depending on feed composition, relative volatility and product purity specifications. The energy savings are due to reduced mixing loss at the interconnections. In addition we my also have capital savings that comes from both compactness and reduced internal flow rates which can be used to reduce equipment size (or increase production for the same internal flows). The potential savings are also higher for more difficult splits.

Although the ideas and theory behind the Petlyuk arrangement were known for some time, the first industrial implementation put into use was, as mentioned, not before the mid 1980's. The column, when built by BASF in Ludwigshafen, Germany, was built as a dividing wall column (DWC) ([17]). The dividing wall column (Figure 2.4) is thermodynamically equivalent to the Petlyuk arrangement, but the two columns are incorporated into a single shell. As the name suggests, the column is divided vertically into main sections by a partitioning wall. The side where the feed enters replaces the prefractionator column in the Petlyuk arrangement. In addition to the energy efficiency benefits, the dividing wall column can also save additional capital investment and plot space taken up by the equipment.

Ever since the first implementation, BASF has been the world leader in developing and operating dividing wall columns. At present there are around 70 DWCs in operation in BASF plants worldwide ([8]). The development of the dividing wall columns by BASF are closely related to their co-operation with equipment manufacturer J. Montz, who have delivered most of the columns or column internals for BASF. A major breakthrough in the development of DWCs that significantly increased the rate of implementations was the introduction of the non-welded partition wall by Montz ([16]).

After the success of BASF, other companies have followed suit and the number of DWCs in operation now count more than 100 [8].

2.1.1 The Kaibel column

It was the paper by Dr. Gerd Kaibel [17] of BASF in 1987 that got the world's attention to the dividing wall columns of BASF and sparked interest in the academic community. In the same article, a four-product dividing

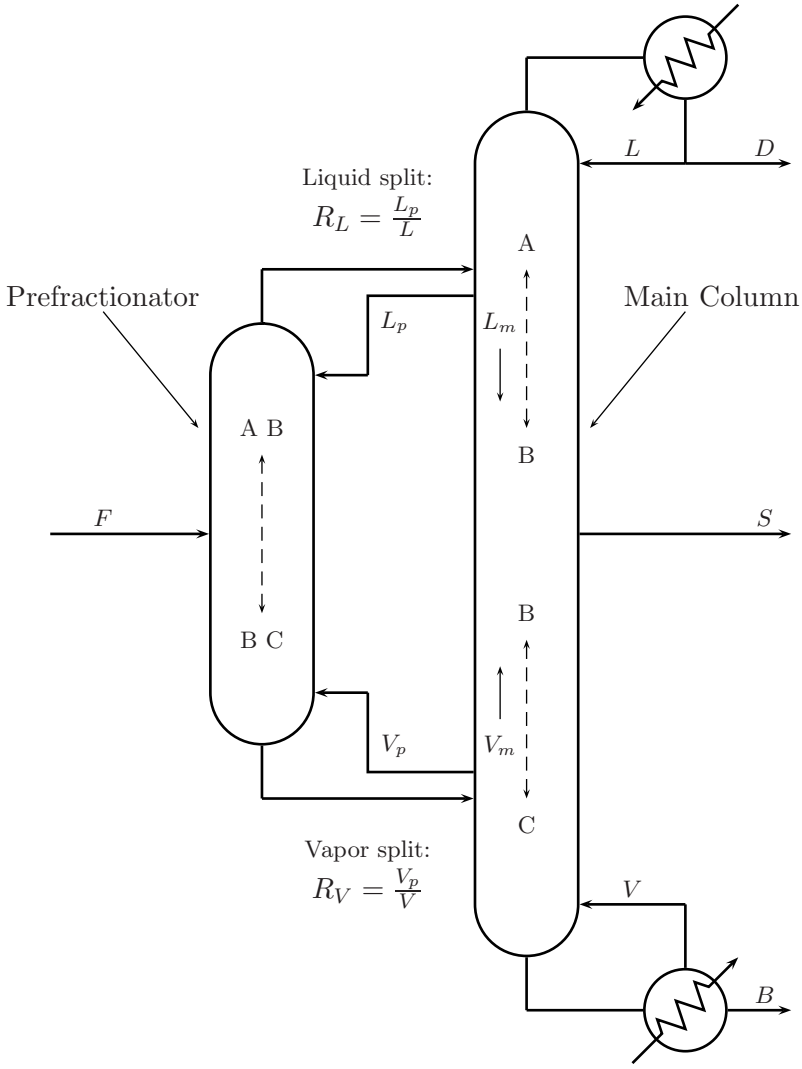

Figure 2.3: Detailed Petlyuk arrangement.

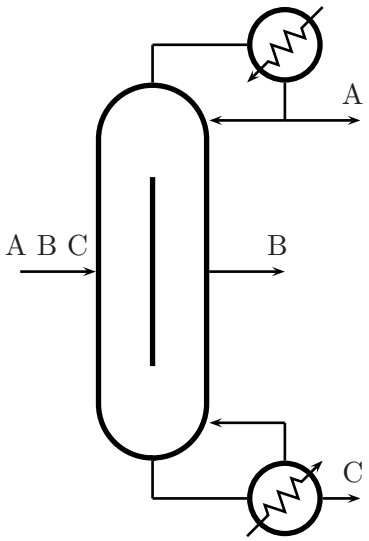

Figure 2.4: Dividing wall column

wall column was for the first time described. With this arrangement (Figure 2.5), a four-component mixture can be completely separated into pure products and thus replace a sequence of three conventional distillation columns. Obviously, the potential for capital investment savings is large, and the configuration has also been shown to reduce energy requirements compared to the conventional sequence. We denote the column configuration the "Kaibel column" [7] as a tribute to its inventor, and the Kaibel column is the main focus of this work. The world's first industrial-scale Kaibel column has recently been put into operation by BASF (Olujic, 2009 [28]). The column, a packed dividing wall column operated under vacuum is another example of BASF's co-operation with J. Montz.

With the correct design and operation, the Kaibel column may effectively reduce the required heat input by at least 20% [7, 12], but for a thermodynamically optimal configuration for a four-component mixture, more coupled sections are required. Figure 2.6 shows what can be termed a Petlyuk arrangement for a four-component mixture. Such a column has yet to be realized, but a recent paper by Dejanovic et al [9] goes a long way to show the feasibility of its design and potential benefits.

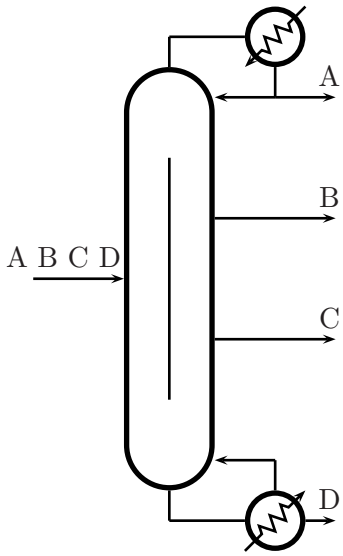

Figure 2.5: Kaibel column. A 4-product dividing wall column

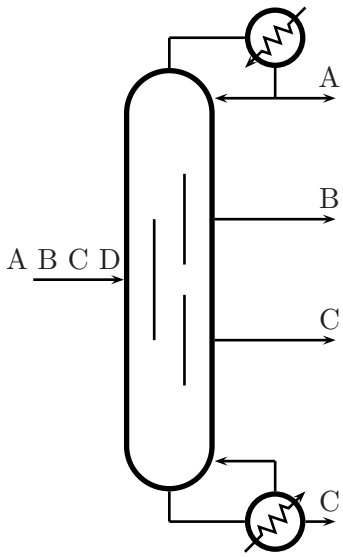

Figure 2.6: A 4-product Petlyuk arrangement with multiple partition walls.

2.2 Control and operation of dividing wall columns

Problems regarding control and operability of dividing wall columns have often been named as a contributing factor in explaining the slow emergence of the columns in the process industry [8, 18, 30].

One of the first papers published on control of dividing wall columns was by Wolf and Skogestad [41]. They studied the Petlyuk column and used 3-point composition control of the products. There were no operational problems for the system when using reflux (L), side-stream flow (S) and vapour boil up rate (V) as the manipulated variables. They also tried to utilize the liquid split (R_L) for a fourth loop, controlling the composition of one of the impurities in the side-stream (S used to control the other impurity), but discovered discontinuities in the feasible range.

Halvorsen and Skogestad [14] showed how liquid and vapour splits are related to vapour boil up rate in a Petlyuk column and suggested to use the liquid split for control to minimize the energy input to the column. They suggested some candidate control variables and described the ideal self-optimizing control properties of such measurements. Temperature differences in the column were one of the suggested measurements, but no dynamic simulation results were presented.

Mutalib and Smith [25] did dynamic simulations of a system by controlling the three product compositions. They discuss the impact of liquid and vapour splits but decide to keep the ratios fixed. In a second paper, Mutalib et al. [26] present further simulations in addition to results from pilot plant experiments. Here they use temperatures instead of compositions as controlled variables, however they fix only two temperatures and leave the side-stream rate fixed, which results in poor disturbance rejection.

Mizsey et al. [23] and Serra et al. [31] also studied the Petlyuk column choosing control the three product compositions while keeping the liquid split fixed.

Adrian et al. [1] compared using three single temperature loops (PI-controllers) against a (multivariable) model predictive controller (MPC). They used the reflux (L) to control a temperature in the top of the prefractionator, the side-stream rate (S) to control a temperature in the bottom section and the liquid split (R_L) to control a temperature in the main column above the side draw. They concluded that MPC showed superior control behaviour to that of the decentralized feedback loops. However, it should be noted that the vapour boil up V was kept fixed during the PI experiments, while it was used as an extra input for the MPC experiment.

Alstad and Skogestad [3] applied self-optimizing control ideas to find

combinations of measurements to be controlled using the liquid split (and vapour split), while controlling the product purities at their specifications using reflux, boil up and side-stream rate. The objective was to minimize the energy input to the Petlyuk column.

Wang and Wong [40] studied a high-purity Petlyuk arrangement. They used three stabilizing temperature control loops, with one temperature fixed in the prefractionator and two in the main column. The temperature near the bottom of the prefractionator was controlled using the reboiler duty (vapour boil up), while the temperatures in the main column were controlled using the reflux and side-stream rates. While the authors stress the effect of liquid and vapour splits on the column they choose to fix the splits and instead treat them as disturbances. Using the temperatures above with composition control in a cascade structure they improve the performance.

Ling and Luyben have recently published two papers [19, 20] concerning control of the column. In the first paper they propose a decentralized control configuration where four compositions are controlled. In addition to the product compositions, they select to control the composition of the heaviest component at a location near the top of the prefractionator using the liquid split as the manipulated variable. They report that using the liquid split in this manner indirectly minimizes the energy input required for the separation. In the second paper, the authors replace composition control for temperature control. They use SVD-analysis (singular value decomposition) to select temperature measurement locations and apply four temperature feedback loops. They find that although the column is stabilized, the product compositions deviate in the face of feed composition disturbances. Later, the authors change the controlled variables to control four temperature differences instead of single temperatures and find that this improves the results.

Finally, van Diggelen et al. [39] compared a number of different decentralized control configurations and more advanced multivariable controllers on a dynamic model of a Petlyuk column. The objective for all was to control the product compositions at their setpoints. In the case for the decentralized configurations three composition loops are closed, while the liquid split is kept constant. They found that while the decentralized PI controllers work, disturbances are controlled faster using MIMO (multi-input, multi-output) controllers.

2.3 Previous experimental work

There are not many published data from laboratory experiments with dividing wall columns available and even less from operating columns in the industry. Nevertheless, there are some academic groups that have developed pilot plant columns and published results from their experiments.

Mutalib et al. [26] from UMIST (Manchester, UK) reported from a dividing wall column with an inside diameter of 0.305 m and a height of 11 m. They used structured packing material (Gempak 4A) and a metal plate was placed vertically inside the middle section to form the dividing wall. The plate was placed closer to the feed side to make the cross-sectional areas of the prefractionator and main column correspond to the vapour split ratio specified in their simulation studies. The liquid split is distributed by first withdrawing the liquid from the top section above the wall into a buffer tank, and then redirecting the liquid to either side of the wall at a predetermined ratio. Methanol, Iso-propanol and butanol made up an equimolar feed mixture and were fed to the column at 75 l/h. The condenser was open to atmospheric pressure.

Adrian et al. [1] conducted experiments at BASF's miniplant lab at Ludwigshafen, Germany. The setup included a column where the dividing wall section were represented by to columns in parallel (similar setup to the one presented in this thesis, Figure 7.1). The inner diameters of the parallel sections were 40 mm while the upper and lower sections were 55 mm. The total height of the column was 11.5 m and the entire column was insulated with active heat compensation. The liquid split was distributed in a similar way as in the UMIST column, however here it was actively used for control. The authors used a feed mixture of butanol (15 % wt), pentanol (70 % wt) and hexanol (15 % wt) fed at a rate of 2 to 3 kg/h. They operated the column at 900 mbar.

The most recent experimental study published is that of Niggemann et al. [27]. Their group is based at Hamburg University of Technology, Germany. The dividing wall column set up in their lab was built into one shell with an inner diameter of 68 mm. The total height of the column was approximately 12 m and equipped with Montz B1-500 structured packing. The liquid split was operated using a magnetically actuated swinging funnel at the top of the vertical division, but the split ratio was kept constant (50:50) during the reported experiments. The study used a feed mixture of n-hexanol, n-octanol and n-decanol and achieved product purities of around 99 % wt. The authors present steady-state results and subsequent model validation from their experiments and do not discuss the control system

in detail. An interesting result from their experiment is that heat transfer across the dividing wall may influence the hydraulics of the column to such an extent that the vapour distribution (vapour split) is affected. The added condensation and evaporation effects cause changes in the pressure drop in the relevant sections and thereby the vapour distribution.

2.4 Conclusions

Dividing wall columns are not a new invention, but it is really only in the last 10 to 15 years that their application has become relatively widespread. A thermally coupled column such as the Petlyuk column has the potential for large energy savings when compared to a traditional distillation sequence. It also offers capital investment savings since less equipment is required. When realized as dividing wall column, built into one column shell, the capital investment cost is even less, and there is the added benefit of smaller plot space necessary in the processing plant.

Fear of control and operational problems regarding the more complex configuration of a dividing wall column is often blamed for the slow spread of the columns in the process industry. Some authors also claim that there is a direct conflict between the controllability of a dividing wall column and operating the column in an energy efficient way [1].

Chapter 3

Optimal operation of the Kaibel column

3.1 Introduction

To define optimal operation we must decide what the objectives of the operation are. Usually the operation is to perform a certain task with some specifications on quantity and quality. To find optimal operation, we can measure the performance according to our defined criterion, which generally is to maximize profit subject to satisfying given constraints and specifications. Depending on the situation, this can be translated to more specific objectives such as maximize throughput, maximize quality (purity), minimize energy, minimize time etc.

3.1.1 Cost function

We define a general economic objective function, namely to minimize the cost J:

$$(-J) = \sum_{i=1}^{m} w_{p,i} P_i - \sum_{j=1}^{n} w_{f,j} F_j - \sum_{k=1}^{o} w_{e,k} E_k \tag{3.1}$$

where w_p, w_f, and w_e denote the weighting (normally prices) of the products P_i, the feedstocks F_j and the energy utilities E_k respectively. In some cases, the prices $w_{p,i}$ are functions of the composition of the flows. In other cases, the prices are fixed, provided the compositions are within their specifications.

The optimization problem then becomes:

$$\min_{\mathbf{u}} J \tag{3.2}$$

subject to

$$\begin{aligned} \mathbf{f}(\mathbf{x}, \mathbf{u}, \mathbf{d}) &= 0 \\ \mathbf{h}(\mathbf{x}) &\leq 0 \end{aligned} \tag{3.3}$$

where $\mathbf{f} = 0$ expresses the model equations and the equality constraints and $\mathbf{h} \leq 0$ the inequality constraints. $\mathbf{x}$ is the vector of model states, $\mathbf{u}$ represent the model inputs and $\mathbf{d}$ is the vector of process disturbances.

3.2 Plantwide control

To achieve optimal operation, or indeed any functioning operation, of a dividing wall column, we need a control system. In the process of the designing a complete control system for a plant (or in this case a Kaibel distillation column), the structural decisions involved in designing a control *structure* are important. Skogestad and Postlethwaite [37] identify the following decisions involved in control structure design:

- The selection of controlled outputs (a set of variables which are to be controlled to achieve a set of specific objectives).
- The selection of manipulated inputs and measurements (sets of variables which can be manipulated and measured for control purposes).
- The selection of a *control configuration* (a structure of interconnecting measurements/commands and manipulated variables).

Skogestad [35] has proposed a systematic procedure called plantwide control that is a useful approach to the decisions above:

"Top-down":

(i) Identify operational constraints and indentify a scalar cost function J that characterizes optimal operation.

(ii) Identify degrees of freedom (manipulated inputs u) and in particular identify the ones that affect the cost J (in process control, the cost J is usually determined by the steady-state).

(iii) Analyze the solution of optimal operation for various disturbances, with the aim of finding primary controlled variables ($y_1 = z$) which, when kept constant, indirectly minimize the cost ("self-optimizing control", further discussed in Section 4.2.2)

(iv) Determine where in the plant to set the production rate.

"Bottom-up":

(v) *Regulatory/base control layer*: Identify additional variables to be measured and controlled (y_2), and suggest how to pair these with manipulated inputs.

(vi) *"Advanced"/supervisory control layer* configuration: Should it be decentralized or multivariable?

(vii) *On-line optimization layer*: Is this needed or is a constant setpoint policy sufficient ("self-optimizing control")

In this chapter we initiate the above procedure by looking at steps (i) and (ii). In Section 3.3 we apply the approach for various operating modes of the Kaibel column. Chapter 4 will focus on step (iii), that is finding primary controlled variables where the selection of controlled outputs is done using methods related to self-optimizing control. Step (v) in the bottom-up analysis is investigated in Chapters 5 and 6.

3.3 Modes of operation

The performance objective to minimize the cost in Eq. 3.1 is typical in considering the operation of a whole plant, and to include the all aspects of the economic performance, additional terms and parameters would probably be included. But, the idea of optimal operation can also be applied on a single unit such as a distillation column. The operational objective of a distillation column is largely dependent on its role in the plant (process). The task of a column could be to remove small amounts of undesirable components from a feedstock, providing a rough separation of petrochemicals before further separation or to produce high purity products as the last major process unit in the plant. The definition of an objective function for optimal operation thus depends on the purpose of the unit.

Below we give four different examples of the operation of a Kaibel distillation column, depending on the task given to the column. The purpose of this is to illustrate the procedures of the plantwide control approach and further that the operational objective may have an influence on the controlled variables selected to achieve optimal operation.

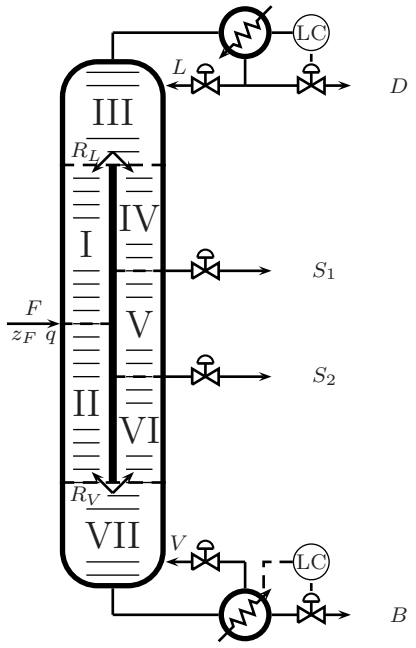

Figure 3.1: The Kaibel column with section numbering (I-VII) and input variables.

3.3.1 Column information and assumptions

The Kaibel column is modeled as a stage-by-stage column with equilibrium stages. The column has 12 stages in each of the two prefractionator sections (I-II) and 8 stages in the other five sections (see Figure 3.1 and refer to Appendix A for more information).

In the analysis below we assume that there are initially seven degrees of freedom for optimization including the feed rate, F. The other degrees of freedom are vapour boil up rate (V), liquid reflux rate (L), the two side-stream rates (S_1 and S_2), the liquid split ratio (R_L) and the vapour split ratio (R_V). The distillate rate (D) and the bottoms product rate (B) are in all cases assumed to be used for inventory control of the condenser and reboiler respectively (usually referred to as the LV-configuration for binary columns). In addition, the feed composition (z_F) is fixed as an equimolar mixture and the feed liquid fraction (q) is the same for all modes ($q = 0.9$).

3.3.2 Mode 1. Maximize purity

It is quite common, from an economical perspective if energy is relatively cheap, that it is optimal to maximize the purity of all the product streams from a distillation column, or equivalently to minimize the sum of its impurities:

$$J = \sum impurities = \sum P_i(1 - x_{i,P_i}) \tag{3.4}$$

where i denotes both the product number and the main component in this product. In the simplest case, we minimize the sum of impurities with no weighting included. The impurity sum cost in Eq. 3.4 can be derived from the general cost in Eq. 3.1 if we assume that the main component in all products are of equal value and there is no income from impurities, and in addition the energy costs are fixed.

We make the following additional assumptions:

Given feed, F. The feed to the column is assumed given by an upstream process or set at a constant rate. The feed rate will be included in the disturbance vector in the following analysis.

Given boil up, $V = V_{max}$. We assume that heat input to the column and hence boil up is set at a constant rate. This will be optimal if energy is relatively cheap as this will minimize the amount of impurities in the product streams.

For a case with four main components (A,B,C,D) and two side streams the cost function then becomes:

$$\begin{aligned} \min_{u_0} J &= D(1 - x_{A,D}) + S_1(1 - x_{B,S_1}) \\ &\quad + S_2(1 - x_{C,S_2}) + B(1 - x_{D,B}) \end{aligned} \tag{3.5}$$

Degrees of freedom - active constraints

In this mode, F and V are treated as active constraints and we are left with 5 unconstrained degrees of freedom for optimization: $\mathbf{u^T} = [L\ S_1\ S_2\ R_L\ R_V]$

3.3.3 Mode 2: Minimize energy usage

One of the great benefits of the Kaibel column is the potential for energy savings compared with separation in a series of columns, and will perhaps in the future be the principal reason for installing such a column. Thus, an operator having installed a Kaibel column may want to take full advantage

of the reduced energy cost of operation and for a given product specification, minimize energy input to the column.

In the following, we relate energy usage to the vapour boil up, V, and the optimization problem can be formulated as follows, again with the feed rate set:

$$\min_{\mathbf{u}} J = V \tag{3.6}$$

given feed, F.

where in the constraints $\mathbf{h}$ of Equation 3.3 are included the product specifications, which are here selected to be:

$$\begin{bmatrix} x_{A,D} \\ x_{B,S_1} \\ x_{C,S_2} \\ x_{D,B} \end{bmatrix} = \begin{bmatrix} 0.975 \\ 0.94 \\ 0.94 \\ 0.975 \end{bmatrix}$$

Note that product purities are specified by equality (=) constraints, whereas one generally requires "$\geq$" for product specifications.

Degrees of freedom - active constraints

Assuming the four product specifications are active, we need to use 4 inputs to control these active constraints. We are then left with 2 inputs for optimization (minimizing the energy usage in (3.6): $\mathbf{u^T} = [R_L \ R_V]$

Remark : We must also assume that we are directly producing the final products, and can not make them, for example, by overpurification and mixing with the feed. It seems that such an assumption would be unnecessary because overpurification normally costs energy. However, as shown by Alstad et al. [2] this is not always the case in a Petlyuk column because overpurification may be achieved "for free" because the column may be "unbalanced". Nevertheless, the possible energy savings by overpurifications are small, and are unlikely to be worth the complication of remixing to get the final products, so we here assume that all purity constraints are active.

3.3.4 Mode 3: Maximum profit with uneven pricing

In this scenario, energy is cheap (as in Mode 1), but two of the products are more valuable than the other two. An industrial example could be the separation of iso-pentane (A), n-pentane (B), iso-hexane (C) and n-hexane (D), where the iso-alkanes (A and C) are the more valuable as octane

boosters. In our case we use the components A,B,C,D and we set the product values according to table 3.1 (The components are modelled as Methanol, Ethanol,n-Propanol and n-Butanol). In the distillate and side-stream 2, the price is paid for the main component only (so the impurity have zero value), while in the first side-stream and bottoms product the price is the same for all components.

Table 3.1: Product values

Product stream	Value, w_i (\$/t)	Component
Distillate	200	A
Side-stream 1	150	Any (sold as fuel)
Side-stream 2	200	C
Bottoms	150	Any (sold as fuel)
Feed	150	

Again, we fix the vapour boil-up rate and the optimal operation problem can be stated as:

$$\min_{\mathbf{u_0}} J = -\Big(Dx_{A,D}w_D + S_1 w_{S_1} + S_2 x_{C,S_2} w_{S_2} + B w_B\Big) \tag{3.7}$$

subject to

given feed. F

given boil up, $V = V_{max}$.

Note that the flows in the objective function (3.7) are here given on a mass basis.

Degrees of freedom - active constraints

The degrees of freedom are here the same as in the maximum purity mode (section 3.3.2). We have two constrained degrees of freedom (F, V) and five unconstrained:
$\mathbf{u^T} = [L\ S_1\ S_2\ R_L\ R_V]$

3.3.5 Mode 4: Maximum throughput

In most cases, the prices are such that profit increases when the feed rate increases (although the profit pr. kg may drop because the efficiency drops). Thus, if feed is available and there is a market for the products, maximizing the throughput will lead to maximized profit. For a distillation column, this

can be translated into maximizing the feed flowrate, F. When maximizing throughput of a process, there will be one or more limiting factors (bottlenecks), typically depending on equipment size, utility loads etc. In our case we define a set of product specifications and assume that the vapour boil-up, V, will be the limiting bottleneck. Thus, $V = V_{max}$ and

$$\min_{\mathbf{u_0}} J = -F \tag{3.8}$$

subject to

given purity specifications, $x_i \geq x_{i,spec}$.

given boil up, $V = V_{max}$.

Degrees of freedom - active constraints

Assuming that the 4 product specifications are active, we are then left with two unconstrained degrees of freedom. For example R_V may be used in addition to F:
$\mathbf{u^T} = [F\ R_V]$.

3.3.6 Discussion

Table 3.2 summarizes the data for the four modes of which some will be further studied in the next chapters.

Mode 1. Apparently the separation is simplest in the bottom part of the column, because we note from Table 3.2, that the overall maximum purity is obtained when the bottom product is 99.5 % whereas the other products range in purity from 93.6 % (S_1) to 97.0 % (D).

Mode 2. While keeping the product specifications the energy consumption is reduced from $V = V_{max}$ to V_{min}=2.80.

Mode 3. The objective here is to maximize the production of component A (in product D) plus the production of component C (in product S_2). As expected the purities of these products are then relatively high (98.3 % and 97.4 %) compared to the other modes.

Mode 4. It is possible to increase the throughput by 7 % before reaching the constraint on boil up (V_{max}). Except for the boil up, V, not being a degree of freedom, and all flows being 7 % higher, this mode is identical with Mode 2.

In the following we consider mainly modes 1 and 2.

Table 3.2: Overview of operational modes. Number of unconstrained degrees of freedom in each mode and the corresponding nominal optimal input values. The values of the constrained variables are shown in bold.

	Mode 1	Mode 2	Mode 3	Mode 4
No. of unconstr. DOF's	5	2	5	2
Optimal inputs				
F	**1.0000**	**1.0000**	**1.0000**	1.0708
L	2.8492	2.6537	2.8594	2.8416
V	**3.0000**	2.8017	**3.0000**	**3.0000**
S_1	0.2494	0.2437	0.2681	0.2609
S_2	0.2497	0.2523	0.2396	0.2702
R_L	0.2572	0.2353	0.2642	0.2353
R_V	0.3770	0.3611	0.3850	0.3611
D	0.2508	0.2480	0.2406	0.2655
B	0.2501	0.2560	0.2518	0.2741
Nominal purities				
$x_{A,D}$	0.9703	**0.9750**	0.9830	**0.9750**
x_{B,S_1}	0.9361	**0.9400**	0.8946	**0.9400**
x_{C,S_2}	0.9589	**0.9400**	0.9737	**0.9400**
$x_{D,B}$	0.9949	**0.9750**	0.9900	**0.9750**

Chapter 4

Selection of measurements and controlled variables for optimal operation

4.1 Introduction

A typical control system is organized in a hierarchical structure, see Figure 4.1, divided into several layers that operate on different time-scales. The *control layer*, which is the subject of this thesis, is often divided into two sub-layers that are the *supervisory control* and *regulatory control* layers. In supervisory control the *primary controlled variables* deal with slow actions while the *secondary controlled variables* in the regulatory control level deal with stabilization and fast dynamics.

The subject of this chapter is how to select the primary controlled variables for the supervisory control level. Two methods related to *self-optimizing control* (see section 4.2.2 below) are applied to Kaibel column examples introduced in Chapter 3.

4.2 Selecting primary controlled outputs for the Kaibel column

While the regulatory control layer deals with stabilization of the plant, the supervisory (or advanced) control layer should make sure that the operational objectives of the plant are met. These objectives define *optimal operation* as was discussed in Chapter 3 for the Kaibel column. Thus, the primary controlled variables should be chosen based on the economic cost

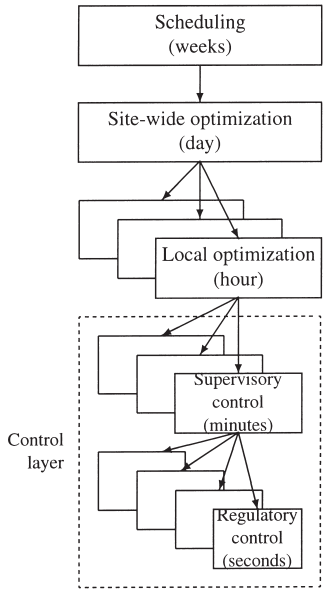

Figure 4.1: Typical control system hierarchy in a chemical plant [37]

function for the operational mode of the column.

Through the plantwide control approach referred to in the previous chapter and applying the steps of the *top-down analysis* outlined in Section 3.1.1, we now want to select the primary controlled variables for the Kaibel column.

4.2.1 Constrained and unconstrained degrees of freedom

To achieve optimal operation, the active constraints should be controlled at their constraint values. If, after controlling the active constraints, there are remaining unconstrained degrees of freedom, then we need to find a control policy for how they should be used.

With the active constraint loops closed (including control loops on top and bottom levels using D and B), the model is linearized around the nominal optimal point to yield

$$\Delta \mathbf{y}_0 = \mathbf{G}^{y_0} \Delta \mathbf{u} + \mathbf{G}_d^{y_0} \Delta \mathbf{d} \tag{4.1}$$

where $\mathbf{u}$ denotes the remaining unconstrained degrees of freedom, $\mathbf{y_0}$ the available measurements are the temperatures of each stage including the reboiler. The unconstrained degrees of freedom $\mathbf{u}$ vary depending on the

mode. The disturbances **d** generally include the feed conditions and the active constraints.

4.2.2 Self-optimizing control

Self-optimizing control is a term used to describe controlled variables that when controlled at constant setpoints indirectly keep the process near its optimal operating point. Skogestad [33] gives the following definition:

> *Self-optimizing control is when we can achieve an acceptable loss with constant setpoint values for the controlled variables without the need to re-optimize when disturbances occur.*

The loss is defined as the difference between the objective function value using the constant setpoint policy and the true optimal objective function value for a disturbance **d**:

$$L = J(\mathbf{u}, \mathbf{d}) - J_{opt}(\mathbf{d}) \tag{4.2}$$

4.2.3 Minimum singular value rule

In this work we make use of the Singular Value Rule of Halvorsen et al. [13]to find the best set of temperatures to control. The procedure is summarized here.

1. Using a linear model we scale the inputs $\mathbf{u_j}$ such that a unit deviation in each input has the same effect on the cost function J. $\mathbf{u_{scl,j}} = 1/\sqrt{[\mathbf{J_{uu}}]_{jj}}$.

2. For each candidate controlled variable, we obtain its optimal variation due to disturbances $\Delta\mathbf{y_{opt,i}}$. Assuming the setpoints are nominally optimal, $\Delta\mathbf{y_{opt,i}} = [\mathbf{G}\mathbf{J_{uu}}^{-1}\mathbf{J_{ud}} - \mathbf{G_d}]_i\mathbf{d}$.

3. For each candidate controlled variable, we obtain its expected implementation error n_i (sum of measurement error and control error).

4. Using the sum of the magnitudes of $\Delta\mathbf{y_{opt,i}}$ and n_i (often called "span"), we scale the candidate controlled variables. $\mathbf{c_{scl,i}} = |\Delta\mathbf{y_{opt,i}}| + |n_i|$.

5. We then compute the scaling matrices, $\mathbf{D_c} = diag\{\mathbf{c_{scl,i}}\}$, and $\mathbf{D_u} = diag\{\mathbf{u_{scl,j}}\}$ and obtain the scaled model $\mathbf{G'} = \mathbf{D_c}^{-1}\mathbf{G}\mathbf{D_u}$.

6. Finally, we select as candidates those sets of controlled variables that correspond to a large value of the minimum singular value $\underline{\sigma}(\mathbf{G'})$.

4.2.4 Exact local method

It had been shown by Alstad et al. [4] that the worst case loss for the expected disturbances and implementation error is

$$L_{wc} = \max_{\left\| \begin{matrix} \mathbf{d'} \\ \mathbf{n^{y'}} \end{matrix} \right\|_2 \leq 1} L = \frac{1}{2}\bar{\sigma}([\mathbf{M_d} \quad \mathbf{M_n}])^2 \tag{4.3}$$

4.2.5 Measurement combinations

We may also select combinations of measurements as controlled outputs to improve performance.

$$\mathbf{c} = \mathbf{H}\mathbf{y} \tag{4.4}$$

As shown by Alstad et al.[4] the optimal measurement combination can be solved explicitly for the exact local method:

$$\mathbf{H}^T = (\widetilde{\mathbf{F}}\widetilde{\mathbf{F}}^T)^{-1}\mathbf{G}^y(\mathbf{G}^{yT}(\widetilde{\mathbf{F}}\widetilde{\mathbf{F}}^T)^{-1}\mathbf{G}^y)^{-1}\mathbf{J}_{uu}^{1/2} \tag{4.5}$$

4.3 Results

The above methods for selecting controlled outputs have been applied to the Kaibel column. In Chapter 3 several modes of operation for the Kaibel column was introduced. Here, the first two modes are analyzed using different methods. First, the results for the mode where the objective is to maximize all of the product purities is presented. The minimum singular value rule is used to select single measurements. Next we show results for the mode where the goal is to minimize energy usage subject to purity constraints on the products. In this case, the exact local method and extended nullspace method is applied to find combinations of measurements to control.

4.3.1 Mode 1. Maximize purity

As shown in Chapter 3, we defined the objective function to be the sum of all impurity streams:

$$\begin{aligned} \min_{u_0} J &= D(1 - x_{A,D}) + S_1(1 - x_{B,S_1}) \\ &\quad + S_2(1 - x_{C,S_2}) + B(1 - x_{D,B}) \end{aligned} \tag{4.6}$$

and we defined five variables as unconstrained degrees of freedom for optimization:

$$\mathbf{u^T} = [L\ S_1\ S_2\ R_L\ R_V] \tag{4.7}$$

However, as the vapour split (R_V) is not (yet) an adjustable variable online, we chose to leave it out of the input set. Instead, the implementation of a fixed vapour split was treated as a disturbance in the analysis. After finding the optimal operating point (Table 3.2), the model was linearized (Eq. 4.1) and further optimizations were performed to determine the matrices $\mathbf{J}_{uu}$ and $\mathbf{J}_{ud}$ with the following inputs and disturbances:

$$\mathbf{u^T} = [L\ S_1\ S_2\ R_L] \tag{4.8}$$

$$\mathbf{d}^T = [V \quad R_V \quad F \quad z_A \quad z_B \quad z_C \quad q] \tag{4.9}$$

Using $\mathbf{J_{uu}}$ and $\mathbf{J_{ud}}$ the optimal variation in each temperature, $\Delta\mathbf{y}_{opt}$, was calculated with respect to the expected disturbances. The optimal variation in temperatures of the column is plotted in Figure 4.2. We note that the stages around the feed show most variation in temperature. This is to be expected with the feed disturbances and these sections can experience relatively large composition changes with all components present. The optimal variation has been used as a criterion [22] for selecting controlled variables, which generally favors stages near the column ends where composition (and temperature) changes tend to be small. Figure 4.2 confirms this as the temperature variation is smallest at the two ends and near the side-streams.

A measurement error of 0.5K was added to the optimal variation for each measurement, to obtain the span and the output scaling matrix $\mathbf{D_c}$ was computed.

The input scaling, $\mathbf{D_u}$, was obtained from $\mathbf{J_{uu}}$, and the scaled gain matrix, $\mathbf{G_s}$ was computed from Eq. 4.10:

$$\mathbf{G_s} = \mathbf{D}_c^{-1}\mathbf{G}\mathbf{D}_u \tag{4.10}$$

The scaled gains from the individual inputs can be seen in Figures 4.3 a) and b).

Using the branch and bound algorithm by Cao [6] to find the maximum minimum singular value we obtained the best set of four temperatures to keep constant:

$$\mathbf{c}_y^T = [T_{10} \quad T_{35} \quad T_{45} \quad T_{57}] \tag{4.11}$$

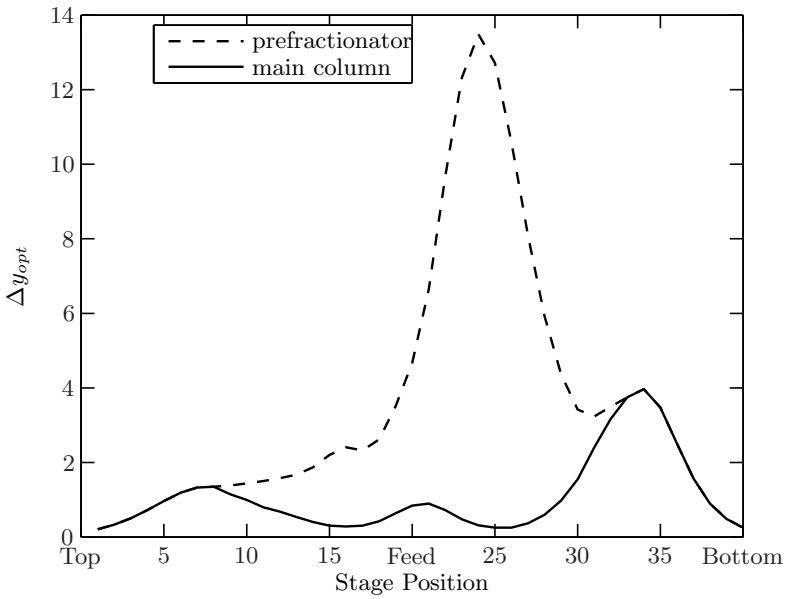

Figure 4.2: Optimal variation in outputs.

The corresponding minimum singular value equates to:

$$\underline{\sigma}(\mathbf{G}_s) = 15.27 \tag{4.12}$$

The temperature locations can be seen in Figure 4.4. We observe that each of the four "main" sections of the column is represented by one temperature. We have temperature T_{10} in the prefractionator just above the feed. The three near- or ideally binary sections bounded by the product outlets have from the top the temperatures T_{35}, T_{45} and T_{57} respectively. All temperatures can be said to be near the middle of the sections. These locations are exactly where we would expect to place measurements were we to fix variables for regulatory control (i.e. stabilizing the column dynamically, which is the topic of chapters 5 and 6). Here, these temperatures are the result of the minimum singular value rule which looks for temperatures that are economically optimal (steady-state) to keep constant. So at this point in the analysis, the set looks like a promising candidate for both (economically-) optimal and stabilizing control.

The minimum singular value method combined with an effective branch and bound algorithm can easily generate a ranking of all the possible combinations. The ten best sets for this mode are listed in Table 4.1, ranked by minimum singular value. There are no great differences in the location

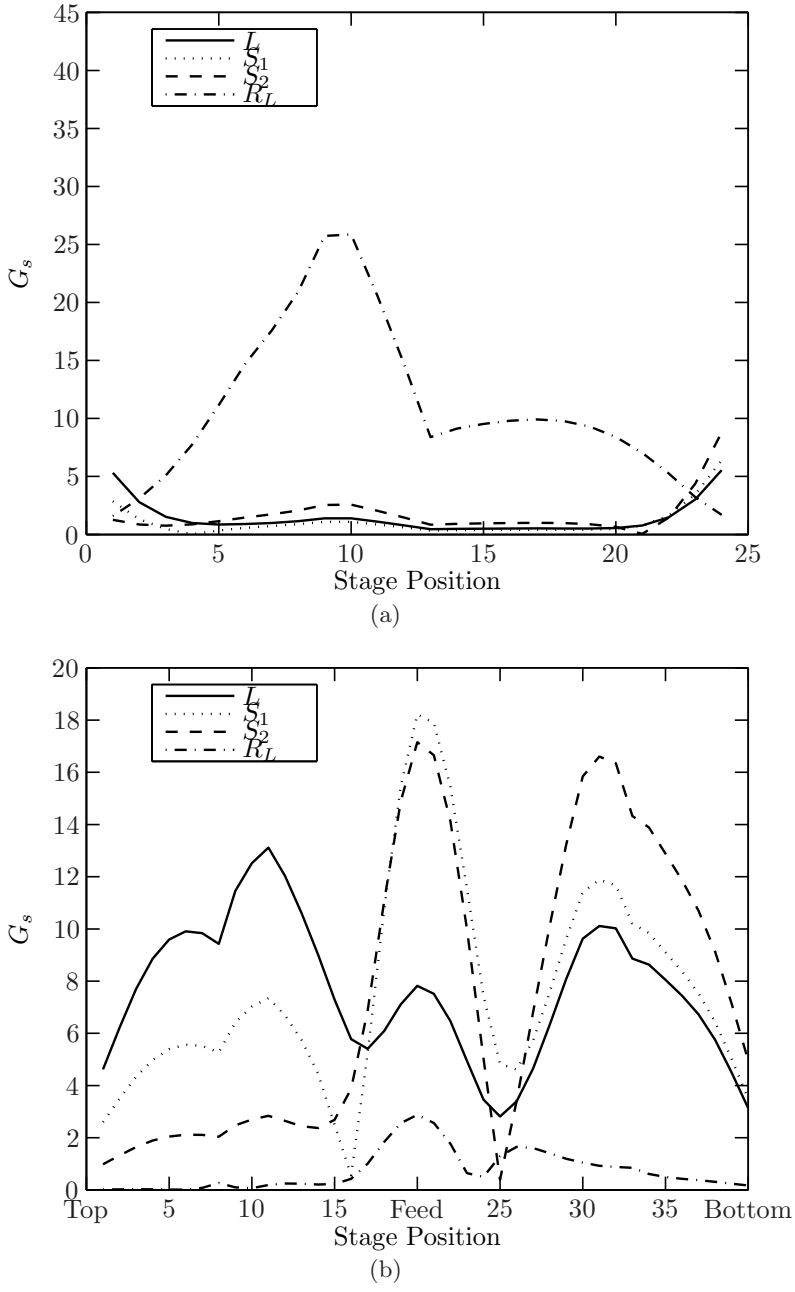

Figure 4.3: Scaled gains. (a) Prefractionator. (b) Main column.

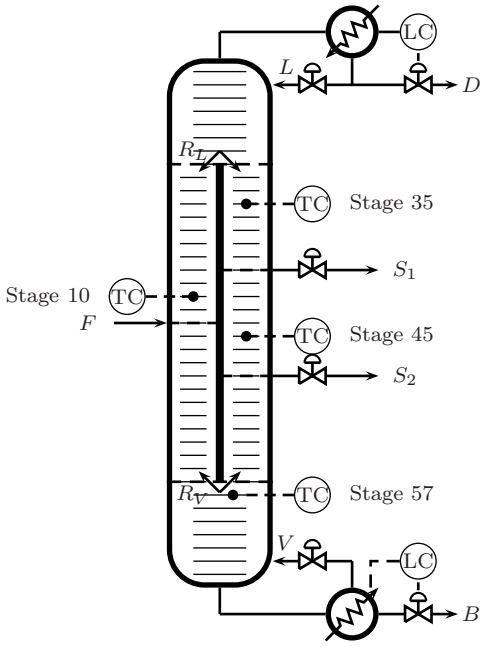

Figure 4.4: Temperature locations selected using the minimum singular value rule.

Table 4.1: Sets of controlled temperatures

Rank	Stage no.				$\underline{\sigma}(\mathbf{G_s})$	Loss
1	10	35	45	57	15.2671	0.0021
2	9	35	45	57	15.2669	0.0021
3	10	35	45	58	15.2668	0.0021
4	10	35	45	56	15.2668	0.0021
5	9	35	45	58	15.2667	0.0021
6	9	35	45	56	15.2667	0.0021
7	10	35	46	57	15.2666	0.0021
8	10	35	46	58	15.2664	0.0021
9	9	35	46	57	15.2664	0.0021
10	9	35	46	58	15.2663	0.0021

of the temperature measurements chosen or the resulting singular value. Stage 10 is sometimes exchanged with stage 9 above while the temperature at stage 35 is chosen in all ten sets. In the section between the side draws, temperature T_{45} is chosen in the first six sets while the last temperature varies between stages 56 and 58. From these results there should be practically no difference of choosing any of these temperature measurements for a constant setpoint policy.

Remark: In this example, each of the temperature locations found were as mentioned within a separate section of the column. This is by no means guaranteed by the minimum singular value method, as the method does not discriminate between column sections nor take into account pairing of the measurements and inputs.

Pairing

The temperature measurements in set $\mathbf{c}_y$ are easy to pair with the available manipulated variables. Simply by looking at Figure 4.4 we see that the liquid split, R_L, can be paired with T_{10}, the reflux, L, should be paired with T_{35}, side-stream 1, S_1, with T_{45} and that side-stream 2, S_2 should be paired with temperature T_{57}. The control configuration may however not always be obvious and we can make use of the steady-state RGA (Relative Gain Array, [37]) to discriminate between alternative pairings. The RGA-number is a measure of the diagonal dominance (of the matrix) and we can use it to avoid pairings with close interactions in a decentralized control structure. We should, preferably pair on RGA-elements close to one and avoid pairing on negative RGA-elements. For the set $\mathbf{c}_y$ the steady-state RGA is:

$$RGA(0) = \left[\begin{array}{c|cccc} & L & S_1 & S_2 & R_L \\ \hline T_{10} & -0.0036 & -0.0135 & 0.0119 & 1.0052 \\ T_{35} & 1.0265 & -0.0210 & -0.0000 & -0.0054 \\ T_{45} & -0.0234 & 1.0644 & -0.0404 & -0.0006 \\ T_{57} & 0.0005 & -0.0298 & 1.0284 & 0.0008 \end{array}\right] \tag{4.13}$$

We see that the RGA confirms our intuitive pairing. Now, the resulting control configuration for the Kaibel column can bee seen in Figure 4.5.

Loss evaluation

The control configuration in Figure 4.5 was developed by applying a decentralized control structure to the four individual measurements (temperatures) resulting from the minimum singular value method. The intention

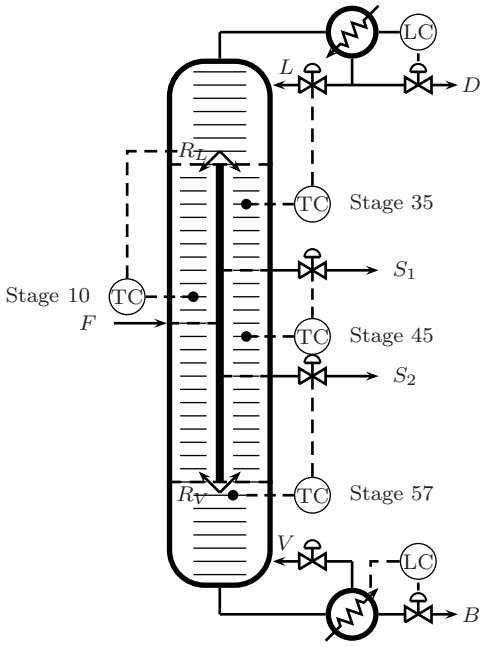

Figure 4.5: Final control configuration for Mode 1.

being, that keeping these four temperatures constant at their nominal (optimal) setpoints will lead to small economic loss in spite of disturbances. To verify that this policy works we need to test it on the full non-linear model of the Kaibel column. Table 4.2 shows the loss associated with various disturbances for the column. The disturbances defined are in the vapour boil-up (V), the vapour split (R_V), and in the feed conditions where feed rate (F), feed heat (q) and the feed compositions (z_i) are all varied. Note that a positive change in component A, B or C is accompanied by a corresponding reduction in component D. The table shows the product purities resulting after the imposed disturbances as well as the value of the objective function, J. Included are also the truly optimal values of the objective function ($J_{opt,d}$) that are calculated by reoptimizing for the given disturbance (the vapour-split, R_V, has been kept constant in all cases). The final table column shows the percentage loss in the objective function compared to the truly optimal value. As we can see, this configuration performs really well. The losses imposed by keeping the four temperatures constant are all small with the worst recorded loss at 0.8% for the change in z_C. Notably, for the disturbances in the vapour split (R_V) and feed heat (q) the control system moves the column towards its optimal operating point.

Table 4.2: Effect of disturbances on product purities and objective function.

Disturbance	$x_{A,D}$	x_{B,S_1}	x_{C,S_2}	$x_{D,B}$	J	$J_{opt,d}$	Loss (%)
Nominal	0.9703	0.9361	0.9589	0.9949	0.0349	0.0349	0.000
ΔV + 10%	0.9731	0.9369	0.9596	0.9952	0.0338	0.0337	0.088
ΔR_V = + 10 %	0.9692	0.9364	0.9593	0.9949	0.0350	0.0350	0.013
ΔF = + 10 %	0.9672	0.9348	0.9565	0.9947	0.0403	0.0403	0.174
Δz_A = + 20 %	0.9663	0.9351	0.9590	0.9956	0.0374	0.0373	0.312
Δz_B = + 20 %	0.9676	0.9340	0.9577	0.9956	0.0394	0.0393	0.414
Δz_C = + 20 %	0.9705	0.9361	0.9572	0.9956	0.0370	0.0367	0.800
Δq = + 10 %	0.9699	0.9354	0.9584	0.9950	0.0353	0.0353	0.002

Summary

In this section we have looked for primary controlled variables for a Kaibel column where the operational objective is to maximize the purity of all four product streams (Mode 1). We identified four available degrees of freedom (manipulated variables) and decided to look for single temperature measurements as candidate controlled variables. Using a linearized model of the Kaibel column we based the selection of the temperature locations on the minimum singular value method. The temperatures selected were then paired with the available inputs (as seen in Figure 4.5) in a decentralized control configuration. Finally, the configuration was tested with simulations on the full non-linear model. The results (Table 4.2) show that the controlled variables have excellent self-optimizing control properties with small loss in the objective function value after disturbances.

4.3.2 Mode 2: Minimize energy

In the mode where we want to minimize the energy usage subject to quality constraints on the product purities we found that we were left with two degrees of freedom after controlling the active constraints. For control of active constraints, we may use reflux, L, for controlling the distillate purity, $x_{A,D}$, and the vapour rate, V, to control the bottoms purity, $x_{D,B}$. The side-stream purities, x_{B,S_1} and x_{C,S_2} may be paired with the side-stream rates S_1 and S_2 respectively. The remaining unconstrained degrees of freedom are then the split ratios R_L and R_V, and the objective is to find some combinations of variables (measurements) to control at constant setpoints that will keep the process close to optimal operation (with acceptable loss) despite disturbances and implementation error. The following procedure was used:

Step 1. Optimization

The optimization problem in equation 3.6 was solved to find the optimal nominal operating point. The resulting value of the objective function was $V = 2.8017$, and the optimal input values can be seen in Table 3.2.

Step 2. Identification of variables

The linearized model of Equation 4.1 for this case have, as mentioned, the split ratios for inputs, while in the disturbance vector we have included the feed rate (F), feed compositions (z_i), the feed enthalpy (q) as well as the product specifications (active constraints).

$$\mathbf{u} = \begin{bmatrix} R_L \\ R_V \end{bmatrix} \tag{4.14}$$

$$\mathbf{d}^T = \begin{bmatrix} F & z_A & z_B & z_C & q & n_{x_{A,D}} & n_{x_{B,S_1}} & n_{x_{C,S_2}} & n_{x_{D,B}} \end{bmatrix} \tag{4.15}$$

$$\mathbf{y}_0 = \begin{bmatrix} T_1 \\ T_2 \\ \vdots \\ T_{65} \end{bmatrix} \tag{4.16}$$

Step 3. Scaling of variables

Each measurement is scaled with its corresponding implementation error ($|n_{y_{0,i}}|$). In this case all the measurements are temperatures, and they are given the same error of 0.5 K.

Each disturbance is scaled with its corresponding expected disturbance ($|\Delta d_{k,max}|$). In this example the feed rate and feed enthapy are given a 10% maximum expected disturbance and 5 % for the feed compositions.

The inputs are scaled using the Hessian matrix $\mathbf{J_{uu}}$.

We then have the following scaling matrices

$$\mathbf{W_n^{y_0}} = \begin{bmatrix} |n_{y_{0,1}}| & & \\ & \ddots & \\ & & |n_{y_{0,n_{y_0}}}| \end{bmatrix} \mathbf{W_d} = \begin{bmatrix} |\Delta d_{1,max}| & & \\ & \ddots & \\ & & |\Delta d_{n_d,max}| \end{bmatrix} \tag{4.17}$$

Step 4. Selection of measurements

For this mode, the objective was to test out the possibility of controlling measurement combinations, rather than just individual measurements as for mode 1. This obviously gives a smaller loss, and is more complicated. However, the use of both R_L and R_V for optimizing control is in itself already a very complex operational policy by industrial standards, so using measurement combinations is from this point of view not a significant addition in complexity. Originally, when this work started, the aim was to use the "nullspace" method, which gives zero loss when there is no measurement noise, and which requires a minimum of $n_y = n_u + n_d = 2 + 9 = 11$. We select to use temperature measurements only. However, with 65 possible measurements there are extremely many possible combinations, and to select a set of 11 measurements we decided to maximize the minimum singular value of the scaled augmented process model $\tilde{\mathbf{G}}^{y_0}$.

A branch and bound search give the following measurements*:

$$\begin{aligned} \mathbf{y^T} = \quad & [T_7 \quad T_{12} \quad T_{18} \quad T_{21} \quad T_{24} \\ & T_{28} \quad T_{36} \quad T_{37} \quad T_{44} \quad T_{55} \quad T_{57}] \end{aligned} \tag{4.18}$$

The location of the measurements in the column can be seen in Figure 4.6.

*This is a very demanding computation as there are 8.95×10^{12} possible combinations

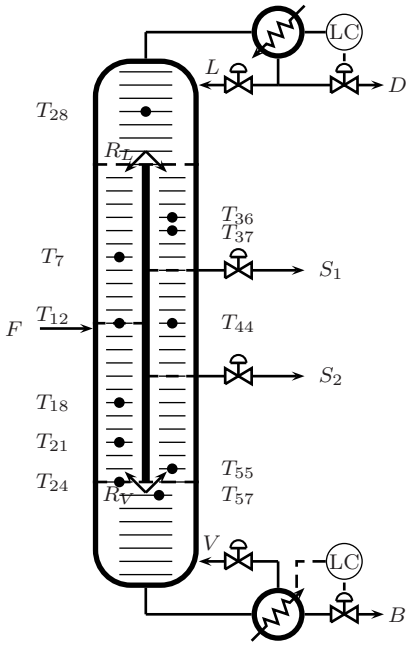

Figure 4.6: Temperature locations selected.

Step 5. Exact local method

As mentioned, it was originally planned to use the nullspace method. However, the *exact local method* can also include measurement noise in a rigorous fashion, so it was decided to use this method instead. For this method, we can actually use fewer than 11 measurements, but we nevertheless decided to keep the same 11 temperatures.

Using the explicit expression for the optimal $\mathbf{H}$ for combined disturbances and measurement errors we find the linear combination of the measurements to form the self-optimizing controlled variables, $c_{soc,1}$ and $c_{soc,2}$:

$$\begin{aligned} c_{soc,1} &= -0.23T_7 - 0.68T_{12} + T_{18} - 0.30T_{21} + 0.31T_{24} - 0.43T_{28} \\ &\quad -0.45T_{36} - 0.21T_{37} + 0.09T_{44} + 0.56T_{55} - 0.01T_{57} \end{aligned} \tag{4.19}$$

$$\begin{aligned} c_{soc,2} &= 0.19T_7 + 0.53T_{12} - 0.79T_{18} + 0.23T_{21} - 0.25T_{24} + 0.34T_{28} \\ &\quad +0.36T_{36} + 0.17T_{37} - 0.07T_{44} - 0.44T_{55} + 0.01T_{57} \end{aligned} \tag{4.20}$$

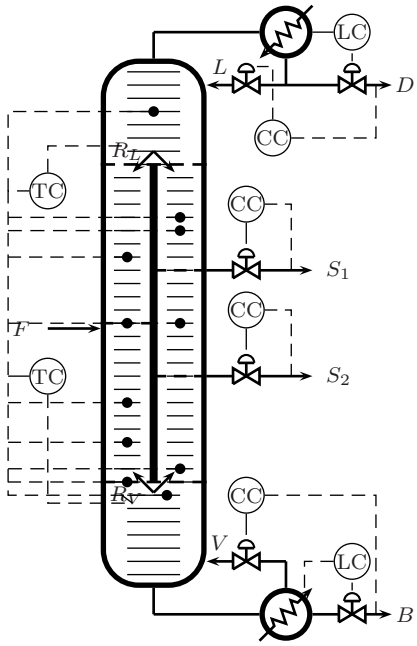

Figure 4.7: Final control configuration for Mode 2.

Loss evaluations

Keeping $c_{soc,1}$ and $c_{soc,2}$ constant the worst case loss ($L_{wc} = \frac{1}{2}(\overline{\sigma}[\mathbf{M}])^2$) comes out as 0.0068 using the linear analysis. This can be compared with the loss when we include all available measurements, which is $L_{wc}^{all} = 1.9 \times 10^{-5}$.

To evaluate how the measurement combinations perform as controlled variables we test the control configuration (Figure 4.7) on the full nonlinear model. The percentage loss in the objective function for a set of feed disturbances is shown in Table 4.3. The loss is again in comparison to the optimal value of the objective function for the given disturbance. Just as we saw for Mode 1, the self-optimizing control variables are able to effectively keep the system near the true optimal point when disturbances enter.

Summary

In this section the basis has been a Kaibel column with the operational objective of minimizing the energy usage while keeping the product purities at specified values (Mode 2). We had shown (Chapter 3) through the plantwide control approach that we had two steady-state degrees of freedom available for optimizing control. We decided to look for combinations of measure-

Table 4.3: Disturbance loss

disturbance	magnitude	%-loss
ΔF	$+10\%$	0.0
ΔF	-10%	0.0
$\Delta z_{A,F}$	$+5\%$	0.0086
$\Delta z_{A,F}$	-5%	0.0107
$\Delta z_{B,F}$	$+5\%$	0.0058
$\Delta z_{B,F}$	-5%	0.0065
$\Delta z_{C,F}$	$+5\%$	0.0079
$\Delta z_{C,F}$	-5%	0.0028
Δq	$+10\%$	0.0254
Δq	-10%	0.0218

ments to form self-optimizing controlled variables that could be paired with the available degrees of freedom. Using the exact local method of Halvorsen and Alstad on a linearized model we found a set of temperature measurements that were linearly combined to form the self-optimizing controlled variables. Using the full model of the Kaibel column for validation, we have shown that the resulting control configuration provides excellent tracking of the true optimal points when the system is exposed to disturbances.

4.4 Conclusions

In this chapter, two examples of selecting controlled variables for optimal operation of a Kaibel column have presented. The two examples have different operational objectives (Mode 1 and Mode 2), as defined in Chapter 3. In the first example the selection of controlled variables were based on the minimum singular value method, and single temperature measurements were chosen and paired with the available inputs. The second example, concerning Mode 2, which involves minimizing energy input to the column, several measurements were combined to form new self-optimizing variables. The resulting control configurations both show excellent self-optimizing properties that give small loss from the true optimal using constant setpoints.

Chapter 5

Regulatory layer of Kaibel and Petlyuk columns

5.1 Introduction

This chapter introduces some more practical aspects of how to operate a dividing wall column, and in particular how to design the regulatory control layer. While in the previous chapter we defined the steady-state optimal operation, we will here focus on how to operate the column in practice, where the goal is to achieve acceptable operation using simple control policies.

In particular, we will investigate the importance of properly adjusting the liquid split ratio, R_L, which determines the relative amount of reflux to the two sides of the dividing wall.

Furthermore, we would like to compare the same analysis on both the Kaibel column and on a Petlyuk column. Are there any inherent differences in the operation of these two types of dividing wall column?

The example used is taken from Section 3.3.2 where the overall objective (Equation 5.1) is to minimize the sum of the impurity flows of all product streams (for a Kaibel column).

$$\begin{aligned} J &= D(1 - x_{A,D}) + S_1(1 - x_{B,S_1}) \\ &\quad + S_2(1 - x_{C,S_2}) + B(1 - x_{D,B}) \end{aligned} \tag{5.1}$$

This cost objective of minimizing the "impurity sum" is a reasonable regulatory control objective because it avoids that we get drift in the column with breakthrough of undesirable components. Note that we want the regulatory layer to be independent of changes in the primary control objectives, for example, changes in product composition specifications, which may depend on price changes and disturbances.

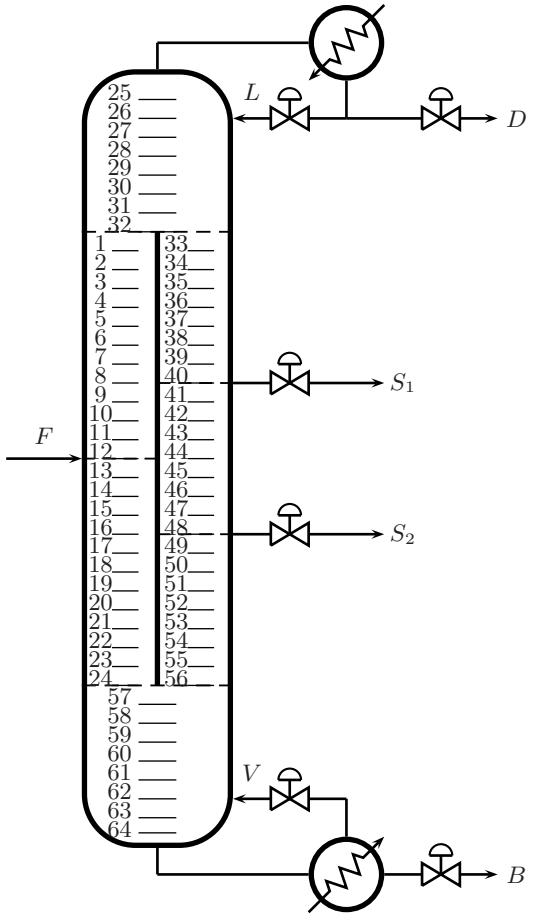

Figure 5.1: Kaibel dividing wall column. Stage numbering

5.1.1 Loss definition

Throughout this chapter we compare the resulting objective function value (impurity flows) after changes in the inputs and disturbances (J_d) relative to the truly optimal J for the given disturbance, $J_{opt,d}$ (re-optimized with respect to L, S_1, S_2 and R_L):

$$Loss = \frac{J_d - J_{opt,d}}{J_{opt,d}} \tag{5.2}$$

5.2 Kaibel Column

We start by analyzing the Kaibel dividing wall column (Figure 5.1). We assume a fixed feed rate (F), fixed vapour boil up rate ($V = V_{max}$) and fixed vapour split ratio (R_V). Assuming that the distillate (D) and bottoms (B) flows are used for level control, the remaining degrees of freedom for control are then the reflux (L), the side stream flows (S_1 and S_2) and the liquid split ratio (R_L).

These remaining four degrees of freedom are sometimes held constant, but preferably they should be adjusted during operation, for example, by keeping selected temperatures constant. This is needed in order to "stabilize" the composition profile in the column. In order to avoid breakthrough of impurities in the products, which would completely change the process model (nonlinear effect), it is important that these loops are quite fast, thus also dynamic effects need to be considered. Three cases are studied in this chapter.

1. One temperature control loop: Reflux, L, is used for temperature control (also used in the other cases).

2. Three temperature control loops: Adding temperature loops for the two side streams (S_1 and S_2).

3. Four temperature control loops: Adding a temperature loop by using the liquid split, R_L.

The three different control configurations are indicated in Figure 5.2, where the locations of the temperature measurements are also indicated. The locations were chosen without a detailed analysis, but were based on dynamic consideration and common recommendations as for example from Skogestad [36] and Luyben [21].

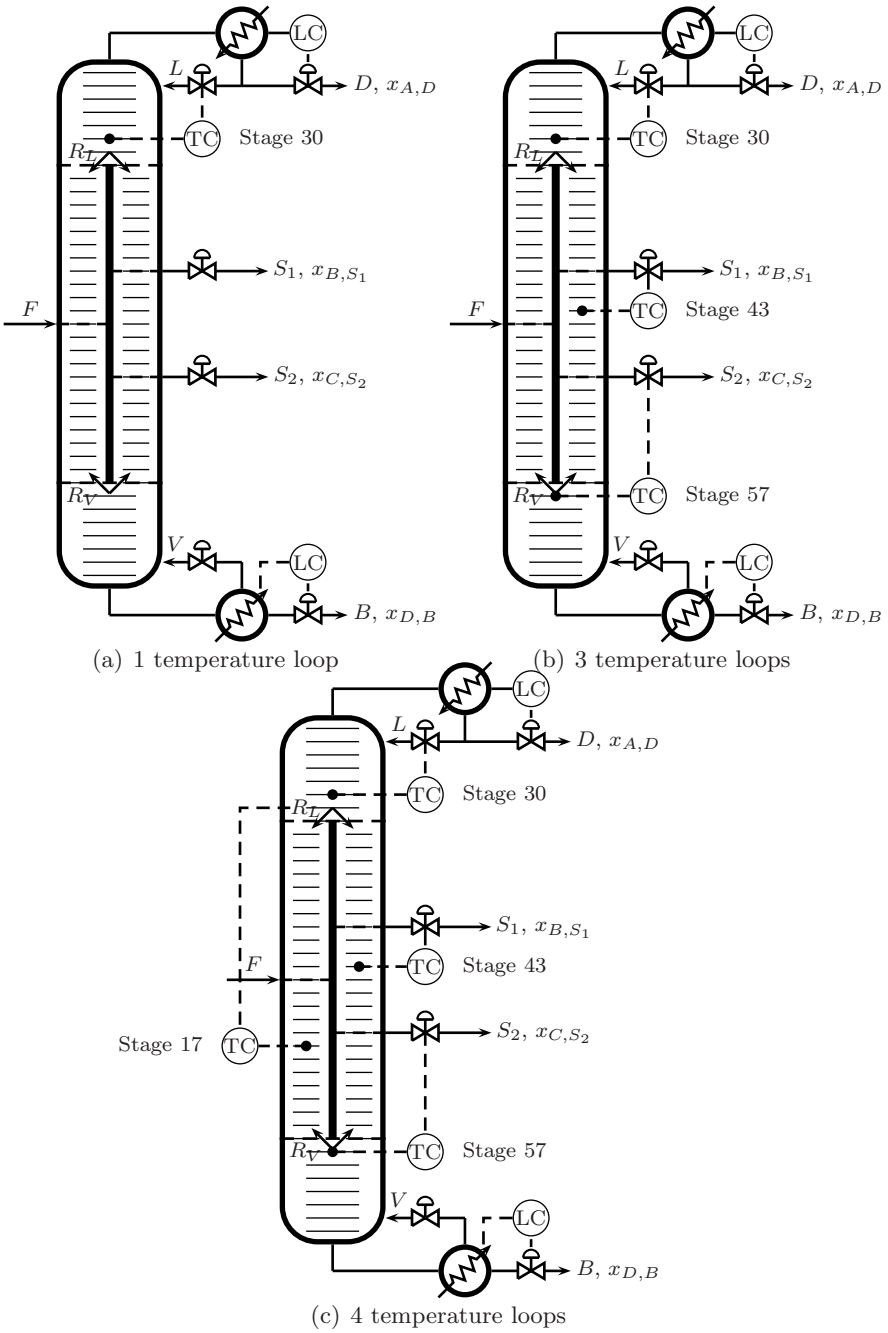

Figure 5.2: Kaibel column control configurations (In all cases F, V and R_V are fixed)

5.2.1 Effect of liquid split ratio

The nominal operating point for the Kaibel column is taken from Chapter 3. We first investigate how the column behaves for the two cases when the liquid split ratio is kept constant and not used for control. Starting from the nominal point we have the first case where only one temperature loop is closed using the reflux, L, as input (Figure 5.2a). The second case is where we have three temperature loops closed, using S_1 and S_2 in addition to L (Figure 5.2b). The setpoints for the temperature controllers are kept at their nominal values, while we vary the liquid split ratio R_L away from its optimal value.

We set $R_L = 0.50R_{L,opt}$ and $R_L = 0.75R_{L,opt}$, which signifies that more (too much) reflux is directed to the main column. Also, we increase R_L by 25 and 50%, which means that more reflux is directed to the prefractionator as compared to the optimal value.

Input values, resulting product purities and objective function value for the case with one temperature loop are given in Table 5.1, while Table 5.2 shows the values for the case with three temperature loops closed.

From the tables we see that changing the liquid split away from its optimal setting has a detrimental effect on the side stream purities. The configuration with three temperature loops performs slightly better than the one-loop configuration, but the differences are relatively small. For the largest positive change in R_L, the three-loop configuration is actually the worst. This is because the controller on side-stream 2 enforces a large flow on the stream with most impurities.

Figure 5.3 shows the temperature profiles in the column for the case with 3 temperature loops. The first (a) is the nominal (optimal) operating point, while the second (b) and third (c) show the profiles when the liquid split is set too low ($0.50R_{L,opt}$) and too high ($1.50R_{L,opt}$) respectively. The three controlled temperatures are all in the main column (as indicated in the figure), so that when more of the reflux is directed to the main column (b), the prefractionator temperature profile is shifted upwards, while the main column profile has less shift. Conversely, when too much reflux is sent to the prefractionator (c), the section is cooled and the profile is "lowered".

The corresponding composition profiles of the prefractionator and main column are shown in Figure 5.4. The effect of an incorrectly set liquid split ratio is readily observed here. When R_L is too low, we can observe a breakthrough of component C in from the top of the prefractionator into the main column (Fig 5.4c). This leads in turn to large impurity in the first side-stream (Fig. 5.4d). Figure 5.4 e) and f) show the composition profiles

Table 5.1: Kaibel column with one temperature loop closed: Effect of changes in R_L

	$\Delta R_{L,-50}$	$\Delta R_{L,-25}$	Nominal	$\Delta R_{L,+25}$	$\Delta R_{L,+50}$
R_L	**0.1286**	**0.1929**	**0.2572**	**0.3215**	**0.3858**
F	1.0000	1.0000	1.0000	1.0000	1.0000
$z_{i,F}$	0.2500	0.2500	0.2500	0.2500	0.2500
V	3.0000	3.0000	3.0000	3.0000	3.0000
R_V	0.3770	0.3770	0.3770	0.3770	0.3770
L	2.8547	2.8525	2.8492	2.8457	2.8502
$S1$	0.2494	0.2494	0.2494	0.2494	0.2494
$S2$	0.2497	0.2497	0.2497	0.2497	0.2497
D	0.2453	0.2475	0.2508	0.2543	0.2498
B	0.2556	0.2534	0.2501	0.2466	0.2511
$x_{A,D}$	0.9759	0.9733	0.9703	0.9701	0.9704
x_{B,S_1}	0.7166	0.8223	0.9361	0.8788	0.8055
x_{C,S_2}	0.7163	0.8455	0.9589	0.8907	0.8208
$x_{D,B}$	0.9406	0.9855	0.9949	0.9977	0.9918
J	0.1626	0.0932	0.0349	0.0657	0.1027

Table 5.2: Kaibel column with 3 temperature loops closed: Effect of changes in R_L

	$\Delta R_{L,-50}$	$\Delta R_{L,-25}$	Nominal	$\Delta R_{L,+25}$	$\Delta R_{L,+50}$
R_L	**0.1286**	**0.1929**	**0.2572**	**0.3215**	**0.3858**
F	1.0000	1.0000	1.0000	1.0000	1.0000
$z_{i,F}$	0.2500	0.2500	0.2500	0.2500	0.2500
V	3.0000	3.0000	3.0000	3.0000	3.0000
R_V	0.3770	0.3770	0.3770	0.3770	0.3770
L	2.8559	2.8533	2.8492	2.8455	2.8499
$S1$	0.2880	0.2812	0.2494	0.2234	0.1996
$S2$	0.2268	0.2213	0.2497	0.2741	0.3221
D	0.2441	0.2467	0.2508	0.2545	0.2501
B	0.2411	0.2508	0.2501	0.2480	0.2282
$x_{A,D}$	0.9760	0.9734	0.9703	0.9701	0.9703
x_{B,S_1}	0.7141	0.8109	0.9361	0.9388	0.9105
x_{C,S_2}	0.8071	0.9283	0.9589	0.8701	0.7339
$x_{D,B}$	0.9950	0.9949	0.9949	0.9971	0.9985
J	0.1332	0.0769	0.0349	0.0576	0.1113

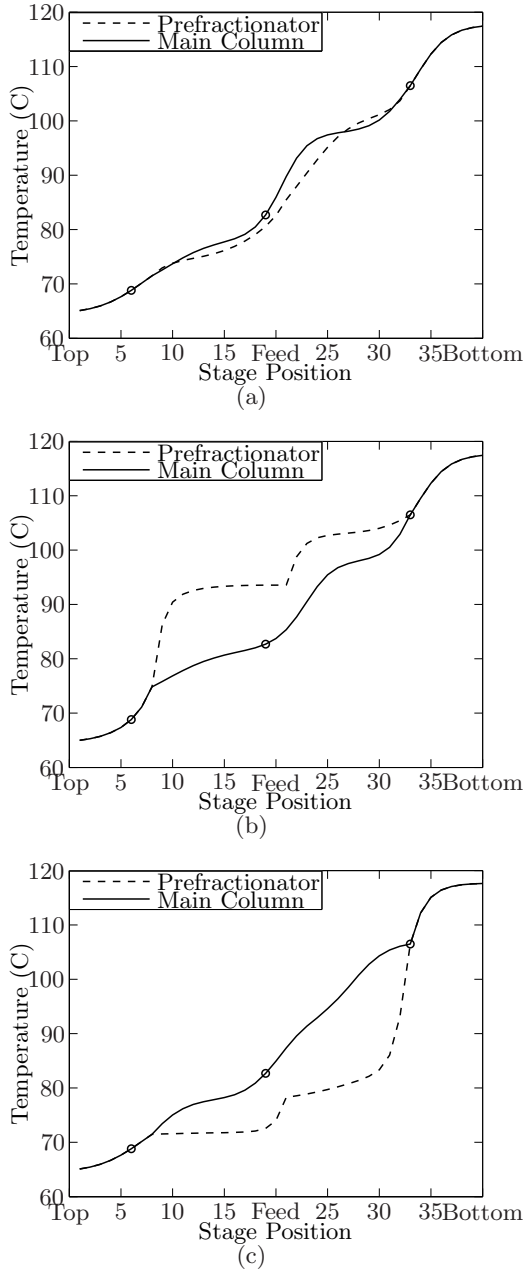

Figure 5.3: Kaibel column with 3 temperature loops closed: Column temperature profiles. (a) Nominal profile, (b) $R_L = 0.50R_{L,opt}$, (c) $R_L = 1.50R_{L,opt}$. Controlled temperatures are circled.

when R_L is set too high. Here we get breakthrough of component B from the bottom of the prefractionator into the main column. This prevents us from reaching high purity in the second side-stream.

In both the cases where the liquid split ratio is implemented incorrectly we observe large reductions in the side-stream product purities (Table 5.1 and Table 5.2). Clearly, it is important to achieve the right split of the reflux for the successful operation of the Kaibel column.

Before we look into how to adjust the liquid split ratio, we will see how the single-loop and 3-loop configurations perform under some different disturbances.

5.2.2 Disturbance rejection

The two control configurations (1-loop and 3-loop) are subjected to disturbances in feed rate (F), feed composition (z_F) and vapour split (R_V). The feed is increased by 10 %. The disturbance in feed composition is a 20 % increase in $z_{B,F}$ with corresponding reduction in $z_{D,F}$. For the vapour split, both a 10 % and a 50 % increase is simulated. To compare the results of the simulations, we have reoptimized the solution with respect to L, S_1, S_2 and R_L for each disturbance with R_V fixed. The optimal values can be seen in Table 5.3.

Table 5.3: Kaibel column: Optimal operating point for disturbances. R_V is fixed

	Nominal	ΔF_{+10}	$\Delta z_{B,F,+20}$	$\Delta R_{V,+10}$	$\Delta R_{V,+50}$
F	1.0000	1.1000	1.0000	1.0000	1.0000
$z_{i,F}$	0.2500	0.2500	0.3000	0.2500	0.2500
V	3.0000	3.0000	3.0000	3.0000	3.0000
R_L	0.2572	0.2443	0.2386	0.2967	0.4552
R_V	0.3770	0.3770	0.3770	0.4147	0.5655
L	2.8492	2.8340	2.8491	2.8491	2.8486
S_1	0.2494	0.2745	0.3004	0.2493	0.2484
S_2	0.2497	0.2745	0.2489	0.2498	0.2506
D	0.2508	0.2760	0.2509	0.2509	0.2514
B	0.2501	0.2750	0.1997	0.2500	0.2496
$x_{A,D}$	0.9703	0.9680	0.9645	0.9692	0.9630
x_{B,S_1}	0.9361	0.9329	0.9369	0.9364	0.9352
x_{C,S_2}	0.9589	0.9579	0.9567	0.9593	0.9590
$x_{D,B}$	0.9949	0.9946	0.9955	0.9949	0.9943
$J_{opt,d}$	0.0349	0.0403	0.0395	0.0350	0.0371

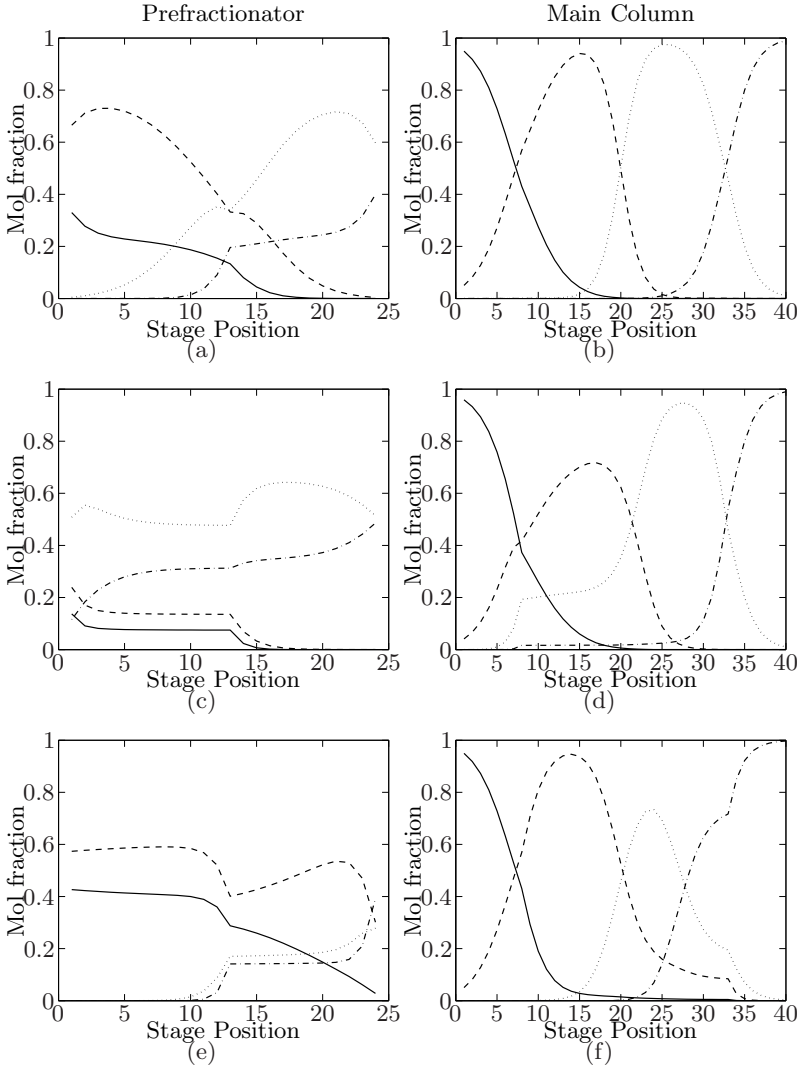

Figure 5.4: Kaibel column with 3 temperature loops closed: Composition profiles of prefractionator and main column. (a) and (b) nominal operating point, (c) and (d) R_L is too low, (e) and (f) R_L is too high. (—— component A, − − − component B, · · · component C, − · − component D)

Table 5.4: Kaibel column with 1 temperature loop closed: Effect of disturbances

	Nominal	ΔF_{+10}	$\Delta z_{B,F,+20}$	$\Delta R_{V,+10}$	$\Delta R_{V,+50}$
F	1.0000	1.1000	1.0000	1.0000	1.0000
$z_{B,F}$	0.2500	0.2500	0.3000	0.2500	0.2500
V	3.0000	3.0000	3.0000	3.0000	3.0000
R_L	0.2572	0.2572	0.2572	0.2572	0.2572
R_V	0.3770	0.3770	0.3770	0.4147	0.5655
L	2.8492	2.8330	2.8493	2.8520	2.8764
$S1$	0.2494	0.2494	0.2494	0.2494	0.2494
$S2$	0.2497	0.2497	0.2497	0.2497	0.2497
D	0.2508	0.2770	0.2507	0.2480	0.2236
B	0.2501	0.3239	0.2502	0.2529	0.2773
$x_{A,D}$	0.9703	0.9692	0.9703	0.9723	0.9813
x_{B,S_1}	0.9361	0.9586	0.9658	0.8642	0.4993
x_{C,S_2}	0.9589	0.8896	0.7925	0.8883	0.4963
$x_{D,B}$	0.9949	0.8485	0.7989	0.9875	0.8820
J	0.0349	0.0955	0.1181	0.0718	0.2876
Loss (%)	-	137	199	105	675

Tables 5.4 and 5.5 show the relevant inputs, resulting purities and objective function values after the disturbances for the two configurations. Here, the three-loop configuration is clearly better than the case with only one temperature loop as can be expected. However, the large change in vapour split (R_V) cannot be handled by either configuration.

The dynamic responses for the case with three temperature loops are shown in Figure 5.5.

5.2.3 Using liquid split for feedback control

So far liquid split ratio (R_L) has been kept constant, while using the reflux and side stream flows to control selected temperatures. However, the liquid split is also a degree of freedom that can be used for control. We will now add an additional temperature using R_L to the Kaibel dividing-wall column, and compare the performance to the previous configurations.

Kaibel column with four temperature loops

The fourth temperature loop is added to "stabilize" the prefractionator profile using the liquid split as manipulated variable. The temperature selected should be in the prefractionator section of the column, and the particular stage location used here was chosen considering the steady-state

Table 5.5: Kaibel column with 3 temperature loops closed: Effect of disturbances

	Nominal	ΔF_{+10}	$\Delta z_{B,F,+20}$	$\Delta R_{V,+10}$	$\Delta R_{V,+50}$
F	1.0000	1.1000	1.0000	1.0000	1.0000
$z_{B,F}$	0.2500	0.2500	0.3000	0.2500	0.2500
V	3.0000	3.0000	3.0000	3.0000	3.0000
R_L	0.2572	0.2572	0.2572	0.2572	0.2572
R_V	0.3770	0.3770	0.3770	0.4147	0.5655
L	2.8492	2.8492	2.8502	2.8502	2.8636
$S1$	0.2494	0.2494	0.2968	0.2968	0.0705
$S2$	0.2497	0.2497	0.2541	0.2541	0.4483
D	0.2508	0.2508	0.2498	0.2498	0.2364
B	0.2501	0.2501	0.1994	0.1994	0.2447
$x_{A,D}$	0.9703	0.9692	0.9704	0.9723	0.9812
x_{B,S_1}	0.9361	0.9364	0.9363	0.8510	0.4594
x_{C,S_2}	0.9589	0.9426	0.9362	0.9444	0.4963
$x_{D,B}$	0.9949	0.9952	0.9962	0.9947	0.9951
J	0.0349	0.0430	0.0433	0.0614	0.2696
Loss (%)	-	6.7	9.6	75.4	627

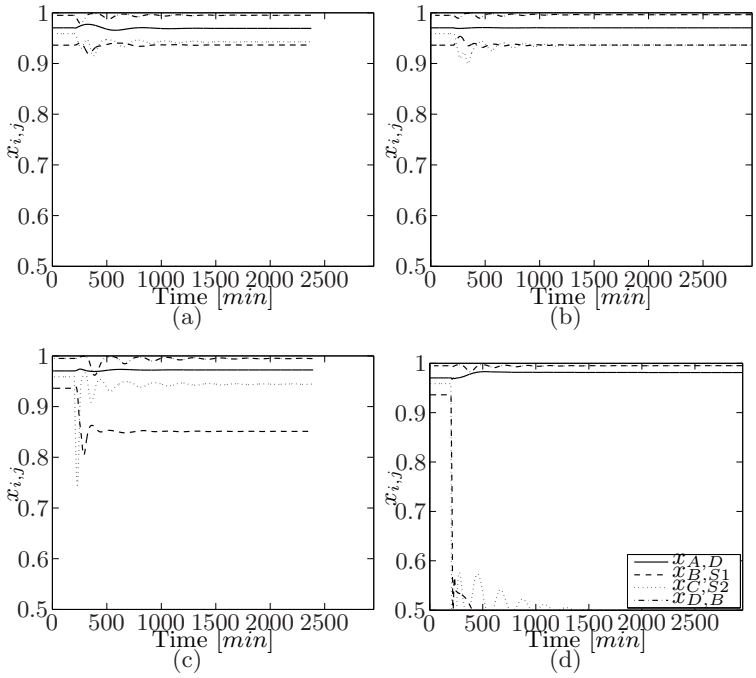

Figure 5.5: Kaibel column with 3 temperature loops closed: Disturbance responses (a) $F + 10\%$, (b) $z_{B,F} + 20\%$, (c) $R_V + 10\%$ and (d) $R_V + 50\%$

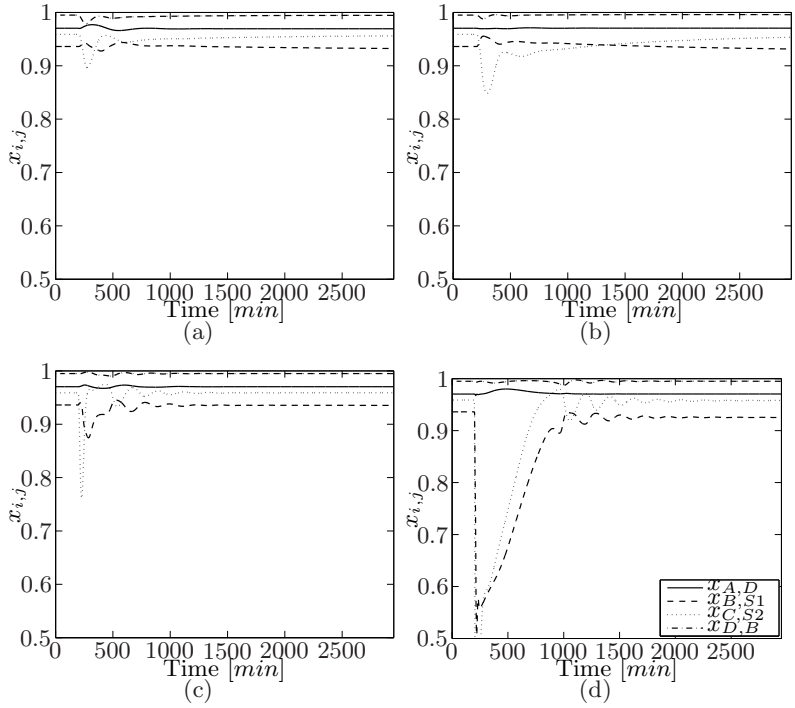

Figure 5.6: Kaibel column with four temperature loops closed: Disturbance responses (a) $F + 10\%$, (b) $z_{B,F} + 20\%$, (c) $R_V + 10\%$ and (d) $R_V + 50\%$

gain and the stage-to-stage temperature difference, but no detailed analysis was made.

With four temperature loops now closed, we subject the model to the same disturbances as above. The dynamic responses for the configuration can be seen in Figure 5.6. Although the response to the changes in vapour split in Figures 5.6 (c) and 5.6 (d) show some dynamic variation, the extra temperature loop manages to reduce the loss in purity considerably as compared to the configurations where R_L is not used for control. The resulting purities, inputs, objective function value and percentage loss are given in Table 5.6 for the four disturbances. The table shows that the control configuration give very good disturbance rejection, and for the smaller change in R_V, nearly zero loss.

Summary

The performance of all three control configurations are summarized in Table 5.7. Here we see clearly the improvement achieved when using the liquid

Table 5.6: Kaibel column with 4 temperature loops closed: Effect of disturbances

	Nominal	ΔF_{+10}	$\Delta z_{B,F,+20}$	$\Delta R_{V,+10}$	$\Delta R_{V,+50}$
F	1.0000	1.1000	1.0000	1.0000	1.0000
$z_{B,F}$	0.2500	0.2500	0.3000	0.2500	0.2500
V	3.0000	3.0000	3.0000	3.0000	3.0000
R_L	0.2572	0.2434	0.2371	0.2969	0.4549
R_V	0.3770	0.3770	0.3770	0.4147	0.5655
L	2.8492	2.8349	2.8528	2.8496	2.8532
$S1$	0.2494	0.2746	0.3032	0.2498	0.2532
$S2$	0.2497	0.2753	0.2500	0.2499	0.2510
D	0.2508	0.2751	0.2472	0.2504	0.2468
B	0.2501	0.2750	0.1996	0.2499	0.2491
$x_{A,D}$	0.9703	0.9694	0.9706	0.9703	0.9705
x_{B,S_1}	0.9361	0.9324	0.9315	0.9354	0.9254
x_{C,S_2}	0.9589	0.9562	0.9535	0.9590	0.9580
$x_{D,B}$	0.9949	0.9945	0.9958	0.9949	0.9950
J	0.0349	0.0406	0.0405	0.0351	0.0380
Loss (%)	-	0.7	2.5	0.3	2.4

split for control. The results confirm the findings of Halvorsen et al. [13], that either R_L or R_V needs to be adjusted online. Even for large disturbances in vapour split, the configuration with four temperature loops closed has very low loss.

Table 5.7: Kaibel column: Summary of objective function after disturbances.

	1 loop		3 loops		4 loops	
	J $\left[\frac{mol}{min}\right]$	Loss $[\%]$	J $\left[\frac{mol}{min}\right]$	Loss $[\%]$	J $\left[\frac{mol}{min}\right]$	Loss $[\%]$
Nominal	0.0349	-	0.0349	-	0.0349	-
$\Delta F = +10\%$	0.0955	137	0.0430	6.7	0.0406	0.7
$\Delta z_{B,F} = +20\%$	0.1181	199	0.0433	9.6	0.0405	2.5
$\Delta R_V = +10\%$	0.0718	105	0.0614	75	0.0351	0.3
$\Delta R_V = +50\%$	0.2876	675	0.2696	627	0.0380	2.4

5.3 Petlyuk Column

The Petlyuk column (Figure 5.7) modelled here is similar to the Kaibel column in that it has the same number of stages in each column section except for the prefractionator sections which have 8 stages above the feed (section 1) and 8 stages below the feed (section 2), as opposed to 12 in each for the Kaibel column. It has also one column section less than the Kaibel column since we here only have 3 product streams. We use 3 components, which are the same components as the three heaviest in the Kaibel model (these are modeled as ethanol, propanol and butanol, but mainly referred to as A, B and C). The feed is again equimolar, but we have halved the ratio of vapour boil up to feed flow (V/F) as compared to the Kaibel column to account for the easier separation. The nominal optimal operating point for the Petlyuk arrangement is found by optimization with the objective to minimize total impurity flow in the products.

Analogous to the investigations on the Kaibel column, we want to look at control configurations for the Petlyuk column with varying number of temperature loops. The control configurations can be seen in Figure 5.8.

1. One temperature control loop: Reflux, L, is used for temperature control (Also used in the other cases) (Fig. 5.8a).

2. Two temperature control loops: Adding a temperature loop for the side stream (Fig 5.8b).

3. Three temperature control loops: Adding a temperature loop for the liquid split, R_L (Fig 5.8c).

Initially, we will look at the two configurations that do not include R_L as an input.

5.3.1 Effect of liquid split ratio

For the two configurations (Figure 5.8 a) and b)), we set the liquid split ratio away from the optimum value and observe how this affects the product purities. The changes in R_L are $\pm 25\%$ and $\pm 50\%$ of the optimal value.

Input values, resulting product purities and objective function values for the case with one temperature loop can be seen in Table 5.8, while the values for the column with two temperature loops closed are shown in Table 5.9. The final objective function values do not differ markedly for the two configurations, although the total impurity for the negative perturbations in R_L for the one-loop configuration is about twice that of the two-loop column.

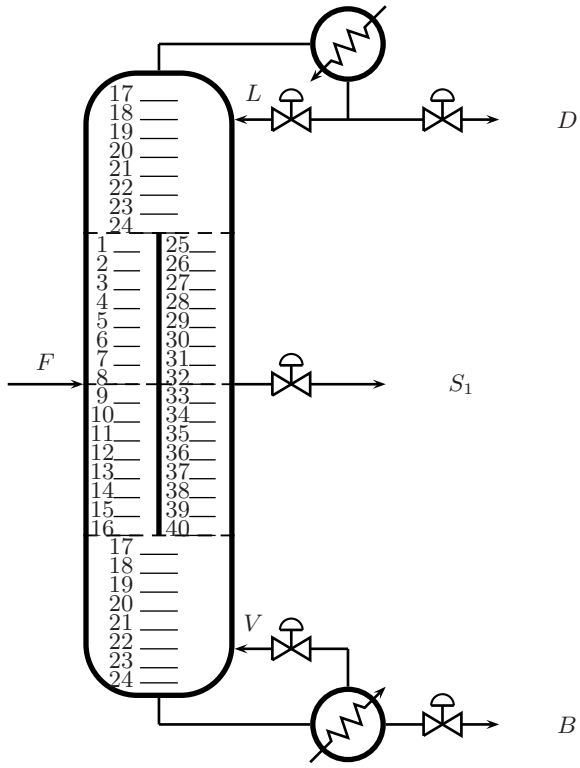

Figure 5.7: Petlyuk dividing wall column. Stage numbering

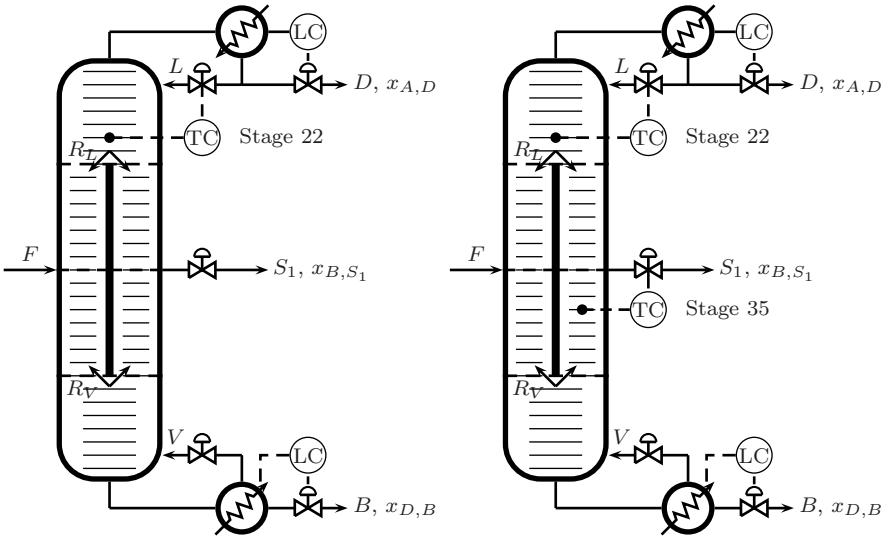

(a) 1 temperature loop

(b) 2 temperature loops

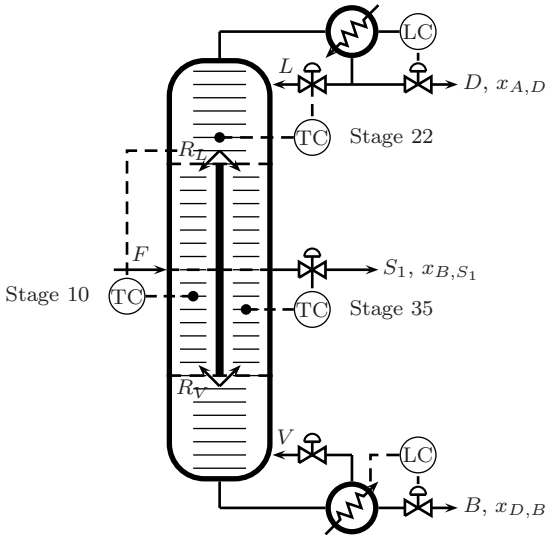

(c) 3 temperature loops

Figure 5.8: Petlyuk column control configurations (In all cases F, V and R_V are fixed)

Table 5.8: Petlyuk column with 1 temperature loop closed: Effect of changes in R_L

	$\Delta R_{L,-50}$	$\Delta R_{L,-25}$	Nominal	$\Delta R_{L,+25}$	$\Delta R_{L,+50}$
R_L	**0.1658**	**0.2487**	**0.3316**	**0.4145**	**0.4974**
F	1.0000	1.0000	1.0000	1.0000	1.0000
$z_{i,F}$	0.3333	0.3333	0.3333	0.3333	0.3333
V	1.5000	1.5000	1.5000	1.5000	1.5000
R_V	0.5346	0.5346	0.5346	0.5346	0.5346
L	1.2987	1.2744	1.2673	1.2695	1.2786
$S1$	0.3356	0.3356	0.3356	0.3356	0.3356
D	0.3013	0.3256	0.3327	0.3304	0.3214
B	0.3631	0.3388	0.3317	0.3339	0.3430
$x_{A,D}$	0.9881	0.9868	0.9862	0.9863	0.9866
x_{B,S_1}	0.7997	0.9144	0.9646	0.9442	0.8826
$x_{C,B}$	0.8310	0.9346	0.9849	0.9642	0.9043
J	0.1322	0.0552	0.0215	0.0352	0.0765

For the positive perturbations, the one-loop configuration performs slightly better than the one with two temperature loops. Interestingly, this is the same as for the Kaibel column.

The temperature profiles of the Petlyuk column operating points for case 2 can be seen in Figure 5.9. Like for the Kaibel column we observe the shifting of the prefractionator temperature profile with varying R_L.

The composition profiles of the Petlyuk column operating points can be seen in Figure 5.10. The Petlyuk column arrangement does not require a sharp split between adjacent components in the prefractionator as the Kaibel column. However, for successful operation, the A/C split must be achieved in the prefractionator in the Petlyuk column. For an incorrectly implemented reflux split (R_L), we can see from Figure 5.10 c) and d) that some of component C is carried over the top of the prefractionator, causing the side-stream product to be less pure.

5.3.2 Disturbance rejection

As with the Kaibel column we apply disturbances to the two control configurations of the Petlyuk column. The disturbances introduced are the same as for the Kaibel column example above. That is, 10% increase in F, 20% increase in $z_{B,F}$, and 10% and 50% increase in R_V. The feed composition increase in component B also implies a corresponding reduction in component C. Also here we include the reoptimized values for each disturbance for comparison. The optimal inputs can be seen in Table 5.10.

Table 5.9: Petlyuk column with 2 temperature loops closed: Effect of changes in R_L

	$\Delta R_{L,-50}$	$\Delta R_{L,-25}$	Nominal	$\Delta R_{L,+25}$	$\Delta R_{L,+50}$
R_L	**0.1658**	**0.2487**	**0.3316**	**0.4145**	**0.4974**
F	1.0000	1.0000	1.0000	1.0000	1.0000
$z_{i,F}$	0.3333	0.3333	0.3333	0.3333	0.3333
V	1.5000	1.5000	1.5000	1.5000	1.5000
R_V	0.5346	0.5346	0.5346	0.5346	0.5346
L	1.2997	1.2746	1.2673	1.2694	1.2777
$S1$	0.3997	0.3574	0.3356	0.3282	0.3135
D	0.3003	0.3254	0.3327	0.3306	0.3223
B	0.3000	0.3173	0.3317	0.3412	0.3642
$x_{A,D}$	0.9882	0.9869	0.9862	0.9863	0.9866
x_{B,S_1}	0.8128	0.9122	0.9646	0.9520	0.8986
$x_{C,B}$	0.9836	0.9903	0.9849	0.9520	0.8702
J	0.0833	0.0388	0.0215	0.0367	0.0834

Table 5.10: Petlyuk column: Optimal operating point for disturbances R_V fixed

	Nominal	ΔF_{+10}	$\Delta z_{B,F,+20}$	$\Delta R_{V,+10}$	$\Delta R_{V,+50}$
F	1.0000	1.1000	1.0000	1.0000	1.0000
$z_{B,F}$	0.3333	0.3333	0.4000	0.3333	0.3333
V	1.5000	1.5000	1.5000	1.5000	1.5000
R_L	0.3316	0.3159	0.3096	0.3822	0.5888
R_V	0.5346	0.5346	0.5346	0.5881	0.8020
L	1.2673	1.2447	1.2675	1.2669	1.2661
S_1	0.3356	0.3716	0.4041	0.3343	0.3314
D	0.3327	0.3653	0.3325	0.3331	0.3339
B	0.3317	0.3631	0.2634	0.3326	0.3346
$x_{A,D}$	0.9862	0.9835	0.9828	0.9844	0.9531
x_{B,S_1}	0.9646	0.9505	0.9635	0.9655	0.9351
$x_{C,B}$	0.9849	0.9795	0.9813	0.9838	0.9769
$J_{opt,d}$	0.0215	0.0318	0.0254	0.0221	0.0449

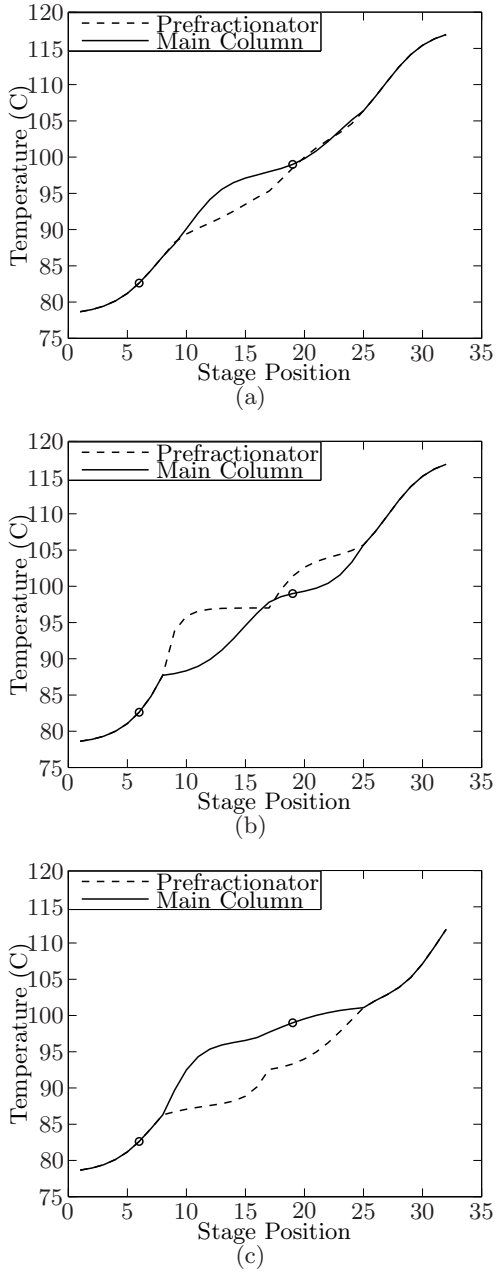

Figure 5.9: Petlyuk column with 2 temperature loops closed: Column temperature profiles. (a) Nominal profile, (b) $R_L = 0.50R_{L,opt}$, (c) $R_L = 1,50R_{L,opt}$. Controlled temperatures are circled.

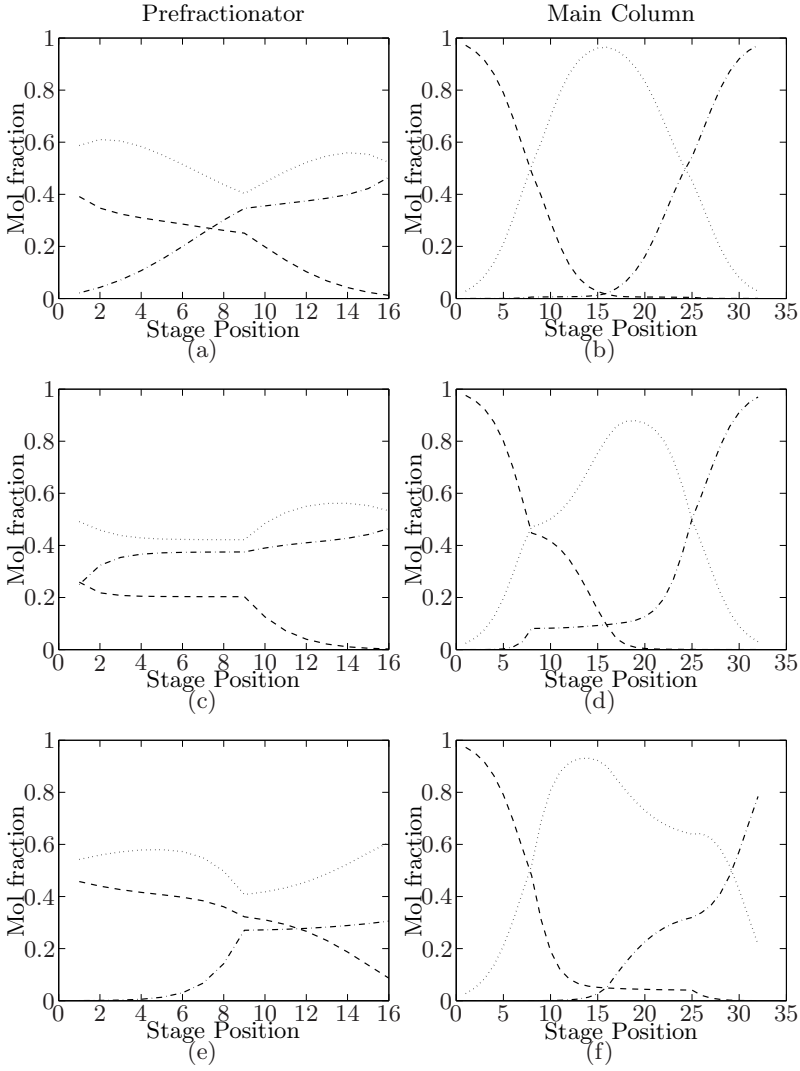

Figure 5.10: Petlyuk column with 2 temperature loops closed: Composition profiles of prefractionator and main column. (a) and (b) nominal operating point, (c) and (d) R_L is too low, (e) and (f) R_L is too high. ($- - -$ component A, $\cdots$ component B, $- \cdot -$ component C)

Table 5.11: Petlyuk column with 1 temperature loop closed: Effect of disturbances

	Nominal	ΔF_{+10}	$\Delta z_{B,F,+20}$	$\Delta R_{V,+10}$	$\Delta R_{V,+50}$
F	1.0000	1.1000	1.0000	1.0000	1.0000
$z_{B,F}$	0.3333	0.3333	0.4000	0.3333	0.3333
V	1.5000	1.5000	1.5000	1.5000	1.5000
R_L	0.3316	0.3316	0.3316	0.3316	0.3316
R_V	0.5346	0.5346	0.5346	0.5881	0.8020
L	1.2673	1.2454	1.2688	1.2763	1.4006
S_1	0.3356	0.3356	0.3356	0.3356	0.3356
D	0.3327	0.3646	0.3312	0.3237	0.1994
B	0.3317	0.3997	0.3332	0.3407	0.4650
$x_{A,D}$	0.9862	0.9849	0.9863	0.9867	0.9911
x_{B,S_1}	0.9646	0.9644	0.9731	0.9354	0.5308
$x_{C,B}$	0.9849	0.9062	0.7933	0.9557	0.6699
J	0.0215	0.0550	0.0824	0.0411	0.3127
Loss (%)	-	73.0	224	86.0	596

Table 5.12: Petlyuk column with 2 temperature loops closed: Effect of disturbances

	Nominal	ΔF_{+10}	$\Delta z_{B,F,+20}$	$\Delta R_{V,+10}$	$\Delta R_{V,+50}$
F	1.0000	1.1000	1.0000	1.0000	1.0000
$z_{B,F}$	0.3333	0.3333	0.4000	0.3333	0.3333
V	1.5000	1.5000	1.5000	1.5000	1.5000
R_L	0.3316	0.3316	0.3316	0.3316	0.3316
R_V	0.5346	0.5346	0.5346	0.5881	0.8020
L	1.2673	1.2357	1.2696	1.2696	1.4438
S_1	0.3356	0.3665	0.4050	0.4050	0.6043
D	0.3327	0.3643	0.3304	0.3304	0.1562
B	0.3317	0.3693	0.2646	0.2646	0.2395
$x_{A,D}$	0.9862	0.9849	0.9863	0.9867	0.9926
x_{B,S_1}	0.9646	0.9551	0.9614	0.9312	0.5495
$x_{C,B}$	0.9849	0.9697	0.9768	0.9908	0.9996
J	0.0215	0.0331	0.0263	0.0314	0.2735
Loss (%)	-	4.1	3.5	42.1	509

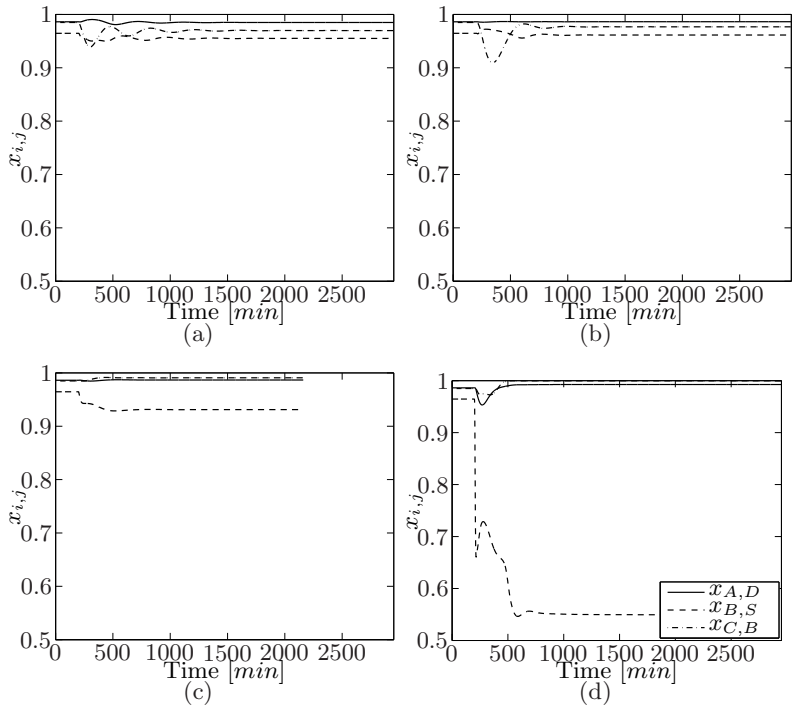

Figure 5.11: Petlyuk column with 2 temperature loops closed: Disturbance responses (a) $F + 10\%$, (b) $z_{B,F} + 20\%$, (c) $R_L + 10\%$ and (d) $R_V + 50\%$

Tables 5.11 and 5.12 show the relevant inputs, resulting purities and objective function values after the disturbances for the two configurations. We observe that the two-loop configuration can handle the disturbances generally much better than the one-loop implementation, which is to be expected. For the large disturbance in R_V, however, both configurations are far off the optimum. The one-loop configuration have large impurities in both side stream and bottoms stream, while the two-loop configuration only suffers the impurity of the side stream (the distillate and bottoms get more pure).

The dynamic responses to the disturbances for the case with two temperature loops can be seen in Figure 5.11. The effect of the large change in R_V on the side stream composition is clearly visible.

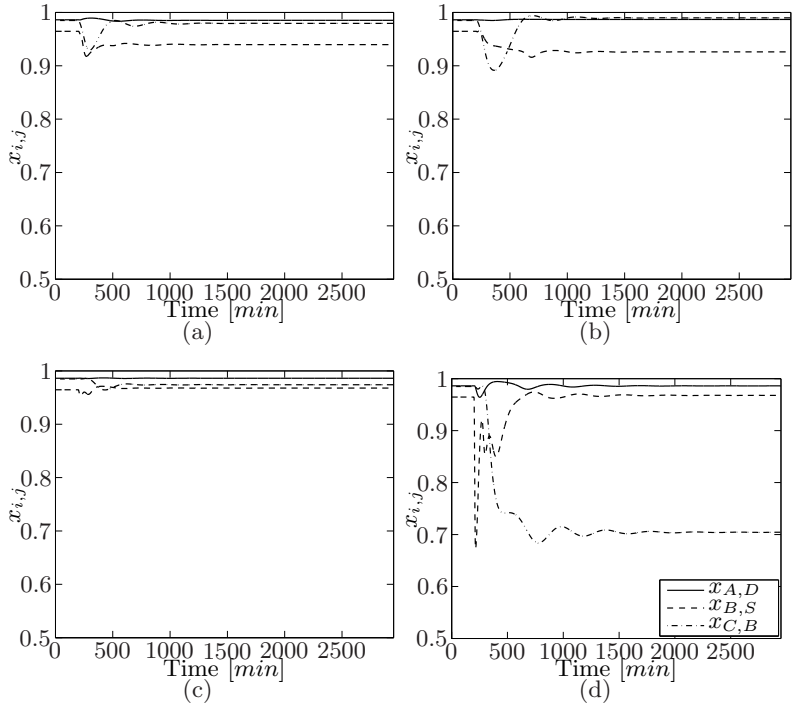

Figure 5.12: Petlyuk column with three temperature loops closed: Disturbance responses (a) F+10%, (b) $z_{B,F}$+20%, (c) R_V+10% and (d) R_V+50%

5.3.3 Petlyuk column with three temperature loops

Similarly to the Kaibel column we also include an extra temperature loop using the liquid split for the Petlyuk dividing-wall column. Figure 5.8 (c) shows the temperature loop that has been added. Again, we choose to control a temperature in the prefractionator section of the column.

The three-loop configuration is also tested with the selected disturbances defined above, and response plots for the column are shown in Figure 5.12. We notice that the extra loop cannot readily reject the large change in the vapour split, contrary to what we saw for the Kaibel column, although a straight comparison is not justified since the increase in R_V in absolute terms is larger in this case. The inputs, resulting product purities, objective function values and loss for the disturbance simulations can be seen in Table 5.13. We can note that the smaller increase in R_V is handled well by the control system. This suggests that up to a certain point, we may adjust the liquid split to compensate for an incorrectly set vapour split. However,

Table 5.13: Petlyuk column with 3 temperature loops closed: Effect of disturbances

	Nominal	ΔF_{+10}	$\Delta z_{B,F,+20}$	$\Delta R_{V,+10}$	$\Delta R_{V,+50}$
F	1.0000	1.1000	1.0000	1.0000	1.0000
$z_{B,F}$	0.3333	0.3333	0.4000	0.3333	0.3333
V	1.5000	1.5000	1.5000	1.5000	1.5000
R_L	0.3316	0.2844	0.2479	0.4081	0.7141
R_V	0.5346	0.5346	0.5346	0.5881	0.8020
L	1.2673	1.2372	1.2782	1.2670	1.2647
S_1	0.3356	0.3766	0.4246	0.3307	0.1966
D	0.3327	0.3628	0.3218	0.3330	0.3353
B	0.3317	0.3606	0.2536	0.3363	0.4681
$x_{A,D}$	0.9862	0.9851	0.9868	0.9862	0.9861
x_{B,S_1}	0.9646	0.9397	0.9260	0.9677	0.9678
$x_{C,B}$	0.9849	0.9795	0.9898	0.9741	0.7044
J	0.0215	0.0355	0.0382	0.0240	0.1494
Loss (%)	-	11.6	50.3	8.6	233

in this case the problem has more to do with the side stream and bottoms rates. They are far off the optimum, and it would be better to keep them constant, though this is not easily achieved in practice.

Summary

The performance of all three control configurations is summarized in Table 5.14. The benefit of the extra (R_L) loop is not so evident here as it was for the Kaibel column, except for the disturbances in R_V. Surprisingly, when the feed composition is changed, the two-loop configuration is considerably better than the three-loop configuration. The locations of the temperature measurements could have a large effect here, and it is likely that other locations can be found that will improve the performance of the three-loop configuration over the other two.

Table 5.14: Petlyuk column: Summary of objective function values after disturbances

	1 loop		2 loops		3 loops	
	J $\left[\frac{mol}{min}\right]$	Loss [%]	J $\left[\frac{mol}{min}\right]$	Loss [%]	J $\left[\frac{mol}{min}\right]$	Loss [%]
Nominal	0.0215	-	0.0215	-	0.0215	-
$\Delta F = +10\%$	0.0550	73	0.0331	4.1	0.0355	12
$\Delta z_{B,F} = +20\%$	0.0824	224	0.0263	3.5	0.0382	50
$\Delta R_V = +10\%$	0.0411	86	0.0314	42	0.0240	8.6
$\Delta R_V = +50\%$	0.3127	596	0.2735	509	0.1494	233

5.4 High-purity dividing-wall columns

In the examples presented above, the product purities have not been particularly high because of the low number of stages modelled. It would therefore be interesting to see if a high-purity column would behave differently and especially whether high-purity columns are more sensitive to the liquid split. In the following we present a Kaibel column and a Petlyuk column with high nominal purities of the products.

5.4.1 High-purity Kaibel column

This column has twice as many stages as the previous model of the Kaibel column. That is, 24 stages in each of the two prefractionator sections and 16 in each of the other column sections. The resulting product purities are all above 99.7% at the nominal optimum.

Effect of liquid split

Following the analysis from the previous section, we first look at the effects of setting the liquid split ratio away from the optimal value for a Kaibel column with 1 and 3 temperature loops closed respectively. The resulting product purities and objective function values can be seen in Table 5.15 for the case with only one temperature loop closed. The results for the column with three temperature loops can are shown in Table 5.16. We can immediately see that this column is more sensitive to an incorrectly set liquid split than the column with lower purities. This agrees with the findings of Halvorsen and Skogestad [14] The second thing to note, is that the effect of the liquid split change is almost the same for the two control configurations.

Table 5.15: High-purity Kaibel column with 1 temperature loop: Effect of changes in R_L

	$\Delta R_{L,-50}$	$\Delta R_{L,-25}$	Nominal	$\Delta R_{L,+25}$	$\Delta R_{L,+50}$
R_L	0.2144	0.3216	0.4288	0.5360	0.6433
F	1.0000	1.0000	1.0000	1.0000	1.0000
$z_{i,F}$	0.2500	0.2500	0.2500	0.2500	0.2500
V	3.0000	3.0000	3.0000	3.0000	3.0000
R_V	0.5407	0.5407	0.5407	0.5407	0.5407
L	2.8520	2.8508	2.8498	2.8497	2.8623
$S1$	0.2496	0.2496	0.2496	0.2496	0.2496
$S2$	0.2498	0.2498	0.2498	0.2498	0.2498
D	0.2480	0.2492	0.2502	0.2503	0.2377
B	0.2526	0.2514	0.2504	0.2502	0.2629
$x_{A,D}$	0.9991	0.9988	0.9984	0.9984	0.9985
x_{B,S_1}	0.5657	0.7380	0.9977	0.8164	0.6218
x_{C,S_2}	0.5388	0.7378	0.9976	0.8164	0.5989
$x_{D,B}$	0.9387	0.9952	0.9984	0.9985	0.9499
J	0.2393	0.1324	0.0020	0.0925	0.2081

Table 5.16: High-purity Kaibel column with 3 temperature loops: Effect of changes in R_L

	$\Delta R_{L,-50}$	$\Delta R_{L,-25}$	Nominal	$\Delta R_{L,+25}$	$\Delta R_{L,+50}$
R_L	**0.2144**	**0.3216**	**0.4288**	**0.5360**	**0.6433**
F	1.0000	1.0000	1.0000	1.0000	1.0000
$z_{i,F}$	0.2500	0.2500	0.2500	0.2500	0.2500
V	3.0000	3.0000	3.0000	3.0000	3.0000
R_V	0.5407	0.5407	0.5407	0.5407	0.5407
L	2.8520	2.8508	2.8498	2.8497	2.8625
$S1$	0.2477	0.2564	0.2496	0.2249	0.2393
$S2$	0.2674	0.2440	0.2498	0.2747	0.2739
D	0.2480	0.2492	0.2502	0.2503	0.2375
B	0.2369	0.2504	0.2504	0.2501	0.2493
$x_{A,D}$	0.9991	0.9988	0.9984	0.9984	0.9985
x_{B,S_1}	0.5657	0.7381	0.9977	0.8850	0.6178
x_{C,S_2}	0.5630	0.7522	0.9976	0.8163	0.6037
$x_{D,B}$	0.9987	0.9984	0.9984	0.9995	0.9998
J	0.2250	0.1283	0.0020	0.0768	0.2004

Table 5.17: High-purity Kaibel column: Optimal operating points for disturbances

	ΔF_{+10}	$\Delta z_{B,F,+20}$	$\Delta R_{V,+10}$	$\Delta R_{V,+50}$
F	1.1000	1.0000	1.0000	1.0000
$z_{i,F}$	0.2500	0.3000	0.2500	0.2500
V	3.0000	3.0000	3.0000	3.0000
R_L	0.4170	0.4113	0.4857	0.7132
R_V	0.5407	0.5407	0.5948	0.8111
L	2.8348	2.8500	2.8499	2.8510
S_1	0.2745	0.2998	0.2496	0.2504
S_2	0.2745	0.2499	0.2499	0.2508
D	0.2652	0.2500	0.2501	0.2490
B	0.1857	0.2003	0.2505	0.2497
$x_{A,D}$	0.9981	0.9983	0.9984	0.9949
x_{B,S_1}	0.9975	0.9972	0.9975	0.9904
x_{C,S_2}	0.9977	0.9976	0.9975	0.9939
$x_{D,B}$	0.9973	0.9986	0.9981	0.9979
$J_{opt,d}$	0.0026	0.0021	0.0021	0.0057

Disturbance rejection

Next, we look at changes in the disturbance variables that we have been using throughout this chapter. The optimal values for the disturbances can be seen in Table 5.17. Table 5.18 shows the resulting purities, input values and objective function values after disturbances have been introduced to the configuration where only the reflux is used for temperature control. Table 5.19 shows the results for the high-purity Kaibel column with three temperature loops closed. Here we see some improvement in going from one to three temperature loops for the feed flow and feed composition changes, but the disturbance in vapour split has nearly the same effect on both configurations. Again, we note that the high-purity column is much more sensitive to these disturbances than the column with low number of stages.

Finally, we add the fourth temperature loop using the liquid split for control. The resulting values after disturbances are given in Table 5.20. The improvement for the feed disturbances is minimal, but for the smaller change in vapour split the extra temperature loop manages to keep operation very close to the optimal point. The large perturbation in R_V however, can not be handled by the control system.

Table 5.18: High-purity Kaibel column with 1 temperature loop closed: Effect of disturbances

	Nominal	ΔF_{+10}	$\Delta z_{B,F,+20}$	$\Delta R_{V,+10}$	$\Delta R_{V,+50}$
F	1.0000	1.1000	1.0000	1.0000	1.0000
$z_{B,F}$	0.2500	0.2500	0.3000	0.2500	0.2500
V	3.0000	3.0000	3.0000	3.0000	3.0000
R_L	0.4288	0.4288	0.4288	0.4288	0.4288
R_V	0.5407	0.5407	0.5407	0.5948	0.8111
L	2.8498	2.8347	2.8498	2.8506	2.9676
$S1$	0.2496	0.2496	0.2496	0.2496	0.2496
$S2$	0.2498	0.2498	0.2498	0.2498	0.2498
D	0.2502	0.2753	0.2502	0.2494	0.1323
B	0.2504	0.3253	0.2504	0.2512	0.3682
x_D	0.9984	0.9982	0.9984	0.9986	0.9993
x_{S_1}	0.9977	0.9991	0.9991	0.8339	0.5003
x_{S_2}	0.9976	0.8993	0.7989	0.8338	0.2643
x_B	0.9984	0.8454	0.7987	0.9965	0.6793
J	0.0020	0.0762	0.1013	0.0842	0.4268
Loss (%)	-	~ 2800	~ 4700	~ 3900	~ 7400

Table 5.19: High-purity Kaibel column with 3 temperature loops closed: Effect of disturbances

	Nominal	ΔF_{+10}	$\Delta z_{B,F,+20}$	$\Delta R_{V,+10}$	$\Delta R_{V,+50}$
F	1.0000	1.1000	1.0000	1.0000	1.0000
$z_{B,F}$	0.2500	0.2500	0.3000	0.2500	0.2500
V	3.0000	3.0000	3.0000	3.0000	3.0000
R_L	0.4288	0.4288	0.4288	0.4288	0.4288
R_V	0.5407	0.5407	0.5407	0.5948	0.8111
L	2.8498	2.8347	2.8498	2.8506	2.9843
$S1$	0.2496	0.2636	0.2654	0.2600	0.2603
$S2$	0.2498	0.2856	0.2843	0.2403	0.3738
D	0.2502	0.2753	0.2502	0.2494	0.1157
B	0.2504	0.2755	0.2001	0.2504	0.2502
x_D	0.9984	0.9982	0.9984	0.9986	0.9995
x_{S_1}	0.9977	0.9989	0.9990	0.8339	0.3915
x_{S_2}	0.9976	0.9593	0.8782	0.8630	0.3945
x_B	0.9984	0.9982	0.9993	0.9985	0.9991
J	0.0020	0.0129	0.0354	0.0768	0.3850
Loss (%)	-	~ 400	~ 1600	~ 3600	~ 6700

Table 5.20: High-purity Kaibel column with 4 temperature loops closed: Effect of disturbances

	Nominal	ΔF_{+10}	$\Delta z_{B,F,+20}$	$\Delta R_{V,+10}$	$\Delta R_{V,+50}$
F	1.0000	1.1000	1.0000	1.0000	1.0000
$z_{B,F}$	0.2500	0.2500	0.3000	0.2500	0.2500
V	3.0000	3.0000	3.0000	3.0000	3.0000
R_L	0.4288	0.4170	0.4113	0.4857	0.5354
R_V	0.5407	0.5407	0.5407	0.5948	0.8111
L	2.8498	2.8348	2.8500	2.8499	2.9401
$S1$	0.2496	0.2653	0.2661	0.2494	0.2605
$S2$	0.2498	0.2839	0.2838	0.2501	0.3293
D	0.2502	0.2752	0.2500	0.2501	0.1597
B	0.2504	0.2756	0.2001	0.2504	0.2505
x_D	0.9984	0.9982	0.9984	0.9984	0.9995
x_{S_1}	0.9977	0.9986	0.9984	0.9979	0.3534
x_{S_2}	0.9976	0.9652	0.8799	0.9958	0.4319
x_B	0.9984	0.9977	0.9992	0.9984	0.9990
J	0.0020	0.0114	0.0351	0.0023	0.3559
Loss (%)	-	~ 340	~ 1600	~ 10	~ 6100

Summary

Table 5.21 summarizes the results of all three control configurations. The high-purity column shows a greater general sensitivity to disturbances than do the column in Section 5.2. There is a large improvement in going from one temperature control loop to three. However, adding the fourth loop to incorporate the liquid split does not increase the feed disturbance rejection significantly. On the other hand, for the small disturbance in the vapour split the result is very good and we have near perfect operation with four temperature loops.

5.4.2 High-purity Petlyuk column

The model of the high-purity Petlyuk column has also two times the number of stages as compared to the Petlyuk column in the previous examples.

The increased number of stages lead to changes in the dynamic behavior of the column, and the temperature to be controlled by the side-stream valve had to be moved down in the bottom section as compared to the column with fewer stages, because of small process gain in the section directly below the side-stream.

Table 5.21: High-purity Kaibel column: Summary of objective function values after disturbances

	1 loop		3 loops		4 loops	
	J $\left[\frac{mol}{min}\right]$	Loss [%]	J $\left[\frac{mol}{min}\right]$	Loss [%]	J $\left[\frac{mol}{min}\right]$	Loss [%]
Nominal	0.0020	-	0.0020	-	0.0020	-
$\Delta F = +10\%$	0.0762	2800	0.0129	400	0.0114	340
$\Delta z_{B,F} = +20\%$	0.1013	4700	0.0354	1600	0.0351	1600
$\Delta R_V = +10\%$	0.0842	3900	0.0768	3600	0.0023	10
$\Delta R_V = +50\%$	0.4268	7400	0.3850	6700	0.3559	6100

Effect of liquid split

The liquid split ratio for the high-purity Petlyuk column is varied around the nominal optimal operating point for the control configurations with one and temperature loops respectively. The input values, resulting purities and objective function values for the case with only one temperature loop can be seen in Table 5.22. Table 5.23 show the values for the case with two temperature loops closed. As for the high-purity Kaibel column, the relative increase in the objective function is very large compared to the column with fewer stages when R_L is set away from its optimal value. We note that the configuration with two loops manages to keep the purities at both column ends, while the configuration with only the "reflux loop" gets large impurities in both side and bottoms streams.

Disturbance rejection

Like with the high-purity Kaibel column, we subject the different control configurations of the high-purity Petlyuk column to selected disturbances. The optimal inputs for the disturbances can be seen in Table 5.24.

The resulting inputs, purities and objective function value for the configuration with one temperature loop is shown in Table 5.25, while the case with two temperature loops is shown in Table 5.26.

Finally, we add the third temperature loop, making use of the liquid split (R_L) for feedback control. The results are shown in Table 5.27. The feed disturbances are handled very well by the control loops and the resulting purities are very close to the optimal values. Again, the small change in vapour split is effectively adjusted for by the liquid split.

Table 5.22: High-purity Petlyuk column with 1 temperature loop closed: Effect of changes in R_L

	$\Delta R_{L,-50}$	$\Delta R_{L,-25}$	Nominal	$\Delta R_{L,+25}$	$\Delta R_{L,+50}$
R_L	**0.1718**	**0.2577**	**0.3436**	**0.4295**	**0.5154**
F	1.0000	1.0000	1.0000	1.0000	1.0000
$z_{i,F}$	0.3333	0.3333	0.3333	0.3333	0.3333
V	1.5000	1.5000	1.5000	1.5000	1.5000
R_V	0.5515	0.5515	0.5515	0.5515	0.5515
L	1.3109	1.2767	1.2667	1.2676	1.2795
$S1$	0.3335	0.3335	0.3335	0.3335	0.3335
D	0.2891	0.3233	0.3333	0.3324	0.3205
B	0.3774	0.3432	0.3332	0.3340	0.3460
$x_{A,D}$	0.9998	0.9998	0.9998	0.9998	0.9998
x_{B,S_1}	0.7729	0.9211	0.9988	0.9890	0.8971
$x_{C,B}$	0.8000	0.9242	0.9996	0.9899	0.9016
J	0.1513	0.0524	0.0006	0.0071	0.0684

Table 5.23: High-purity Petlyuk column with 2 temperature loops closed: Effect of changes in R_L

	$\Delta R_{L,-50}$	$\Delta R_{L,-25}$	Nominal	$\Delta R_{L,+25}$	$\Delta R_{L,+50}$
R_L	**0.1718**	**0.2577**	**0.3436**	**0.4295**	**0.5154**
F	1.0000	1.0000	1.0000	1.0000	1.0000
$z_{i,F}$	0.3333	0.3333	0.3333	0.3333	0.3333
V	1.5000	1.5000	1.5000	1.5000	1.5000
R_V	0.5515	0.5515	0.5515	0.5515	0.5515
L	1.3109	1.2768	1.2667	1.2676	1.2815
$S1$	0.4173	0.3608	0.3335	0.3593	0.4278
D	0.2891	0.3232	0.3333	0.3324	0.3185
B	0.2936	0.3159	0.3332	0.3084	0.2537
$x_{A,D}$	0.9998	0.9998	0.9998	0.9998	0.9998
x_{B,S_1}	0.7984	0.9233	0.9988	0.9273	0.7790
$x_{C,B}$	0.9997	0.9996	0.9996	0.9997	0.9998
J	0.0843	0.0279	0.0006	0.0263	0.0947

Table 5.24: High-purity Petlyuk column: Optimal operating points for disturbances

	ΔF_{+10}	$\Delta z_{B,F,+20}$	$\Delta R_{V,+10}$	$\Delta R_{V,+50}$
F	1.1000	1.0000	1.0000	1.0000
$z_{B,F}$	0.3333	0.4000	0.3333	0.3333
V	1.5000	1.5000	1.5000	1.5000
R_L	0.3201	0.3048	0.3839	0.5955
R_V	0.5346	0.5346	0.5881	0.8020
L	1.2435	1.2668	1.2667	1.2680
S_1	0.3675	0.4010	0.3335	0.3354
D	0.3665	0.3332	0.3333	0.3320
B	0.3660	0.2658	0.3332	0.3326
$x_{A,D}$	0.9997	0.9998	0.9997	0.9952
x_{B,S_1}	0.9968	0.9971	0.9988	0.9875
$x_{C,B}$	0.9994	0.9997	0.9996	0.9984
$J_{opt,d}$	0.0015	0.0013	0.0006	0.0063

Table 5.25: High-purity Petlyuk column with 1 temperature loop closed: Effect of disturbances

	Nominal	ΔF_{+10}	$\Delta z_{B,F,+20}$	$\Delta R_{V,+10}$	$\Delta R_{V,+50}$
F	1.0000	1.1000	1.0000	1.0000	1.0000
$z_{B,F}$	0.3333	0.3333	0.4000	0.3333	0.3333
V	1.5000	1.5000	1.5000	1.5000	1.5000
R_L	0.3436	0.3436	0.3436	0.3436	0.3436
R_V	0.5515	0.5515	0.5515	0.6067	0.8273
L	1.2667	1.2435	1.2668	1.2868	1.3882
$S1$	0.3335	0.3335	0.3335	0.3335	0.3335
D	0.3333	0.3665	0.3332	0.3132	0.2118
B	0.3332	0.3999	0.3332	0.3532	0.4546
x_D	0.9998	0.9997	0.9998	0.9998	0.9999
x_{S_1}	0.9988	0.9985	0.9991	0.9303	0.5648
x_B	0.9996	0.9162	0.7999	0.9350	0.6812
J	0.0006	0.0341	0.0671	0.0463	0.2901
Loss (%)		~ 2200	~ 5100	~ 7600	~ 4500

Table 5.26: High-purity Petlyuk column with 2 temperature loops closed: Effect of disturbances

	Nominal	ΔF_{+10}	$\Delta z_{B,F,+20}$	$\Delta R_{V,+10}$	$\Delta R_{V,+50}$
F	1.0000	1.1000	1.0000	1.0000	1.0000
$z_{B,F}$	0.3333	0.3333	0.4000	0.3333	0.3333
V	1.5000	1.5000	1.5000	1.5000	1.5000
R_L	0.3436	0.3436	0.3436	0.3436	0.3436
R_V	0.5515	0.5515	0.5515	0.6067	0.8273
L	1.2667	1.2435	1.2668	1.2868	1.4293
$S1$	0.3335	0.3682	0.4014	0.3567	0.5370
D	0.3333	0.3665	0.3332	0.3132	0.1707
B	0.3332	0.3653	0.2654	0.3301	0.2923
x_D	0.9998	0.9997	0.9998	0.9998	0.9999
x_{S_1}	0.9988	0.9951	0.9961	0.9341	0.6206
x_B	0.9996	0.9995	0.9997	0.9996	0.9997
J	0.0006	0.0021	0.0017	0.0237	0.2038
Loss (%)	-	~ 40	~ 30	~ 3900	~ 3100

Table 5.27: High-purity Petlyuk column with 3 temperature loops closed: Effect of disturbances

	Nominal	ΔF_{+10}	$\Delta z_{B,F,+20}$	$\Delta R_{V,+10}$	$\Delta R_{V,+50}$
F	1.0000	1.1000	1.0000	1.0000	1.0000
$z_{B,F}$	0.3333	0.3333	0.4000	0.3333	0.3333
V	1.5000	1.5000	1.5000	1.5000	1.5000
R_L	0.3436	0.3331	0.3223	0.3979	0.6403
R_V	0.5515	0.5515	0.5515	0.6067	0.8273
L	1.2667	1.2435	1.2669	1.2669	1.3192
$S1$	0.3335	0.3677	0.4009	0.3337	0.4412
D	0.3333	0.3665	0.3331	0.3331	0.2808
B	0.3332	0.3658	0.2659	0.3332	0.2780
x_D	0.9998	0.9997	0.9998	0.9998	0.9998
x_{S_1}	0.9988	0.9965	0.9973	0.9983	0.7552
x_B	0.9996	0.9995	0.9997	0.9996	0.9997
J	0.0006	0.0016	0.0013	0.0008	0.1081
Loss (%)	-	~ 7	~ 0	~ 30	~ 1600

Table 5.28: High-purity Petlyuk column: Summary of objective function values after disturbances

	1 loop		2 loops		3 loops	
	J $\left[\frac{mol}{min}\right]$	Loss $[\%]$	J $\left[\frac{mol}{min}\right]$	Loss $[\%]$	J $\left[\frac{mol}{min}\right]$	Loss $[\%]$
Nominal	0.0006	-	0.0006	-	0.0006	-
$\Delta F = +10\%$	0.0341	2200	0.0021	40	0.0016	7
$\Delta z_{B,F} = +20\%$	0.0671	5100	0.0017	30	0.0013	0
$\Delta R_V = +10\%$	0.0463	7600	0.0237	3900	0.0008	30
$\Delta R_V = +50\%$	0.2901	4500	0.2038	3100	0.1081	1600

Summary

Table 5.28 summarizes the objective function values of the previous tables for the high-purity Petlyuk column. For the feed disturbances there is a great improvement in going from one to two temperature loops, where the losses are relatively small. However, for the change in vapour split, we see that we need the third temperature loop to compensate by adjusting the liquid split. This is in agreement with the results from the other columns investigated above. Also here, we see that the large disturbance in R_V cannot readily be rejected by any control configuration.

5.5 Conclusions

In this chapter, we have studied the practical implementation of stabilizing control for dividing-wall distillation columns. The examples include the 4-product Kaibel column and the more well-known 3-product Petlyuk column. In the study, we assume that the objective is to maximize the purity of all product streams, and we show that setting the correct liquid split ratio is essential in achieving the potential purities. Control configurations with varying number of temperature loops have been tested and compared. We show that the liquid split can be used to control a temperature in the prefractionator section and thereby reduce the sensitivity to disturbances. Adjusting the liquid split is particularly important in reducing the column's sensitivity to the vapour split ratio. We also show that for high-purity columns the need to adjust the liquid split online is even greater.

Chapter 6

Temperature locations for regulatory control of the Kaibel column

6.1 Introduction

In the previous chapter, we compared strategies with different number of temperature loops being closed, but we did not consider to any depth the location of the temperature measurements on the dynamic and steady-state behavior. This is the topic of this chapter where we consider in more detail the Kaibel column with 4 temperature loops closed.

6.2 Regulatory control layer

The purpose of a regulatory control layer is to stabilize the operation of the plant, here the Kaibel distillation column. Even if the column is not inherently unstable in the mathematical sense, any distillation column will –in addition to drift in the liquid levels, be subject to a "drift" in its composition profile away from the operating point [36].

The regulatory control layer for a distillation column usually includes pressure control and control of liquid levels in the reboiler and condenser. In this work the choice of level control configuration is not investigated, and the most standard $L - V$-configuration is used in all examples. Pressure control is also omitted since the analytical model assumes uniform pressure.

We concentrate on stabilizing the column profile, and the task here is to find a set of secondary variables y_2 to control using manipulated inputs u_2,

to avoid drift. The setpoints for the secondary variables y_{2s} may be used as inputs for the upper layer's primary controlled variables.

6.2.1 Maintaining splits in the Kaibel column

In order to avoid "drift" in the column with undesirable breakthrough of impurities in the product we need to stabilize the column profile, and the conclusion of the previous chapter was that we need to close four temperature loops for the Kaibel column. To understand why this is necessary, note that we can view the Kaibel column as essentially 4 columns within the one (see Figure 6.1). Firstly, in the prefractionator we need to maintain the split between components B and C. In the main column, there are three internal profiles that must be maintained. We need to keep the split between A and B in the top (between the distillate and side-stream 1). In the middle section (between side-streams) there is a B/C-split, and the C/D-split in the bottom (between side-stream 2 and the reboiler) must be maintained. In all, this requires closing 4 regulatory control loops in composition or temperature, and we need to find suitable measurements and pair them with the available inputs. These loops need to be relatively fast, and since composition measurements are usually slow (large effective time delay) and with variable reliability, we propose to use temperatures as the controlled variables.

6.3 Regulatory layer considerations

As mentioned the regulatory control layer should stabilize the plant operation, and the focus is now on dynamic performance as opposed to the steady-state economic criteria used in selecting the primary controlled variables. If possible, we would like the regulatory control to be independent of the layer above. That is, we want the control structure (of the regulatory layer) to be independent of the operational mode (Section 3.3) and the operating point of the column.

We will here apply different criteria for the selection of temperature locations and compare them.

6.3.1 Temperature Locations

The following analysis assumes a temperature measurement on every stage in the column (Figure 6.2). This is unlikely to be found in "real-life" implementations, but we may use the analysis as a design procedure to decide on where in the column to place the temperature sensors. Also, when studying

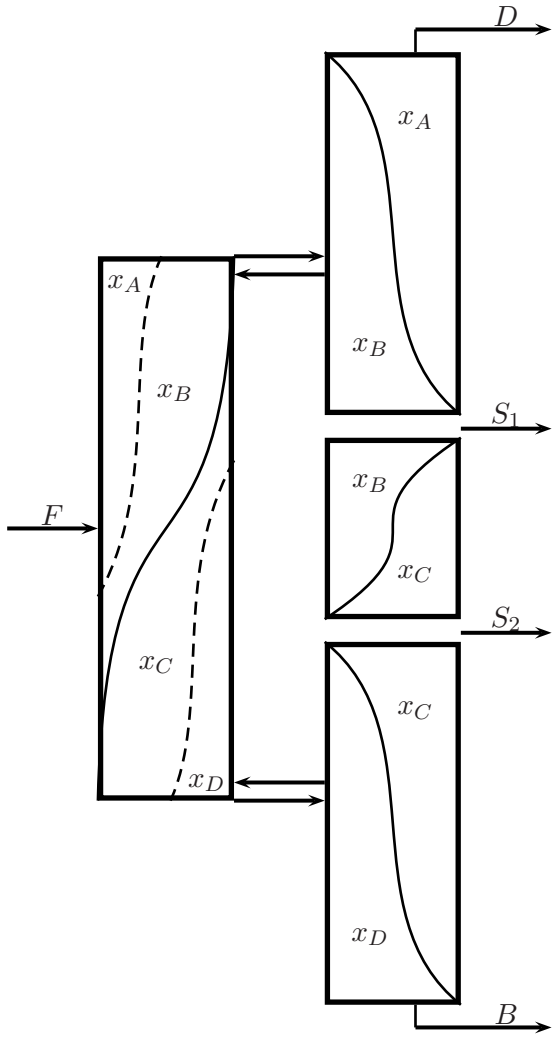

Figure 6.1: The Kaibel column has four internal component splits that need to be maintained for successful opertion. Shown here are hypothetical composition profiles within the column.

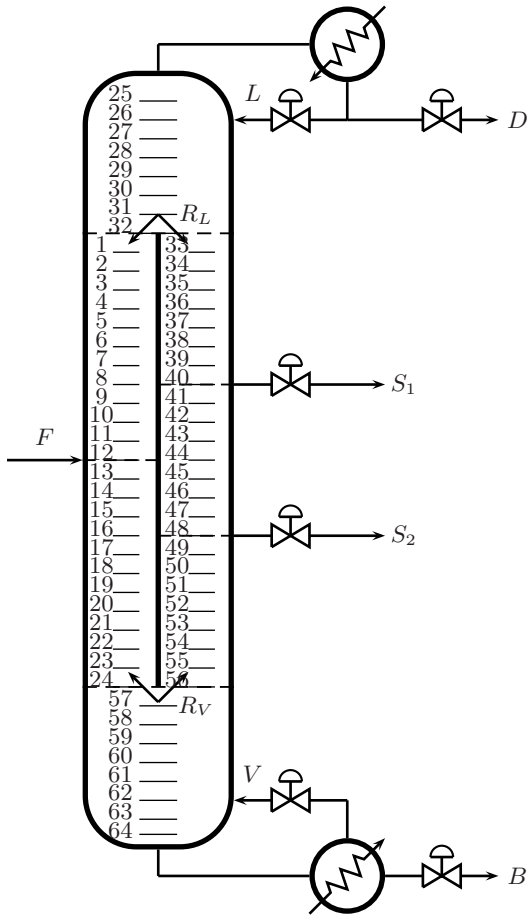

Figure 6.2: Stage numbering

an existing column, the methods and procedures can still be used with a limited number of measurements.

6.3.2 Available inputs

The following working example takes its nominal operating point from Mode 1 in Chapter 3, which is where the purities of all products are maximized. However, the available inputs are considered the same regardless of operating mode and the results for operating point Mode 2 and Mode 3 are given later in the chapter.

Considering the manipulated variables, the feed rate is assumed given, and the vapour split ratio, R_V, is excluded from the input set in all cases. Even though we have included R_V in the top-down analysis (Section 3.1.1),

its practical implementation is still not realiztic in an industrial setting (See Chapter 8). Should a successful implementation of the vapour split as a manipulated variable be achieved it would not significantly change the conclusions in the chapter, because it would replace the liquid split (R_L) which has a very similar effect.

The vapour boil-up rate V is also omitted from the set of available inputs as it is a variable that is likely to saturate (evidently this is the case if nominally $V = V_{max}$ as in some of our cases).

The set of available inputs then becomes:

$$\mathbf{u}_2^T = [R_L \quad L \quad S_1 \quad S_2] \tag{6.1}$$

F, R_V and V are instead treated as process disturbances in the dynamic response simulations later on.

6.4 Criteria for measurement selection

In the literature there are both analytical methods and heuristic rules for choosing the controlled variables and also temperature locations in a distillation column. Several rules are proposed and discussed by Luyben [21], Skogestad [36] and Hori and Skogestad [15].

We will evaluate the following criteria for choosing temperature locations in a Kaibel dividing-wall column:

- Slope criterion
- Sensitivity criterion
- Combine sensitivity and pair close

6.4.1 Slope criterion

We evaluate the temperature change from tray to tray in the column, and select for each of the four "profiles" to be stabilized the tray that experiences the largest temperature change. A large change in temperature indicates in turn that the compositions are changing rapidly, hence giving a large "initial" gain which is good from a dynamic point of view.

The temperature difference from one stage to the next can be seen in Figure 6.3. In the prefractionator, the tray above the feed is chosen; while in the top and bottom the trays just above and below the dividing wall have

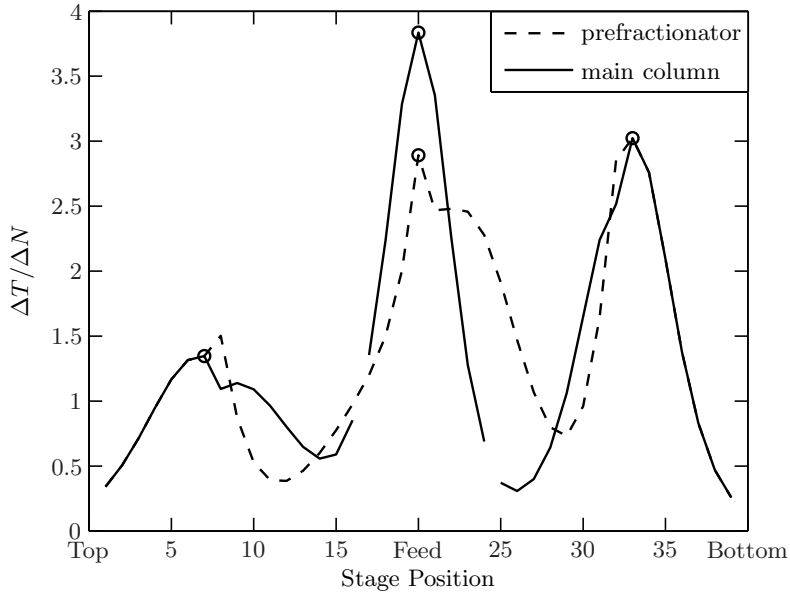

Figure 6.3: Case 1. Temperature difference from one stage to next, $T_{i+1} - T_i$. The chosen temperatures in each section are indicated.

the largest slope. The middle tray in the middle main column section is the fourth temperature. The temperatures chosen are:

$$T_{slope,1} = [T_{12} \quad T_{31} \quad T_{44} \quad T_{57}] \tag{6.2}$$

6.4.2 Sensitivity criterion

The sensitivity criterion has a strong justification in terms of avoiding steady-state drift of the profile. It says that we should find the tray with the largest change in temperature for a change in a manipulated variable. This is the same as maximizing the unscaled steady-state gain. A tray temperature with a large gain will be easier to control than one with a smaller gain.

The steady-state gains of the linearized model can be seen in Figure 6.4. Again we decide to look for a temperature in each of the four main sections of the column. In doing this, we have already decided on the pairing of inputs to outputs, but any other pairing would likely lead to problems with interactions.

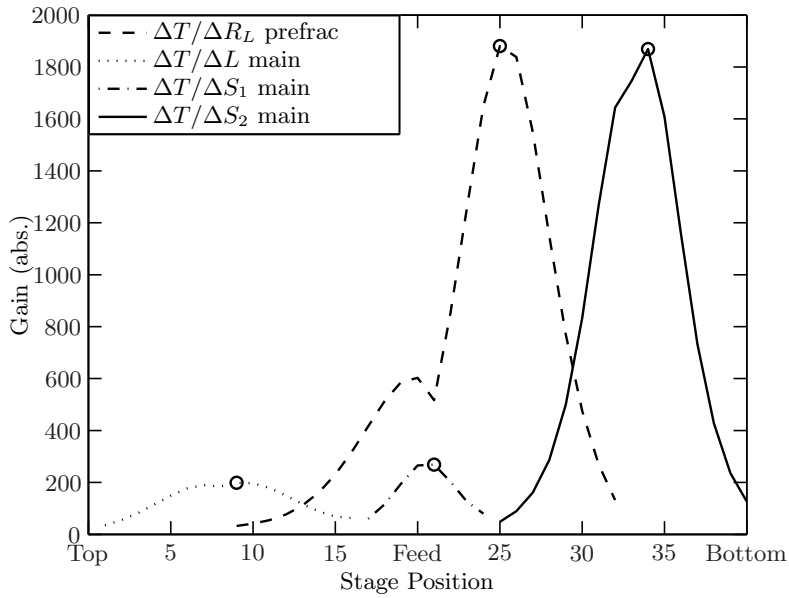

Figure 6.4: Steady-state gains of the column. Note that only the relevant input in each column part (from a dynamic point of view) is shown along with the stage that has the maximum sensitivity.

The four temperatures chosen from the sensitivity criterion are:

$$T_{sens,1} = [T_{17} \quad T_{33} \quad T_{45} \quad T_{58}] \tag{6.3}$$

6.4.3 Combine sensitivity and pair close

To avoid problems with time delay, a rule of thumb is to choose a temperature close to the manipulated variable ("pair close"). The four inputs in our column are all related to liquid streams, and fixing a temperature far down in the column section will introduce larger time delay to the controller than if a temperature was chosen closer to the "origin" of the input. Therefore, we may want to adjust the locations chosen by the sensitivity criterion to make sure we are not introducing large time delays.

In the example above the temperature with the highest sensitivity in the prefractionator (T_{17}) is below the feed and far from the liquid split (R_L) (actually, it may not be that bad, and one could consider using R_V instead if that was available). By moving the controlled temperature above the feed we reduce the time delay. The temperature on stage 10 (T_{10}) seems like a

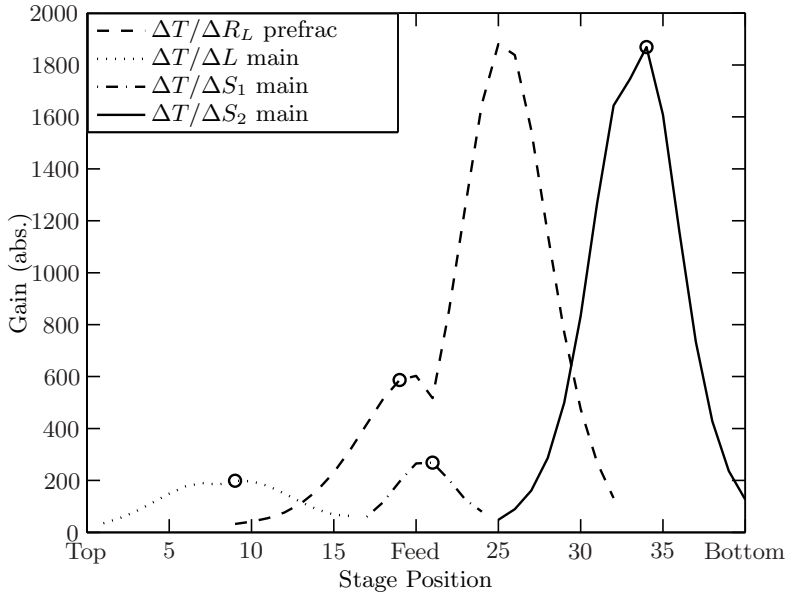

Figure 6.5: Temperature location adjusted to pair controlled variables close to the manipulated variables..

good candidate (See Figure 6.5). It is closer to the input, above the feed stage and still has a reasonably high gain. The other three pairings seem acceptable from a dynamic point of view at first glance. Thus, the four temperatures chosen are:

$$T_{pc,1} = [T_{10} \quad T_{33} \quad T_{45} \quad T_{58}] \tag{6.4}$$

As we can observe, the temperatures chosen by the two (three) criteria do not differ significantly. This is good because it means that the locations are favorable both from a dynamic gain (slope criterion) and steady-state gain (sensitivity criterion) point of view. The largest discrepancy is in the prefractionator where the first criterion places the temperature to be controlled just above the feed stage, while the sensitivity criterion as mentioned chooses a stage further down in the prefractionator.

6.4.4 Other operating modes

In the above analysis the operating point of the Kaibel column was taken from Mode 1 in Chapter 3 where different operating modes for the column were defined. We apply the same criteria also for Mode 2 and Mode 3. The

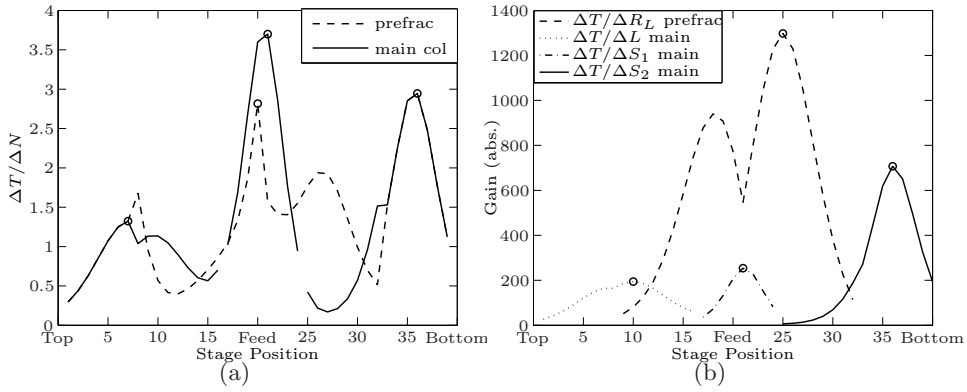

Figure 6.6: Slope-(a) and sensitivity (b) criteria for Mode 2.

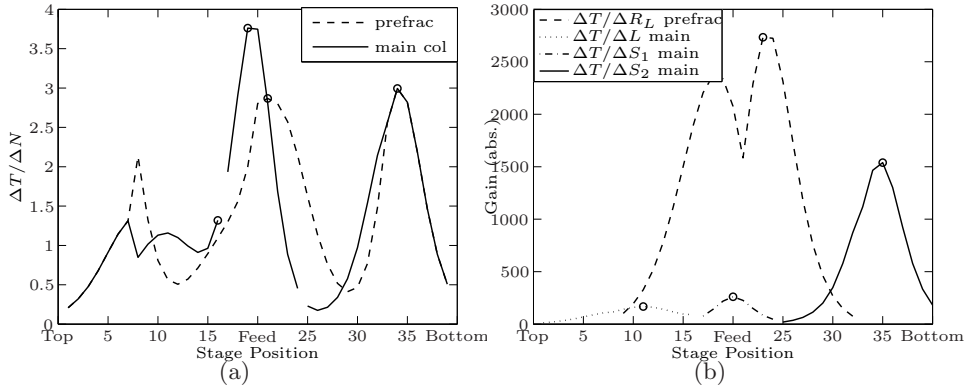

Figure 6.7: Slope-(a) and sensitivity (b) criteria for Mode 3.

plots of slope and sensitivity are shown in Figure 6.6 for Mode 2, while Mode 3 is visualized in Figure 6.7. The results for all three modes are summarized in Table 6.1. As expected, except for the prefractionator, the measurement selection does not differ much when moving to a different operating point. This is important because we want the stabilizing temperature loops (as given by the locations in Table 6.1) to be independent of the plant economics (as given by modes 1, 2 and 3).

6.4.5 The minimum singular value rule

At this point, it is worth to recall a result from Chapter 4, where controlled variables were found for the supervisory control layer. In Section 4.3.1 the minimum singular value rule of Halvorsen [13] was applied to Mode 1 to

Table 6.1: Temperatures for regulatory control

	R_L	L	S_1	S_2
Mode 1				
Slope	T_{12}	T_{31}	T_{44}	T_{57}
Sensitivity	T_{17}	T_{33}	T_{45}	T_{58}
Pair close	T_{10}	T_{33}	T_{45}	T_{58}
Mode 2				
Slope	T_{12}	T_{31}	T_{45}	T_{60}
Sensitivity	T_{17}	T_{34}	T_{45}	T_{60}
Pair close	T_{10}	T_{34}	T_{45}	T_{60}
Mode 3				
Slope	T_{13}	T_{40}	T_{43}	T_{58}
Sensitivity	T_{15}	T_{35}	T_{44}	T_{59}
Pair close	T_{10}	T_{35}	T_{44}	T_{59}

find a set of four temperatures that would, when kept constant, give acceptable loss (with respect to the objective function) when faced with process disturbances. The minimum singular value rule (or 'Max Gain Rule') has also been suggested as criteria for selecting controlled variables for the regulatory control layer [36]. For Mode 1 the previous result can be repeated here and the temperatures found were:

$$T_{minsv} = [T_{10} \quad T_{35} \quad T_{45} \quad T_{57}] \tag{6.5}$$

As we can see, the selected temperatures are very close to the ones selected using the other three criteria. This indicates that, when applied, the control loops will work both as stabilizing controllers and at the same time give small steady-state loss. It must be emphasized, however, that the result from minimum singular value rule depends on the objective function (in this case Mode 1), and is not a general result for the Kaibel column.

6.5 Dynamic simulations

To test the control loops derived in the previous section, we make use of the full dynamic model of the Kaibel column. Since the temperature locations found for the different operating modes were very similar, we choose one set and test it on all three modes. Using the criteria of combining sensitivity and pairing close to the input, the following set is selected from Mode 1:

$$T_{pc,1} = [T_{10} \quad T_{33} \quad T_{45} \quad T_{58}] \tag{6.6}$$

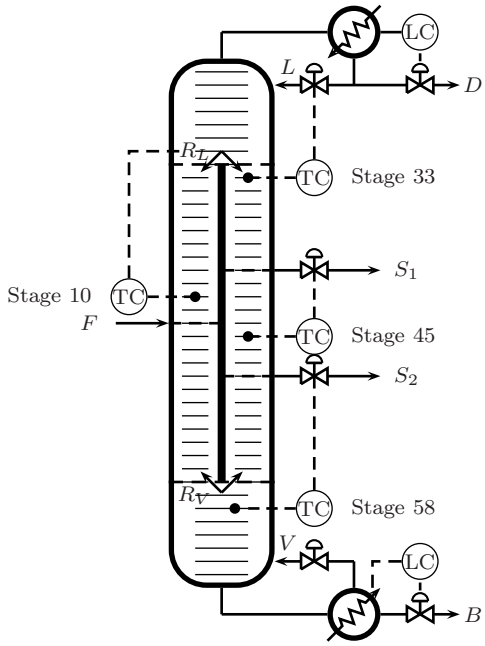

Figure 6.8: Regulatory control layer for the dynamic simulations.

The resulting control loops can be seen in Figure 6.8.

For each operating mode, the same four temperature control loops were applied. The loops were individually tuned for each mode using the SIMC tuning rules (Skogestad, 2003 [34]).

Several disturbances were applied to test the control configuration and four are presented here:

- d_1: 10% increase in feed flow, $F + 10\%$
- d_2: 20% increase of component A in the feed (with a corresponding deacrease in component D), $z_A + 20\%$
- d_3: 10% increase in vapour boil up, $V + 10\%$
- d_4: 10% increase in vapour split ratio, $R_V + 10\%$

The disturbance responses are shown in Figure 6.9. The plots are divided such that Mode 1 is represented in the first column from the left, Mode 2 in the middle and Mode 3 to the right.

Figure 6.10 shows how the product compositions vary for the same disturbances. Note that the compositions are not controlled and the reference lines (dotted blue lines) indicate the initial (steady-state) value only. In the case of Mode 2 they indicate also the product specifications.

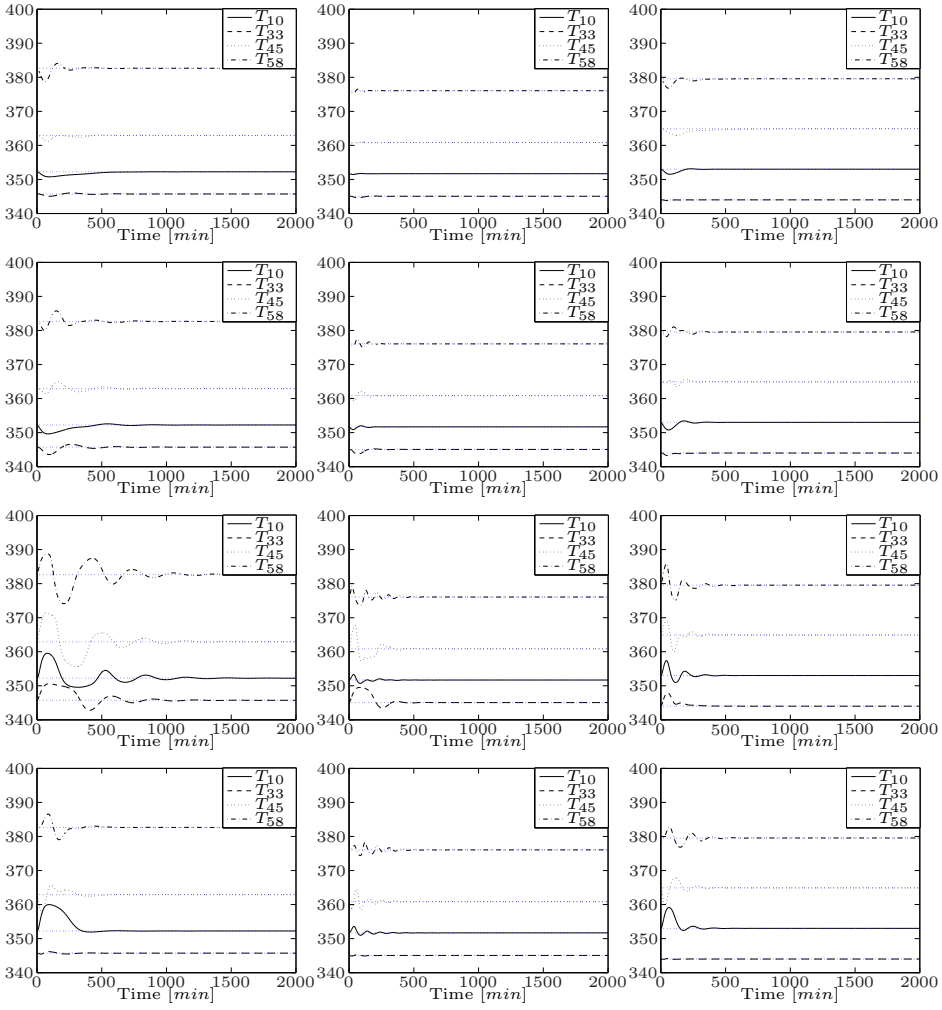

Figure 6.9: Disturbances responses. The columns represents (from the left) operating modes 1, 2 and 3. First row: $F + 10\%$. Second row: $z_{A,F} + 20\%$. Third row: $V + 10\%$. Fourth row: $R_V + 10\%$.

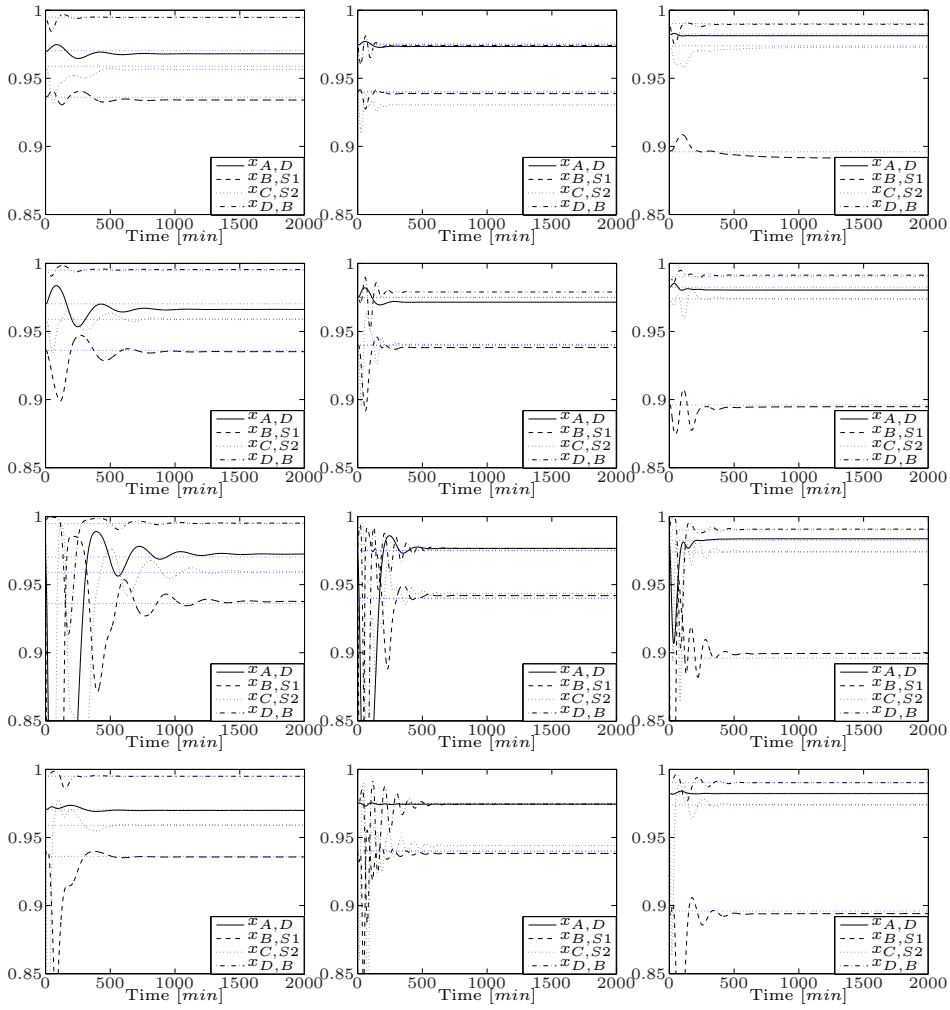

Figure 6.10: Disturbance responses for controlled temperatures found with minimum singular value method (a) $F + 10\%$, (b) $z_{A,F} + 20\%$

6.6 Conclusions

The purpose of the regulatory control layer is to stabilize the plant operation. For a distillation column that means stabilizing the composition profile(s) around its operating point, avoiding "drift" and overcoming process upsets (disturbances). As composition measurements are usually slow and expensive, temperature measurements are recommended here for the regulatory control.

From the results presented here it can be concluded that using four temperature control loops will effectively stabilize the Kaibel distillation column. It has also been shown that good locations for the temperature measurements are independent of the operating mode (economic objective) of the column.

Chapter 7

Pilot plant column

7.1 Introduction

The laboratory Kaibel distillation column was built with the purpose to study its practical operation and control. Experimental results from dividing wall columns are limited in the literature. Some groups have studied the Petlyuk arrangement or equivalent three-product dividing-wall column [1, 26, 27] as described in Chapter 2. We know of one Kaibel column operating for BASF [28], but data from experimental work on the 4-product dividing wall column has not been published to date.

The design chosen for this column was not a dividing-wall column in the strictest sense, but rather a thermodynamically equivalent two-shell realization of a fully thermally-coupled four-product column. The choice was made because it was believed that a two-shell column is easier to build and operate in practice. In addition, it was intended to build the column using glassware column sections of which some were already in stock at the time.

7.2 The column

The Kaibel column was built in the laboratory hall at the Chemical Engineering Department, NTNU. It is supported by an aluminium frame as shown in Figure 7.1. The column itself is made of glass sections produced by Normag Labortechnik in Germany. The standard sections have an inner diameter of 50 mm. They are vacuum jacketed so that the flange size is DN 80. The outer jacket wall has a silver coating to reduce radiation loss, but sight-strips are included to allow some inspection into the inner column. The standard column sections used are 900 and 730 mm respectively,

while the liquid-divider sections (product draws) are 450 mm in length. The "splitting" sections that combine prefractionator and main column shells are custom made into Y-shapes of approximately 500 mm length. The liquid dividers and feed sections have threaded connections (GL25) for product and feed tube attachment. Those parts as well as the Y -sections have extra connections used for inserting temperature sensors inside the column.

7.2.1 The liquid-dividers

The dividers facilitate the liquid draw off via a swinging funnel operated with a solenoid magnet (Fig. 7.2). At the top of the section is a tray that collects liquid into a downcomer. The downcomer leads the liquid into the swinging funnel, and depending on its position, the liquid will either continue down the column as reflux or it will be led into a side pocket and be drawn off as product.

7.2.2 Column connectors

The top Y-piece or splitting section also has a swinging funnel incorporated for the distribution of liquid split between the two columns. Here, a small vertical wall is positioned directly below the funnel outlet and the funnel swings to direct the liquid flow to either side of the wall. The bottom connecting piece has no internals except for a liquid re-distributor which ensures the liquid enters the middle area (away from the section walls) of the bottom section.

7.2.3 Vapour split valves

The original valves installed were butterfly-valves in stainless steel. The flange sizes were equal to the flanges on the glass column sections but to avoid excessive weight, the inner diameter was kept at 80 mm (the normal diameter for a DN 80 flange as there is no double wall here as opposed to the glass sections). The valves had a manual lever with a 90 degree range between fully open and fully closed. These valves were eventually replaced with different type (See Section 7.5.2).

7.2.4 Reboiler

The reboiler is a kettle type boiler made of stainless steel and has a maximum capacity of approximately 15 litres. Electrical heating elements with a combined effect of 3 kW are inserted through the wall near the bottom of the tank. The minimum liquid volume required to cover the elements is

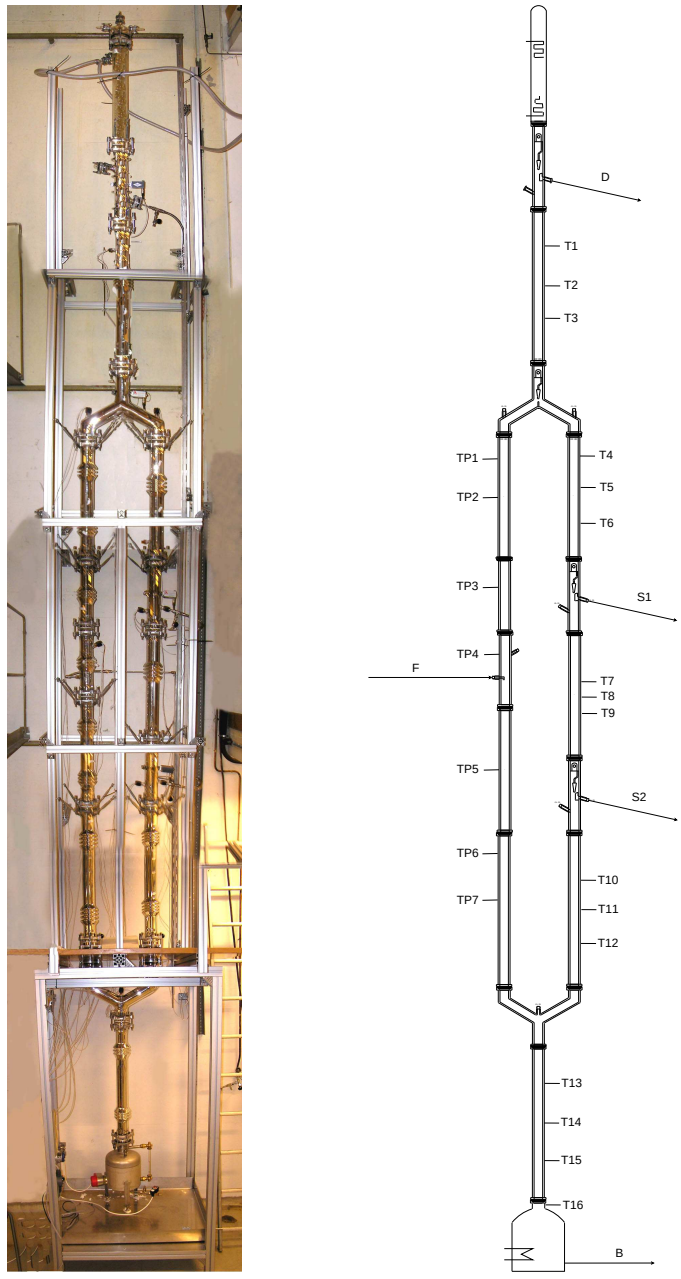

(a) (b)

Figure 7.1: Laboratory Kaibel column. (a) Assembled photo showing column and supporting frame. (b) Scaled drawing indicating streams and the locations of temperature sensors.

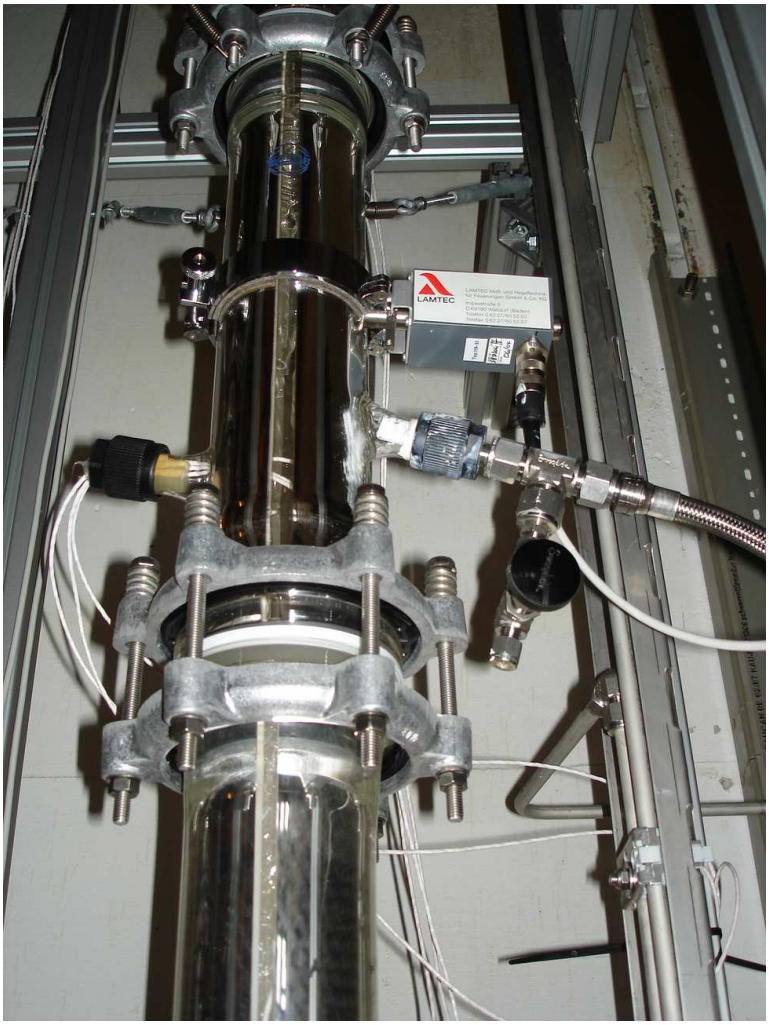

Figure 7.2: Side-stream product draw. Swinging funnel inside column section directs the liquid to the product line or as reflux.

3 litres. A level gauge is attached to the side of the reboiler to allow for monitoring of the liquid level.

7.2.5 Condenser

The condenser sits directly on top of the column as a further extension to the topmost column section. There is no distillate/reflux tank from which the reflux is drawn. Instead the condensed liquid flows back down, countercurrent to the vapour, and into the swinging funnel that directs the liquid to either distillate product or reflux. The swinging funnel thus sets the L/D ratio of flows.

7.2.6 Packing

To facilitate the placement of temperature sensors inside the column sections, it was decided to fill the column with random packing material. For cost effectiveness and simplicity, Glass Raschig rings with a diameter of 6 mm were used.

7.2.7 Assembling the column

The column is mounted inside, and supported by, an aliminium frame. Because of the considerable weight of the stainless steel valves used for vapour split, and that they were to be mounted directly on top of the lower column connector (Y-piece) it was decided that the valves had to be fixed to the supporting frame and thus become the fixation point for the entire column. This was mainly to protect the glass Y-piece from excessive stress from the weight of the valves but also to prohibit the movement of the valves when turning the levers. The fixed point of the column was then about 2 metres above ground level, with the sections below the valves "hanging free". The weight of the reboiler was compensated with springs attached to the column frame. Above the vapour split valves, the column sections are resting on top of each other but their weight is also compensated using springs. 4 springs and adjustable turnbuckles are attached to each flange-connection (Figure 7.3). The springs are adjusted to lift the weight of the section below. The spring system has a dual effect; while lightening the stress on the glass section it also helps in positioning the column.

Figure 7.3: Springs and turnbuckles help centering the column and compensates for the weight of each column section.

7.3 Instrumentation

7.3.1 Measurements

Inside the column, a total of 24 temperature sensors of type PT-100 are placed at various locations (See Figure 7.1b). The individual sensors with wire are inserted in the relevant column section during the filling of the Raschig rings, so that the packing keeps the sensors in place. In addition to the PT-100 elements, thermocouples (type K) are used for external temperature measurements on heat tracing, feed tube and reboiler wall etc.

The only other measurement available is a differential pressure sensor, used to monitor the liquid level in the reboiler.

7.3.2 Actuated inputs

The feed is pumped and metered by a digital diaphragm dosing pump. The dosing rate can be set remotely from the control interface. The pump has a range from 0.2 to 20 l/h.

The bottoms product draw is controlled using a solenoid operated valve (on/off). The rate is set by specifying the switching-frequency.

The three other product draws plus the liquid split divider are all op-

erated by swinging funnels inside the column sections. They act as on-off valves and are controlled using solenoids attached to the outside of the column wall (See below, Section 7.4.2)

The reboiler heat duty is controlled by supplying variable voltage to the heater elements through a thyristor.

7.4 Data acquisition and control

All the measurements and actuators are connected to a Fieldpoint modular I/O system from National Instruments in a central cabinet. The system consists of several interconnected Fieldpoint modules that are either input or output modules. A network interface module, FP-1000, connects the modules to a PC through an RS-232 cable. The PT-100 elements are connected to three modules of type FP-RTD-124 while the differential pressure measurement is connected to an analog input module of type FP-AI-112. An FP-TC-120 connects the thermocouples. The actuators are connected via two FP-AO-200 analog output modules. The analog output modules deliver current output in the range 4-20 mA.

7.4.1 Labview interface

The column is operated using an interface (Figure 7.4) created in the LabVIEW development tool from National Instruments. It is the interface that reads and writes the signals to the Fieldpoint interface module. Measurements are visualized on the computer screen an the values of the actuator can be manipulated. All measurement and actuator signals can be written and stored to a data file during an experiment. The LabVIEW interface also includes the various controllers used in the column operation.

7.4.2 Controllers

There are four PID-controllers implemented through the LabVIEW interface to control the Kaibel pilot column. They are temperature control loops used for keeping selected temperature measurements at their setpoints. The actuators are the four swinging funnels that operate in a timed cycle. The swinging funnels have two positions: The position “at rest”, is the default position when no current is sent to the solenoid. The funnel hangs vertically straight down and the liquid continues down the column. In the case of the liquid split the liquid is sent to the prefractionator side of the column partition. In the “excited” position, the solenoid is activated an the funnel swings towards the column wall sending the liquid into the product line, or

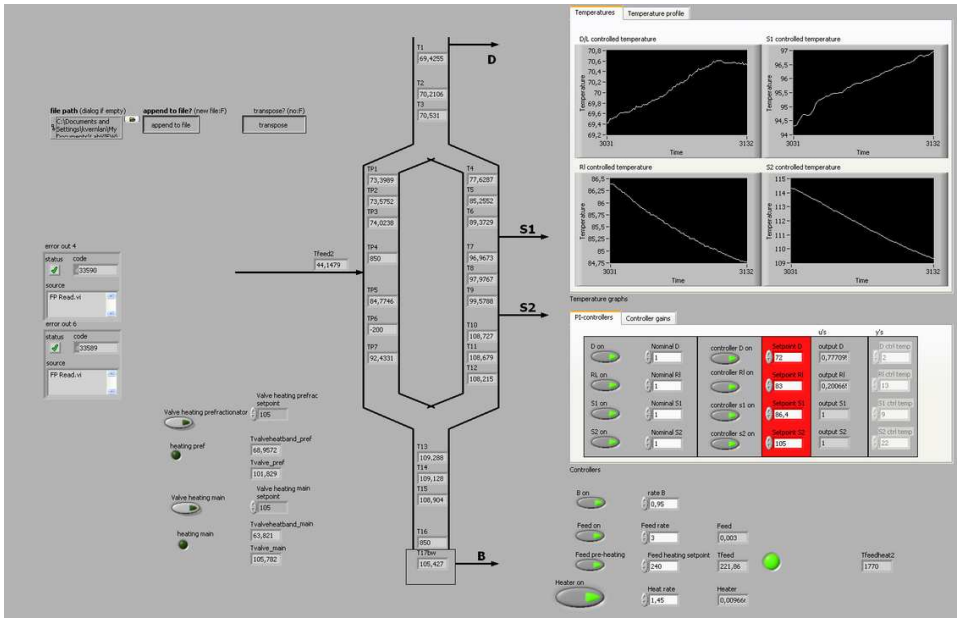

Figure 7.4: Graphical user interface for the column operation

in the case of the liquid split, sends the liquid to the main column side of the partition. A fixed interval of 5 seconds is used, during which the funnel will swing between its end positions at most once each way. The actual manipulated variable is the ratio of the time that the funnel spends in the rested position to the total time of the cycle (5 seconds). Assuming that the liquid flow rate into the funnel is constant during this interval, we can then describe the manipulated variable as the ratio of reflux to the total liquid into the funnel. E.g. for the funnel controlling the distillate product we have:

$$u_D = \frac{L}{L+D} \qquad u_D \in [0,1] \tag{7.1}$$

Thus, for a value of $u_D = 1$ we have total reflux, while a value of $u_D = 0.8$ means that the funnel will move to the side of the wall for one second, then move back to the resting position and remain there for four seconds. The other product draws are defined similarly, while for the liquid split the input is defined as:

$$R_L = u_{R_L} = \frac{L_p}{L_p + L_m} \qquad R_L \in [0,1] \tag{7.2}$$

where L_p and L_m is the liquid flowing to the prefractionator side and main column side of the partition respectively.

The control algorithm used is one of LabVIEW's PID controllers (PID Advanced.vi) with bumpless transfer and anti wind-up. Only proportional and integral action has been used.

In addition to the PID loops, the heating tapes on the feed line and vapour split valves are controlled using thermostat control. These are set manually.

7.5 Manipulating liquid and vapour split

Dividing-wall columns and thermally coupled columns have one feature that distinctly separates it from conventional distillation columns. That is the distribution of liquid and vapour flows to the different column partitions. For a dividing-wall column with the partitioning wall vertically positioned in the middle of the column (i.e. there are column sections above and below the wall), we have what we denote a liquid split at the top of the partition and a vapour split at the bottom. A suitable ratio of flows to either side of the partition is very important to the successful operation of a dividing-wall column.

7.5.1 Liquid split

To achieve the liquid split, a practical solution would be to draw off all liquid above the partitioning wall and transfer it to an intermediate holdup-tank before pumping and metering the liquid back to the column on either side of the dividing wall [1, 26]. Some alternative methods have been reported by the industrial manufacturers:

Julius Montz GmbH (www.montz.de) use a reflux splitter that directs the liquid to two outlets depending on the position of the dividing body, similar in principle to the swinging funnel used in our column. Probably the splitter is located outside the column and depending on the flow rates and sizes involved, the liquid can be returned to the column by pumping power or gravity flow.

Koch-Glitsch have developed a solution [38] with a chimney tray that meters the liquid in a fixed proportion and an external by-pass that can control the liquid split as required. In this case, they use a variable liquid split to compensate for changes in the vapour split.

Both companies say that they use the liquid split for control. Though it is not reported whether they use the liquid split for active feedback control, we have shown earlier that this can be very beneficial and in some cases crucial to achieving optimal operation.

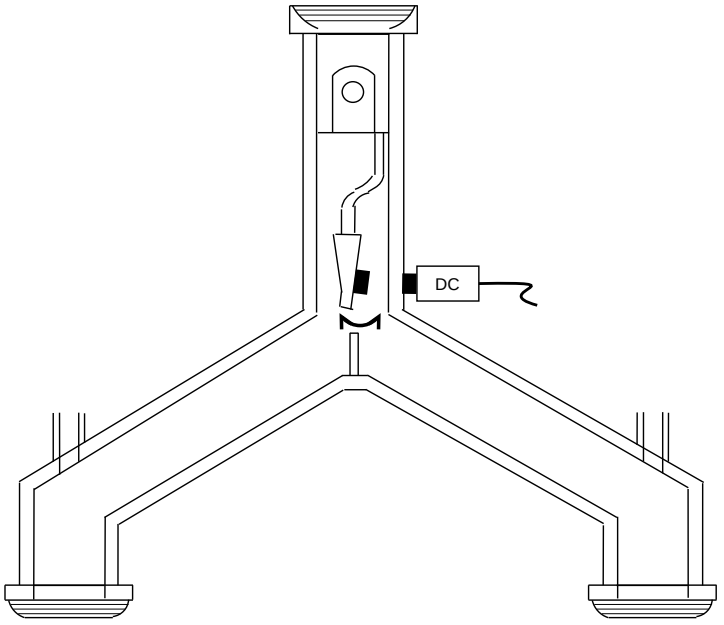

Figure 7.5: Detail of the liquid split section. The solenoid operates the swinging funnel which distributes the liquid reflux to either prefracionator (left) or main column (right). (The nozzles shown on either side are for inserting temperature measurements inside the column.)

The liquid split device used in the laboratory Kaibel column is an internal implementation. As mentioned above, a solenoid operated swinging funnel distributes the liquid to either of the two column sections below it (See Figure 7.5. The funnel is situated in the upper part of the column connector section that connects the two parallel sections. The time spent by the funnel at both extremities determines the liquid split ratio, R_L.

7.5.2 Vapour split

When it comes to the vapour split, there are no reports of adjustable vapour splits in experimental or industrial dividing wall columns*. In the literature (Chapter 2), there is some discrepancy between authors as to whether the vapour split may be regarded as a dynamic degree of freedom or not. Most papers, however, treat the vapour split as a degree of freedom for design

*There exists a patent by Giroux [10] of Phillips Petroleum (1980) that presents a dividing wall column with external valves to control the vapour distribution, but there are no records of its implementation.

only. As an example, the review paper by Dejanovic et al. [8] claims that: "*... vapour split ratio is practically pre-determined in the dimensioning stage and it is self adjusting, so it can not be utilized as a manipulated variable.*"

As a design variable the optimal vapour split ratio is first determined on the basis of the separation to be achieved. Then in the detail engineering phase calculations have to be carried out to determine the pressure drop over the various packing sections and distributors etc, taking into account the liquid load on all sections. The designer can then balance the pressure drop on both sides of the wall by the positioning of the wall. The off-centre positioning of the partition wall in a packed dividing wall column is possible thanks to the non-welded wall technology of Julius Montz GmbH [16].

The vapour split is self adjusting in that it distributes according to the pressure drop on both sides of the wall. However, the distribution (pressure drop) may change with the liquid loads, and as shown by Niggemann et al. [27], heat transfer across the wall may cause condensation and evaporation that have considerable effect on the pressure drop and therefore vapour split ratio. Because of this, a fixed vapour split in the design phase is not necessarily a fixed vapour split during operation and a varying vapour split should at least be considered as a process disturbance. One may argue that if the desired vapour split ratio is not achieved, it can be compensated by adjusting the liquid split. This is true up to a point as we have shown in Chapter 5, but if the ratio is too far off from the optimal value the product purities or at least the column efficiency will suffer. It would therefore be of advantage to the operation of a dividing-wall column, be it with one or more side streams, to be able to adjust the ratio of vapour flows during operation. This is certainly the case if the column is subject to frequent changes in the feed as the optimal settings of both vapour and liquid split ratios will move with varying conditions. If, in addition, a method of adjusting the vapour split was found that was relatively fast and could be manipulated automatically, one would have an extra degree of freedom for control that could be used to increase purities or make the separation more energy efficient in the face of process disturbances.

When planning the construction of the Kaibel pilot column, the idea of a variable vapour split was seen as a particularly interesting challenge. It was therefore decided to attempt to include this with the new apparatus.

7.5.3 Butterfly valves

The first attempt to control the vapour split involved (perhaps naively) inserting standard valves directly into the column sections. Two butterfly valves were installed in parallel above the lower connecting section that

Figure 7.6: Two valves for the adjustment of the vapour split were installed, one on each side of the partition. Here shown under several layers of insulation.

forks the bottom column section into the two separate "columns" of the prefractionator and main column (Fig. 7.6). The valves were with a large bore of almost 80 mm diameter (as compared to 50 mm i.d. of the column sections. This was to allow connection to the column sections which has flanges of DN 80). The valves were adjusted manually using levers.

The large size of the valves was from the start a problem. When going gradually from a fully open position to a fully closed valve, there was no observable redirection of the vapour flow until the very end when the valve was virtually closed. At the time, the only available measurements from which to deduce changes in the internal flows were the temperature sensors, but they should give a clear indication if a change in R_V has occurred. The large diameter of the valve meant that even with only a small opening there were sufficient total area for the flows not to cause significant change in the pressure drop across the valve. Fine adjustment of the valve position was also difficult with the manual levers.

7.5.4 Prototype testing

The experience of the butterfly valves showed that it would be difficult to adjust the vapour flow by constraining the entire cross-section of the column. A method where one could manipulate only the vapour flow after first separating the vapour from the liquid seemed more feasible. This would be analogous to the way the liquid split is performed. A crude experimental rig was set up to test some new ideas for a valve design (Figure 7.7.

To separate liquid from vapour it was decided to design a tray where

the liquid could be collected and passed through a downcomer while the vapour could pass through a separate channel where a variable restriction would manipulate the flow. In the test rig, the tray consisted of an open piece of tube inside a larger tube (forming the column shell). The annulus was blocked off with a rubber gasket, and the liquid collected above the gasket and could be led down past the tray through smaller tubing on the outside of the largest tube. At the vapour exit, above the inner tube, a cap was fixed to form the flow restriction. The cap was fixed below using a spring and above with a retractable string making the cap suspend above the vapour exit. By pulling on the string and fixing it in variable positions, the restriction to the vapour flow could be manipulated.

Two of the above described trays were inserted in the experimental rig shown in Figure 7.7. The rig consisted of 50 mm plastic tubing assembled into a fork-shaped construction. The bottom tube was supplied with an air inlet near the plugged bottom end. The valve trays were placed in parallel in each of the fork ends, and a rotameter was installed above each valve. Water was introduced just above the valve to enable countercurrent air-water flow.

Performing some rudimentary experiments with the rig and the customized trays showed that it was possible control the flow of to either of the two parallel column sections while having a countercurrent flow of water through the sections. The results were promising enough that it was decided to build new valves for the pilot Kaibel column.

7.5.5 Vapour split valves

Building on the principles from the air-water rig, a new vapour split valve was designed and constructed. Figure 7.8 shows a schematic of the design. The valve or column tray is built to fit as a section to the Kaibel pilot column. Liquid is collected on a tray and fed by gravity to a downcomer. The bottom end of the downcomer is truncated so that liquid can accumulate and form a barrier to the vapour. The head of liquid in the downcomer will be balanced by the pressure drop of the vapour across the valve. Vapour is led up past the liquid downcomer and into an area of reduced cross-section. At the exit of this section is a cap fixed to a rack and pinion arrangement that allows its position to be adjusted in the vertical direction. The cap, acting as the "stem" of the valve, is shaped to divert any liquid from above past the vapour exit and down to the tray below. A protruding rim on the cap's underside allows for a tighter fit around the vapour exit channel. Figure 7.9 shows images from the valve internals.

When the valve is fully open (cap in the uppermost position), the pressure drop across the valve is very low, which is an important attribute of

Figure 7.7: Rig for testing new valve solutions using air and water

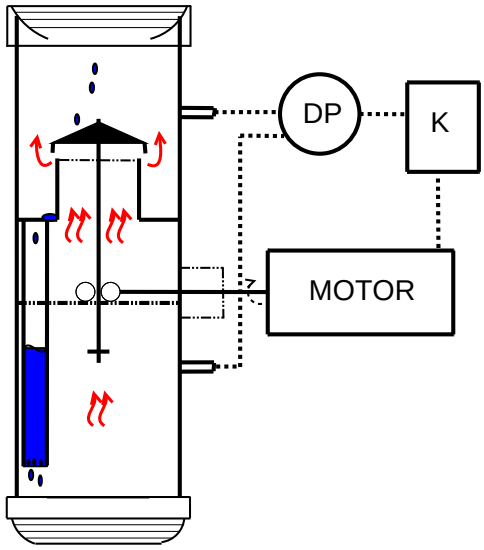

Figure 7.8: Principle drawing of the vapour split valve with a suggested control arrangement.

Figure 7.9: Vapour split valve internals. From top left: Valve in fully open position; Top right: Rack and pinion arrangement. Note the truncated exit of the downcomer; Bottom left: Valve in closed position. The downcomer inlet can be seen to the left; Bottom right: Vapour will flow up through the middle area of reduced cross-section.

the vapour split valve.

The rack and pinion gear is powered by an electric motor attached on the outside of the valve. Position switches protect the gears and motor from damage.

7.6 Acknowledgement

The work on the vapour split valve prototypes (Section 7.5.4) and the design of the final valves (Section 7.5.5) were performed in cooperation with Professor Heinz Preisig.

Chapter 8

Experiments

8.1 Introduction

The laboratory Kaibel distillation column was built with the purpose to study its practical operation and control. In this chapter we discuss some of the challenges faced during the commissioning of the pilot plant and present various experimental results.

8.2 Initial experiments

Early experimental work was concentrated on the practical running of the column and its individual components. The pilot Kaibel was rebuilt a number of times and new problems had to be fixed or improved for each step.

An observation that was made relatively soon after starting experimental work was the lack of reflux available in the upper sections of the column. This was observed by the limited effect on the temperatures in the prefractionator when adjusting the reflux- (liquid-) splitter, R_L, and temperatures recorded in the top section were higher than expected even with total reflux. Measuring the flow from the condenser by temporarily setting $L/(L + D) = 0$ confirmed that distillate and reflux flows combined were at times only slightly higher than the (from mass balance) expected distillate rate. The low reflux rates could also be visually observed through the sight-strips in the top section and liquid-split section.

One cause of the low internal flows in the upper parts of the column was thought to be heat loss to the environment. The column sections themselves are well insulated by the vacuum jackets, but flanges and connections (pipes and sensors) were fitted with insulation to reduce heat loss. The vapour-split valves were heat traced as well as insulated. An infrared camera was

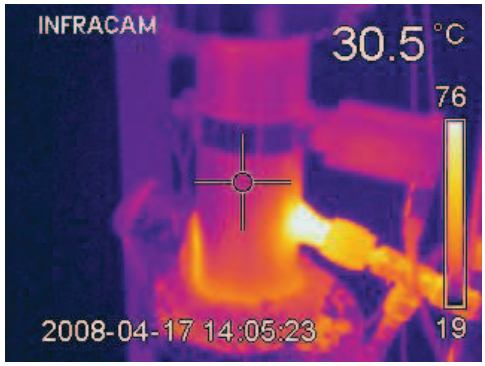

Figure 8.1: Photo of the S_1 side-stream liquid divider taken with an infrared camera. The camera was used to identify sections with large heat losses to the surroundings.

borrowed to identify the largest sources of heat loss (See Figure 8.1). Based on the thermal imaging, more heat insulation was added to the column. There is no doubt that the added insulation was beneficial to the column, but the internal flows in the top did not increase significantly.

To boost the flow of liquid and vapour in the top of the column we wanted of course to increase the vapour boil-up from the reboiler. However, it was clear from early on that the column had a limited hydraulic capacity in the lower end of the column. Flooding was readily observed at the lower junction between the prefractionator and the main column (See Figure 8.2). The bottom section of the column had the same diameter as the other all other sections of the column, and effectively the whole section would flood at relatively low reboiler duties. Thus, from the start the reboiler heat input had to be limited to around 1.3 kW, when it was meant to operate at 2 kW and above (rated at 3 kW).

The limitations caused by having the same internal diameter in all sections of the column is accentuated when one considers the feed mixture used in the experiments. Early trials used an equimolar feed of methanol, ethanol, 1-propanol and n-butanol. With this mixture the volume of butanol is more than twice that of methanol, and the lower parts of the column will naturally have higher loads than in the top.

Knowing that the heat input to the reboiler (and therefore the vapour boil-up) had to be limited, a logical solution would be to lower the feed rate to the column to get a more reasonable ration of boil-up to feed, V/F. Unfortunately, the feed pump was not dimensioned for a lower rate than what was already used. The feed pump (membrane type) was approved for

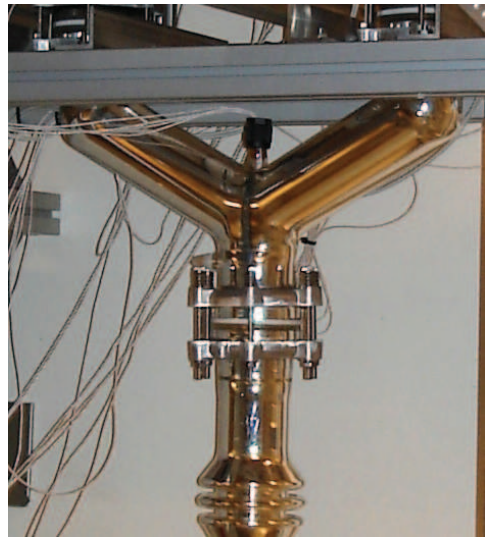

Figure 8.2: The top of the bottom section where the column splits into the prefractionator (left) and main column. Flooding was a problem in this section of the column.

dosing rates from 1 to 20 l/h, but at lower set rates than 3 l/h the pump would not lift the liquid up to the entry point. Therefore, the feed rate was kept at 3 l/h as previously used.

Trials with the column continued despite the limitations described above. The experiments were focused on setting up temperature control loops for the available inputs and tuning the controllers.

8.2.1 Controller tuning

Four temperature control loops were implemented on the column, similarly to the configurations discussed in Chapter 6. The inputs used were the product outlets (actually: $L/(L+D)$, $L_{S_1}/(L_{S_1}+S_1)$ and $L_{S_2}/(L_{S_2}+S_2)$) and the liquid split ratio ($R_L = L_p/(L_p+L_m)$) adjusted with the swinging funnels (See Figure 8.3). The bottoms product outlet valve was intended to be used for controlling the level in the reboiler. However, at the time the differential pressure transmitter installed to do the measurement did not properly function, so the bottoms rate (B) was set manually to a constant rate. A typical set-up of the control loops can be seen in Figure 8.4.

The individual PI-controllers where tuned by first applying open loop step changes in the manipulated variable and then applying Skogestad's SIMC tuning rules [34] to the response. The parameters applied can be

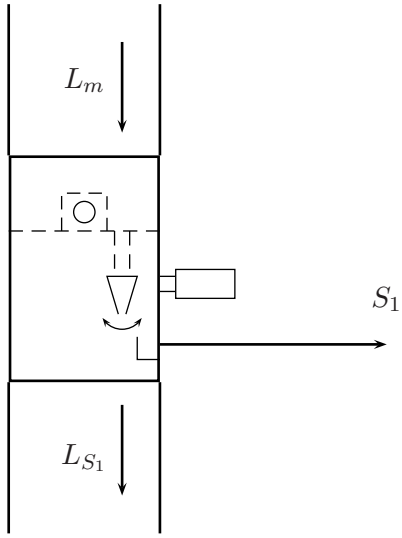

Figure 8.3: Detail of a liquid divider. The product draws are timed to give a ratio of flows.

seen in Table 8.1.

Individually the controllers showed good setpoint tracking. The distillate control loop (as discussed above) and the liquid split controller (see below) had a tendency towards input saturation if setpoints were set outside a fairly limited range.

Below, we give a closer description of the liquid split control and show results from open loop experiments using the vapour split.

8.2.2 Controlling the liquid split

We have previously shown through simulations the importance of adjusting the liquid split for the best operation of the Kaibel column. Particularly, we have used liquid split to control the internal component-split of the prefractionator. The pilot Kaibel has, as mentioned, a liquid-splitter in the form of a column section with an internal swinging funnel that can direct the liquid to either of the two sides of the column partition. The funnel is actuated through a solenoid set to a timed sequence, where the time spent in each position determines the liquid split ratio, R_L.

In the column the liquid split ratio can be set at a constant value from the operating system, but more importantly it can be used as an input to

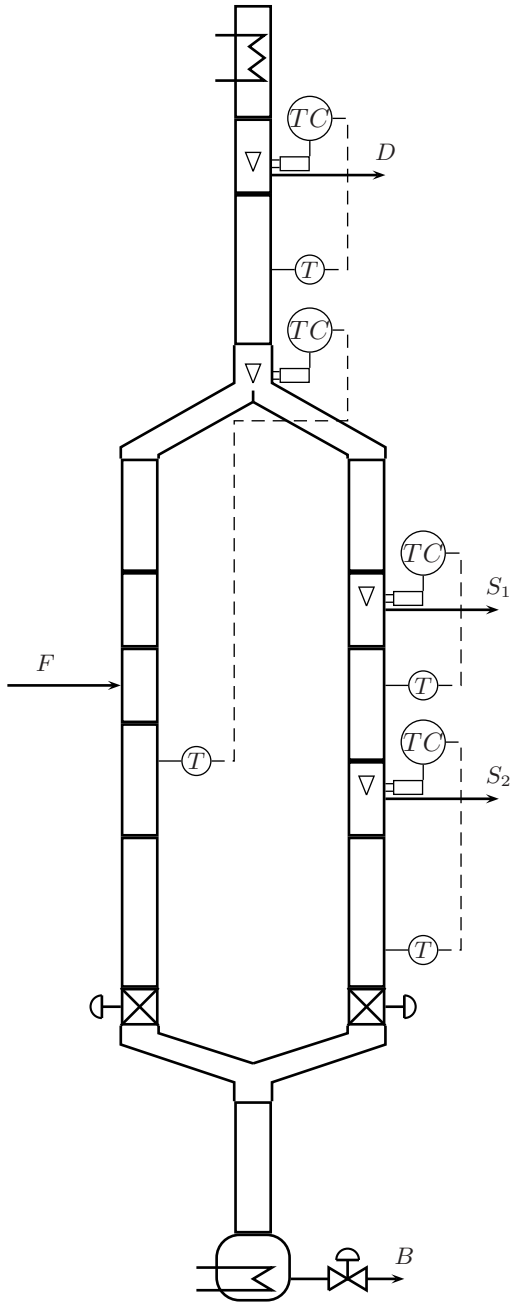

Figure 8.4: Typical control loops for the Kaibel pilot experiments.

Table 8.1: PI-control parameters

Loop	Input	Output	K_C	τ_I (min)
Distillate	$\frac{L}{L+D}$	T2	-1.5	5
Side-stream 1	$\frac{L_{S_1}}{L_{S_1}+S_1}$	T8	-0.11	2.5
Side-stream 2	$\frac{L_{S_2}}{L_{S_2}+S_2}$	T12	-0.43	1.5
Liquid split	$\frac{L_p}{L_p+L_m}$	TP5	-0.86	4

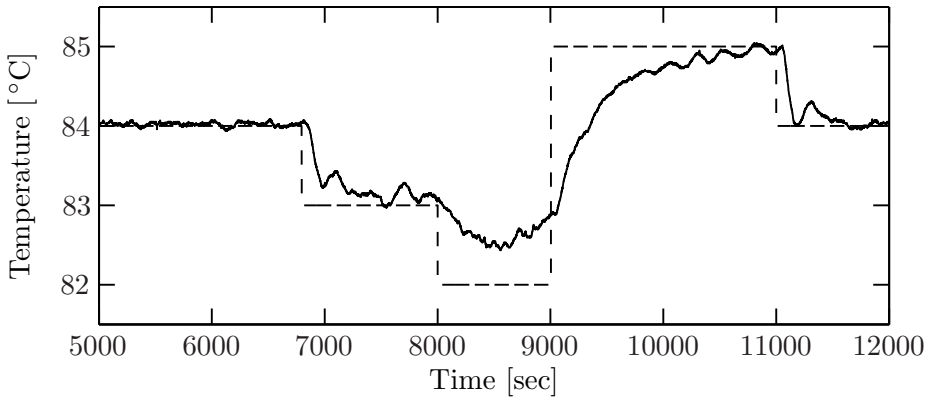

Figure 8.5: Temperature $TP5$ and setpoint

a feedback loop for control. In running the column we have used various temperature measurements in the prefractionator as the controlled variable.

Figure 8.5 shows an example where the liquid split is used to control a temperature in the prefractionator. The temperature measurement ($TP5$) is located approximately 50 cm below the feed entry. The figure shows a series of setpoint changes in the controlled temperature. At t = 6800s, the setpoint is decreased from 84 °C to 83 °C and the temperature responds after some time. However, when the setpoint is further reduced to 82 °C the temperature does not reach the setpoint. In fact, when we look at the liquid split R_L input (Figure 8.6) we can see that the controller saturates, sending all reflux to the prefractionator. At t= 9000s, the setpoint is now increased to 85 °C and the temperature reaches the setpoint after about 2000s. From the input (Fig. 8.6), we see that R_L tends towards a value of around 0.4 - 0.5. Then at t = 11000s, the setpoint is returned to 84 °C with a resulting

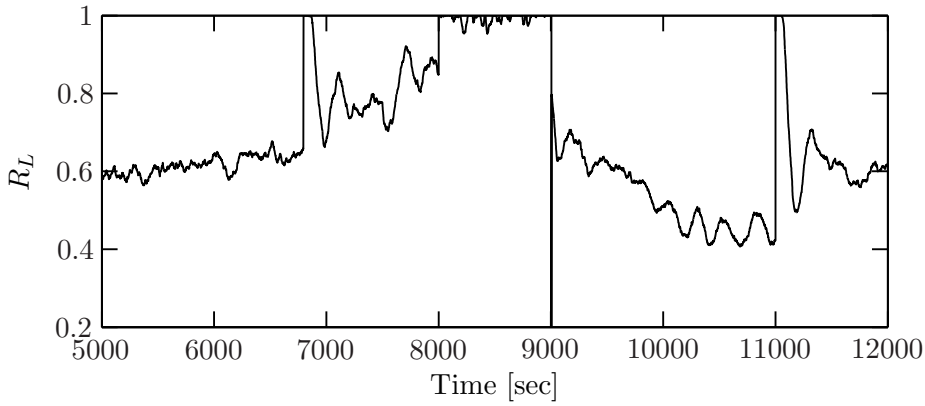

Figure 8.6: R_L controller input

R_L of 0.6.

Discussion: liquid split

The solenoid operated swinging funnel seems to work well in performing the liquid split. Tests have been carried out to verify that the funnel efficiently divides the liquid reflux according to the time spent in each position, and no discrepancies have been found. However, using the liquid split to control the temperature at a position in the prefractionator is not without issues in the laboratory column. Experiments have shown that there is a very limited range of temperatures attainable for any one of the measurements. As seen in Figure 8.6, the input is easily saturated and the liquid splitter will direct the reflux completely to one of the sides. A general observation from experiments is that the prefractionator temperature profile is too "flat". Opposite to the example above, experience have shown that usually the controller will saturate when we try to increase the temperatures in the lower part of the prefractionator.

8.2.3 Manipulating vapour split

With the new vapour split valves installed, some experiments have been performed that show some promise. Whereas adjusting the butterfly valves in practice led to only two valve positions, fully open or fully closed, the new valves can be adjusted to achieve varying vapour flow.

The plots in Figure 8.7 show the temperature responses to step changes in the vapour split, R_V, for the measurements on the main column side (Fig 8.7a) and prefractionator side (Fig 8.7b) respectively. At time $t = 18700$

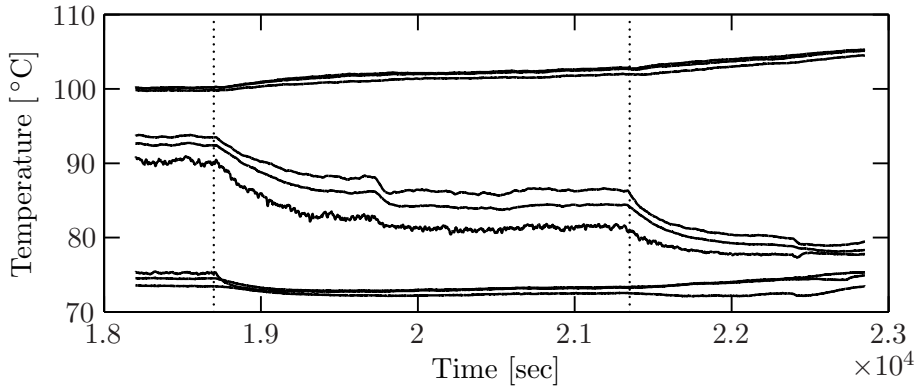

(a) Temperatures on main column side of partition

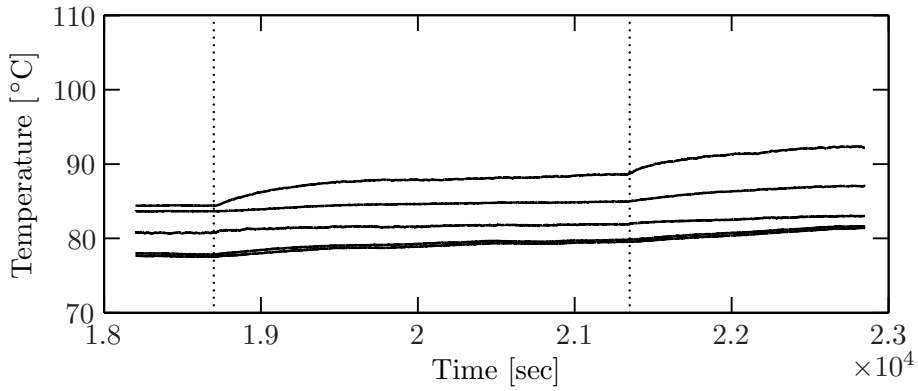

(b) Temperatures on prefractionator side of partition

Figure 8.7: Temperature responses to change in R_V

s the valve on the main column side is moved towards closing, and at t = 21300 s the valve is further closed. We notice that the temperatures in the prefractionator (Fig 8.7b) are increased; indicating that more vapour is being led into these sections. The temperatures below the second sidestream (S_2) are also increased (8.7a), which can be explained by the decrease in lighter components coming down the prefractionator. Further up the main column the temperatures are decreased due to the lowered vapour rate.

These effects are confirmed by simulations. Figure 8.8 shows the resulting temperature responses to step changes in R_V from a simulated Kaibel column. The model* used here has 7 equilibrium stages in the prefraction-

*To date, the majority of experiments have been performed with the purpose of testing

ator (3 above the feed) and 4 stages in each of the 5 sections that make up the main column. The plots show the temperatures at each stage on either side of the "dividing-wall". In the simulation there are no controlled temperatures in the column. Only the reboiler and condenser volumes are controlled using D and B. The initial value of R_V is here set at 0.395, i.e. 39.5 % of the vapour from the bottom section is fed to the prefractionator side of the partition. At time $t = 100$ min, R_V is increased by 5 percentage points, and again at $t = 400$ min to a final value of 0.495. As observed in the experiment, the temperatures in the prefractionator are increased as a result of the increased vapour flow rate to this side of the column (Fig. 8.8b). On the main column side the tendency is again that the stages in the lower region experience increased temperatures, while higher up in the sections the temperatures are decreased.

During the lab experiment, the change caused by closing the vapour-split valve could also be observed from the measured pressure drop across the manipulated valve. With the valve in the open position ($t < 18700$ s) the manometer reading showed a pressure drop of $\Delta P = 8$ mm H_2O. After the first step, the pressure drop increased to 10 mm H_2O and the second step gave a pressure drop of 12 mm H_2O. Figure 8.9 shows how the column temperature profile changes as a result of the steps in R_V. The profiles are shown for time instances before the first step is made (Fig 8.9a), just before the second step (8.9b) and some time after the second step (8.9c). One can clearly see how the middle part of the main column is cooled causing a marked shift in the column temperature profile.

During this experiment, the controllers were set to manual, with the exception of L which was used to control a temperature (T_3) in the top section. After the steps in R_V, this controller eventually saturated and gave close to total reflux in the top. The rates of R_L, u_{S_1} and u_{S_2} were set at 0.3, 0.8 and 0.8 respectively.

Discussion: vapour split

The experiment with the new vapour split valves show that it is possible to manipulate the vapour flow at least to some extent. With reliable measurements of the pressure drop across the valves it would also be possible to adjust the valves online with a constant setpoint on the pressure drop for one of the valves for example. The present valve design is probably not suited for online control, however. The range of valve positions in which

equipment and operating systems. Therefore, the models used in this work has not been validated against experimental data from the laboratory column.

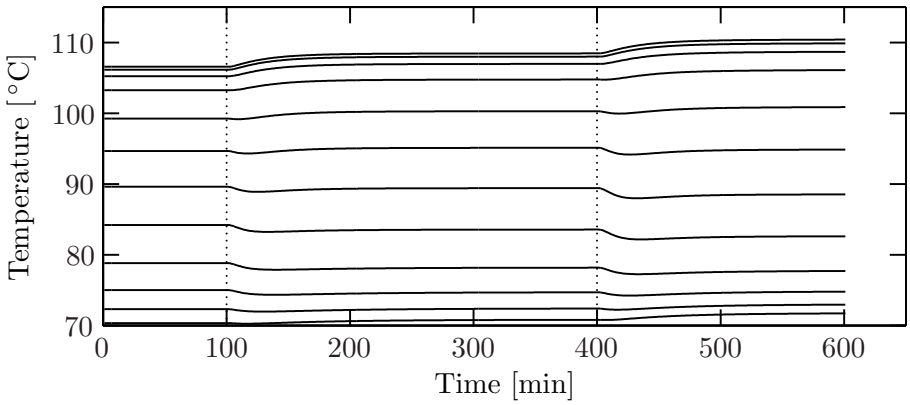

(a) Temperatures on main column side of partition

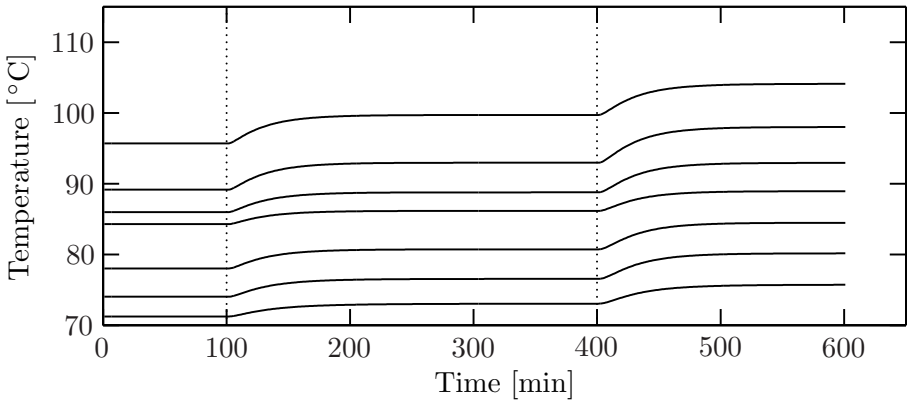

(b) Temperatures on prefractionator side of partition

Figure 8.8: Simulated temperature responses to change in R_V

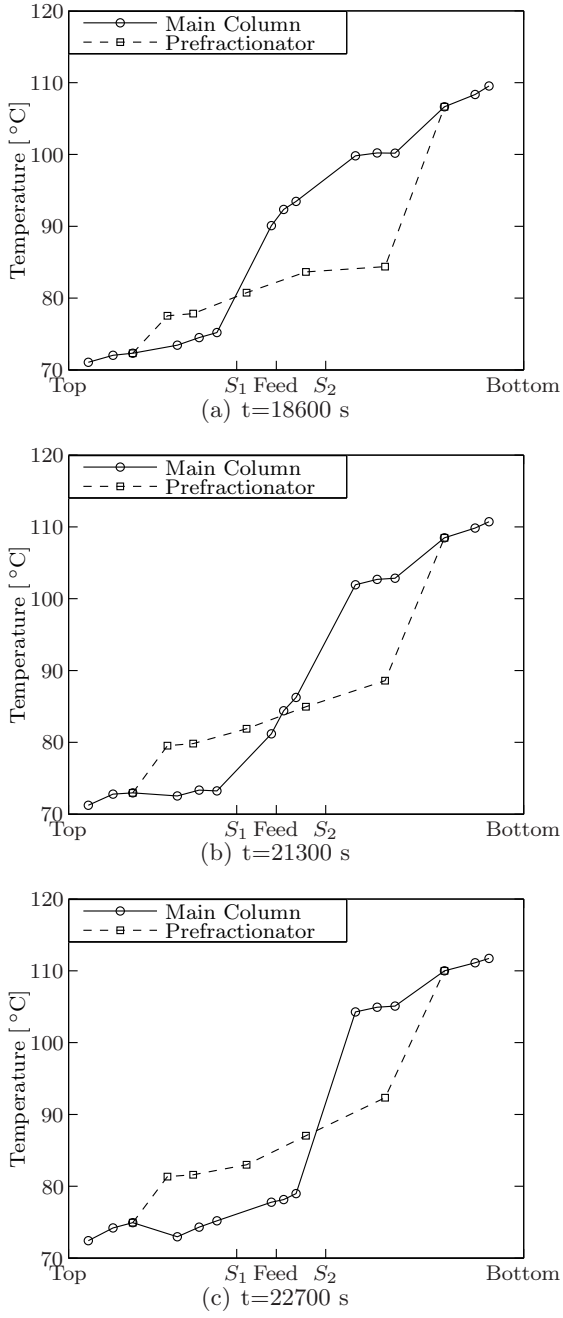

(a) t=18600 s

(b) t=21300 s

(c) t=22700 s

Figure 8.9: Shift in temperature profile after change in R_V. Valve on main column side is closed in two steps. The marked points represent the measurements and the lines are only for visualization.

adjustment has an observable effect is still very limited. Over the full range of positions from fully open to fully closed, more than 95 % of the span is effectively a fully open valve position. With the current step motor this translates to less than 10 half-steps available for real adjustment and a controller would spend most of its time saturated. Resizing the gear system could improve the available input range and make feedback control easier, (but a more thorough redesign of the valve is probably needed for the full range of R_V to be available. For industrial scale applications this type of valve would be impractical, but we believe that the method presented here where the liquid and vapour are separated before adjusting the vapour flow could form the basis for a solution that could also be implemented on a larger scale.

8.2.4 A *leaking* column

As mentioned at the start of the chapter, there were many operational problems discovered with the column after it was put into use. The small diameter of the bottom section limited the vapour boil-up rate and (as a result) there was a lack of reflux in the upper parts of the column. Running experiments with the temperature control loops described above (Figure 8.4) it became apparent that prolonged steady-state operation was not achievable. By measuring the time-averaged flow of the various product streams it was suspected that especially the side-stream rates were much higher than should be expected from the (control) inputs applied. Dedicated runs with total reflux and manual rate settings for the side-streams proved that there was significant leakage from the column to the product streams even though the flow should be zero (total reflux). In the worst cases, up to 1 l/h would exit side-stream 2 into the collection tank. As it turned out, the increased pressure of the column was enough to overcome the small liquid level collected at the product outlet. Essentially a shortcut was created from the column to the product collection tanks. This revelation helped to explain why the column would not reach the desired steady-state and why the internal flows in the upper parts of the column were so low.

8.3 Modified column

Because of the problems identified above were caused by poor design of the column it was eventually decided that the column had to be modified before further progress could be made.

8.3.1 Modifications to the column

A new bottom section and a new junction- (y-shaped) piece with increased internal diameter were ordered and installed. The new sections were 80 mm i.d. instead of the 50 mm used previously. It was not deemed necessary to increase the size of the top section. Another major improvement that was made was to install a throttling valve together with a solenoid (on/off) valve on every product outlet. The solenoid valves are actuated in tandem with the swinging funnels inside each section. In this way, we could stop the unwanted leakage through the product streams.

With the increased diameters in the bottom end of the column, we were able to increase the heat input to the reboiler. Stable operation was now possible at up to 2.2 kW heat input as to 1.4 kW previously. With the new configuration, flooding has been observed in the top section of the column!

8.3.2 Closed loop control of vapour split

An experiment that was run soon after the modifications to the column was to use the vapour split valves in closed loop feedback control. To test the valves, it was decided to attempt to control the temperature difference between the prefractionator and the main column. One temperature was chosen in each section (See Figure 8.10) and the difference between them was made the controlled variable.

The two vapour split valves were arranged in a split-range control logic, with an output range of 0 to 1. An output of 0 would mean that the valve on the main column side was open while the valve on the prefractionator side would be closed. Correspondingly, an output of 1 signifies that the valve on the main column side is closed while the other is open. At an output of 0.5, both valves remain open. Note that a closed valve in this sense is not physically shut tight, but a small opening for the vapour will always be present. As mentioned previously, the effective range of openings of the valves is fairly limited, and we have defined the responsive range as the first 10 steps of the actuator's step motor, from fully closed to fully open. However, this limitation of controller output range can be overcome by using feedback control.

The experiment was run using only methanol and ethanol present in the column, and the column was operated under total reflux. The liquid split ratio R_L was set constant at 0.44 and the heat input to the reboiler was fixed at 1.9 kW.

Figure 8.11 shows the time plot of the controlled variable and the manipulated variable(s). The controlled variable is the temperature in the

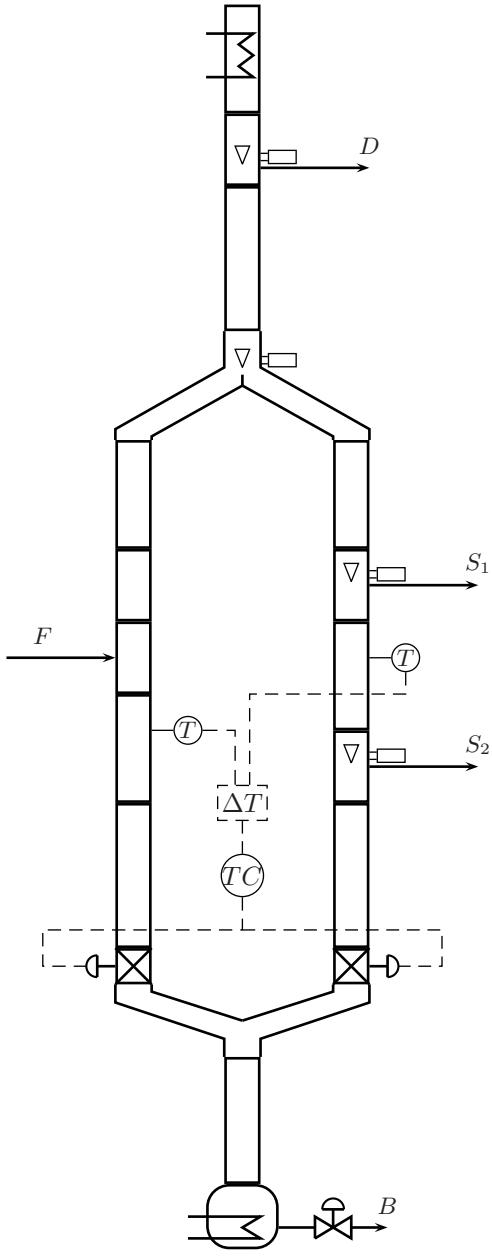

Figure 8.10: Vapour split valves used as manipulated variables. Here used to control the temperature difference across the 'dividing-wall'.

prefractionator ($TP5$) minus a temperature in the main column side ($T9$). From time 0 to 80 minutes a series of setpoint changes are introduced in the range of -3 to 5 °C. We observe that the setpoint is tracked excellently, except for a setpoint of + 5 °C when the controller saturates around 4.5 °C.

From 70 minutes onward, the setpoint remains unchanged at 0 °C and disturbances are introduced by changing the liquid split, R_L. At t = 83 min, the liquid split ratio is increased from 0.44 to 0.46. At t = 92 min, the ratio is reduced to 0.4 and at 110 minutes R_L is set to 0.45. Again, the controller works well and returns the temperature difference to the setpoint.

8.4 Conclusions

We have presented results from experiments with a Kaibel distillation column set up at NTNU. The results show how the prefractionator is successfully stabilized by using the liquid split to control a temperature in the prefractionator at its set point. We show, for the first time, that the vapour split can be manipulated during operation using a novel valve arrangement. Of importance is also that the vapour split can be used for active feedback control of a dividing wall column.

During the first experiments with the column a lot of problems were encountered that prevented proper operation of the column. The problems were mostly related to the column design, and the column and set-up had to be modified several times. A main conclusion has to be that more time should be spent in the design and engineering stage of a project like this before construction is initiated.

After the latest modifications the column is performing well, and hopefully many more experimental results can be presented in the future.

8.5 Acknowledgements

The latest modification work on the pilot plant (Section 8.3.1) was carried out with the help of Deeptanshu Dwivedi, Ivar J. Halvorsen and Mohammad Shamsuzzoha. The closed loop vapor split experiment (Section 8.3.2) was carried out by Deeptanshu Dwivedi and Ivar J. Halvorsen.

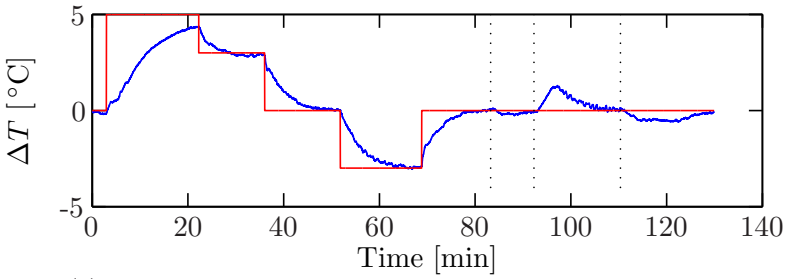

(a) Temperature difference across the partition and setpoint.

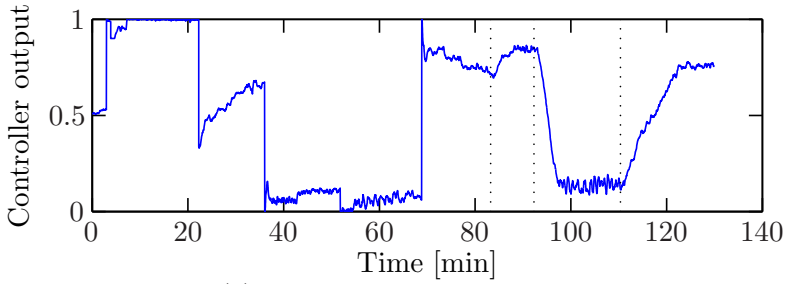

(b) Split-range controller output

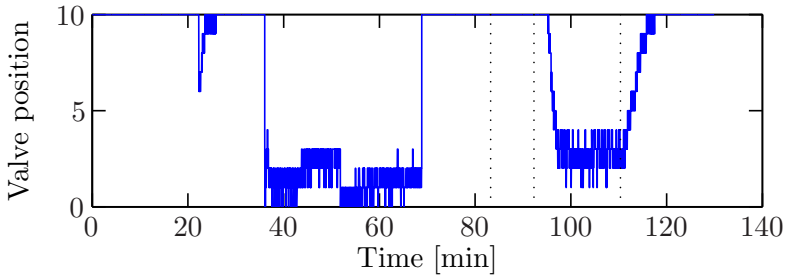

(c) Prefractionator valve position. 0 = max. closure.

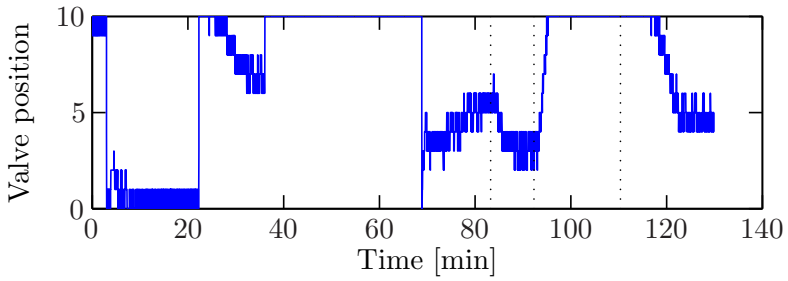

(d) Main column valve position. 0 = max. closure.

Figure 8.11: Experimental results from modified column. The vapour split, R_V, is used to control the difference between two temperatures either side of the column partition as shown in Figure 8.10. Dotted lines represent time of introduced disturbance in the liquid split, R_L.

Bibliography

[1] T. Adrian, H. Schoenmakers, and M. Boll. Model predictive control of integrated unit operations control of a divided wall column. *Distillation & Absorption 2002, Baden-Baden, October 2002*, 2002. See CD02-2; C02-5.

[2] V. Alstad, I. J. Halvorsen, and S. Skogestad. Optimal operation of a petlyuk distillation column: Energy savings by over-fractionating. In *Proceedings European Symposium on Computer Aided Process Engineering (ESCAPE-14). Lisboa, Portugal*, pages 547–552, 2004.

[3] V. Alstad and S. Skogestad. Combinations of measurements as controlled variables: Application to a petlyuk distillation column. *International Symposium of Advanced Control of Chemical Processes (Adchem-2003), Hong Kong, 11-14 Jan.*, 2004.

[4] V. Alstad, S. Skogestad, and E. S. Hori. Optimal measurement combinations as controlled variables. *Journal Of Process Control*, 19(1):138–148, January 2009.

[5] A.J. Brugma. Process and device for fractional distillation of liquid mixtures, more particularly petroleum. *US Patent No. 2,295,256*, 1942.

[6] Y. Cao and P. Saha. Improved branch and bound method for control structure screening. *Chem. Engng. Sci.*, 60:1555–1564, 2005.

[7] A.C. Christiansen, S. Skogestad, and K. Lien. Complex distillation arrangements: Extending the petlyuk ideas. *Computers and Chemical Engineering*, 21(SUPPL.1):S237–S242, 1997.

[8] I. Dejanovic, L. Matijasevic, and Z. Olujic. Dividing wall column-a breakthrough towards sustainable distilling. *Chemical Engineering And Processing*, 49(6):559–580, June 2010.

[9] I. Dejanovic, L. Matijasevic, Z. Olujic, I. Halvorsen, S. Skogestad, H. Jansen, and B. Kaibel. Conceptual design and comparison of four-products dividing wall columns for separation of a multicomponent aromatics mixture. *Distillation & Absorption 2010, A.B. de Haan, H. Kooijman and A. Gorak (Editors)*, 2010.

[10] V.A. Giroux. Fractionation method and apparatus. *US Patent No. 4,230,533*, 1980.

[11] J. Gmehling and J. Onken. *Vapor-liquid equilibrium data collection.* DECHEMA Chemistry Data Series, Frankfurt am Main, 1977.

[12] I. Halvorsen, I. Dejanovic, L. Matijasevic, Z. Olujic, and S. Skogestad. Establishing internal configuration of dividing wall column for separation of a multicomponent aromatics mixture. *Distillation & Absorption 2010, A.B. de Haan, H. Kooijman and A. Gorak (Editors)*, 2010.

[13] I. J. Halvorsen, S. Skogestad, J. C. Morud, and V. Alstad. Optimal selection of controlled variables. *INDUSTRIAL & ENGINEERING CHEMISTRY RESEARCH*, 42(14):3273–3284, 2003.

[14] I.J. Halvorsen and S. Skogestad. Optimal operation of petlyuk distillation: A steady-state behavior. *J. of Process Control, Special issue: Selected Papers from Symposium PSE-ESCAPE '97, Trondheim. Norway, May 1997*, 9(5):407–424, 1999.

[15] E. S. Hori and S. Skogestad. Selection of control structure and temperature location for two-product distillation columns. *Chemical Engineering Research & Design*, 85(A3):293–306, March 2007.

[16] B. Kaibel, H. Jansen, E. Zich, and Z. Olujic. Unfixed dividing wall technology for packed and tray distillation columns. *IChemE Symposium Series*, 152, 2006.

[17] G. Kaibel. Distillation columns with vertical partitions. *Chem. Eng. Technol.*, 10:92–98, 1987. Petluyk.

[18] F. Lestak and C. Collins. Advanced distillation saves energy & capital. *Chemical Engineering*, pages 72–76, July 1997.

[19] H. Ling and W. L. Luyben. New control structure for divided-wall columns. *Industrial & Engineering Chemistry Research*, 48(13):6034–6049, July 2009.

[20] H. Ling and W. L. Luyben. Temperature control of the btx divided-wall column. *Industrial & Engineering Chemistry Research*, 49(1):189–203, January 2010.

[21] W. L. Luyben. Evaluation of criteria for selecting temperature control trays in distillation columns. *JOURNAL OF PROCESS CONTROL*, 16(2):115–134, 2006.

[22] W.L. Luyben. Steady-state energy conservation aspects of distillation column control system design. *I&EC Fund.*, 14(4):321–325, 1975.

[23] P. Mizsey, N.T. Hau, N. Benko, I. Kalmar, and Z. Fonyo. Process control for energy integrated distillation schemes. *Computers and Chemical Engineering*, 22(SUPPL.1):S427–S434, 1998.

[24] D.A. Monro. Fractionating apparatus and method of fractionation. *US Patent No. 2,134,882*, 1938.

[25] M.I. Mutalib and R. Smith. Operation and control of dividing wall distillation columns. part 1: Degrees of freedom and dynamic simulation. *Trans IChemE*, 76(Part A):308–318, March 1998.

[26] M.I. Mutalib, A.O. Zeglam, and R. Smith. Operation and control of dividing wall distillation columns. part 2: Simulation and pilot plant studies uisng temperature control. *Trans IChemE*, 76(Part A):319–334, March 1998.

[27] G. Niggemann, C. Hiller, and G. Fieg. Experimental and theoretical studies of a dividing-wall column used for the recovery of high-purity products. *Industrial & Engineering Chemistry Research*, 49(14):6566–6577, July 2010.

[28] Z. Olujic, M. Jodecke, A. Shilkin, G. Schuch, and B. Kaibel. Equipment improvement trends in distillation. *Chemical Engineering And Processing*, 48(6):1089–1104, June 2009.

[29] F. B. Petlyuk, V. M. Platonov, and D.M. Slavinskii. Thermodynamically optimal method for separating multicomponent mixtures. *International Chemical Engineering*, 5(3):555–561, 1965.

[30] M.A. Schultz, D.G. Stewart, J.M. Harris, S.P. Rosenblum, M.S. Shakur, and D.E. O'Brien. Reduce costs with dividing-wall columns. *Chemical Engineering Progress*, 2002. HS2002-6.

[31] M. Serra, A. Espun?a, and L. Puigjaner. Control and optimization of the divided wall column. *Chemical Engineering and Processing*, 38(4-6):549–562, 1999.

[32] S. Skogestad. Dynamics and control of distillation columns – a tutorial introduction. *Trans. IChemE*, 75(Part A):539–562, 1997. Also Plenary lecture at Distillation and Absorption '97, Maastricht, September 9-10, 1997, C97-5, V1 pp. 23-58.

[33] S. Skogestad. Plantwide control: the search for the self-optimizing control structure. *Journal of Process control*, 10:487–507, 2000. H2000-10.

[34] S. Skogestad. Simple analytic rules for model reduction and pid controller tuning. *J. of Process Control*, 13:291–309, 2003. See C03-1; Nordic Process Control (NPC) Workshop 11, January 9-11, Trondheim, 2003; pages 209-227.

[35] S. Skogestad. Control structure design for complete chemical plants. *Computers and Chemical Engineering*, 28(1-2):219–234, 2004.

[36] S. Skogestad. The dos and don'ts of distillation columns control. *Chemical Engineering Research and Design (Trans IChemE, Part A)*, 85(A1):13–23, 2007.

[37] S. Skogestad and I. Postlethwaite. *Multivariable Feedback Control: Analysis and Design Second Edition.* John Wiley & Sons. Chichester, UK., 2005.

[38] B. Slade, B. Stober and D. Simpson. Dividing wall column revamp optimises mixed xylenes production. *IChemE Symposium Series*, 152, 2006.

[39] R. C. van Diggelen, A. A. Kiss, and A. W. Heemink. Comparison of control strategies for dividing-wall columns. *Industrial & Engineering Chemistry Research*, 49(1):288–307, January 2010.

[40] S. J. Wang and D. S. H. Wong. Controllability and energy efficiency of a high-purity divided wall column. *CHEMICAL ENGINEERING SCIENCE*, 62(4):1010–1025, 2007.

[41] E.A. Wolff and S. Skogestad. Operation of integrated three-product (petlyuk) distillation columns. *Industrial and Engineering Chemistry Research*, 34(6):2094–2103, 1995.

[42] R.O. Wright. Fractionation apparatus. *US Patent No. 2,471,134*, 1949.

Appendix A

Modelling

A.1 Model assumptions

The model used in the computations of this thesis is a stage-by-stage model with the following main assumptions:

- *Constant molar flows*: That is $V_i = V_{i+1}$ and $L_i = L_{i-1}$ for stage i inside a column section.
- *Constant pressure* P.
- *Equilibrium on each stage.*
- *No heat transfer across dividing wall*: This is a good assumption for a two-shell column like the pilot plant described in this thesis. For true dividing wall columns the effect of cross-wall heat transfer will be greater with smaller columnn diameters.
- *Linearized flow dynamics*: The liquid flow dynamics are modeled as

$$L_i = L_{0,i} + \frac{M_i - M_{0,i}}{\tau_L} + (V_{i-1} - V_{0,i-1})\lambda \tag{A.1}$$

  where $L_{0,i}$ and $M_{0,i}$ are the nominal values for the liquid flow and holdup on stage i. τ_L is the liquid time constant and λ is the effect of vapour flow on the liquid flow ('K2'-effect). In this work $\lambda = 0$, which is a good assumption for a packed column (Skogestad, 1997 [32]).

A.2 Kaibel column model

The Kaibel column is modeled using 7 column sections. The two sections in the prefractionator (above and below the feed) consist of 12 equilibrium

stages each, while the rest of the sections each contain 8 stages. Liquid holdup volumes are included for the condenser, reboiler, side product draws (S_1 and S_2) and the liquid split.

Unless otherwise stated in the text, the feed consists of an equimolar mixture of methanol (A), ethanol (B), 1-propanol (C) and 1-butanol (D). The liquid fraction of the feed has a nominal value of $q = 0.9$.

A.2.1 Vapour-Liquid Equilibria (VLE)

Ideal vapour phase is assumed and the vapour-liquid equilibrium for component j is described by the equation:

$$Py_j = x_j \gamma_j P_j^s \tag{A.2}$$

where

$$P = \sum_{j=1}^{n=NC} x_j \gamma_j P_j^s \qquad [mmHg] \tag{A.3}$$

The vapour pressures (P^s) are given by the Antoine equation:

$$\log P_j^s = A_j - \frac{B_j}{T + C_j} \tag{A.4}$$

The activity coefficients (γ_j) are given by the Wilson equation with description and parameters taken from Gmehling and Onken (1977) [11].